Republic of Iraq
Ministry of Higher Education and Scientific Research
University of Babylon
College of Science for Women
Department of Laser Physics

Spectroscopic Study on Organic Dyes as Optical Switches for Laser Applications

A Thesis

Submitted to Council of the College of Sciences for Women University of Babylon in Partial Fulfillment of the Requirements for the Degree of Doctor of Philosophy in Laser Physics and Its Applications

By

Noor Salah Khudhair Abd Ali AL-Busultan

B.Sc. Laser Physics Science. University of Babylon (2012)
M.Sc. Laser Physics Science. University of Babylon (2016)

Supervised by

Dr. Sami Abed Al-Hussein — *Assistant Professor*

Dr. Alaa Hussein Ali — *Senior Researcher*

2023 A.D *1444 A.H*

جمهـــورية العـراق
وزارة التعليم العـالي و البحث العلـمي
جامعة بابل،كلية العلوم للبنات
قسم فيزياء الليزر

دراسة طيفية للصبغات العضوية كمفاتيح بصرية في تطبيقات الليزر

أطروحة مقدمة الى

مجلس كلية العلوم للبنات،جامعة بابل

وهي جزء من متطلبات نيل درجة الدكتوراه فلسفة في العلوم/ فيزياء الليزر وتطبيقاته

من قبل

نور صلاح خضير عبدعلي البوسلطان

بكالوريوس علوم فيزياء الليزر . جامعة بابل (٢٠١٢)

ماجستير علوم فيزياء الليزر. جامعة بابل (٢٠١٦)

بأشراف

د. سامي عبد الحسين
أستاذ مساعد

د. علاء حسين علي
باحث علمي أقدم

٢٠٢٣ م

١٤٤٤ ه

الخلاصه

في هذا العمل تم تصميم دائرة الكترونية خاصة يمكننا من خلالها التحكم في التردد وزمن الضخ ومن خلاله يمكن تقدير زمن الفلورة ولكن أولا قمنا بدراسة الخصائص الطيفية الخطية و اللاخطية للصبغات المستخدمة عن طريق قياس أطياف الامتصاص والفلورة لصبغة الرودامين (R6G)المذابة في الايثانول وصبغة Methyl orange (MO) المذابة في الماء المقطر وفي تراكيز مختلفة .

تم استخدام التراكيز (1×10^{-4},3×10^{-4},3×10^{-5}, 5×10^{-5},and 7×10^{-5}) M لصبغة الرودامين والتراكيز ($1x10^{-4}$,$5x10^{-5}$, $1x10^{-5}$, and $1x10^{-6}$)M لصبغة Methyl orange(MO)حيث تم ملاحظة إن طيف الفلورة والامتصاص لكلا الصبغتين تتأثر بشكل كبير بتغير تركيز الصبغة ونوع المذيب حيث لوحظ كذلك بان هنالك إزاحة حمراء لطيف الفلورة باتجاه الطول الموجي الطويل .

تم دراسة أطياف الامتصاص و الفلورة قبل وبعد إضافة جسيمات الفضة النانوية (AgNPs) بين هذا العمل ان هنالك زيادة في شدة الامتصاص وكبت لطيف الفلورة .الخصائص البصرية اللاخطية للصبغتين تم دراستها باستخدام تقنية Z-Scan ضمن الطيف المرئي باستخدام ليزرات مستمرة الموجة بأطوال موجية nm (405,473,532, 650) أظهرت النتائج ان الخصائص اللاخطية للصبغتين تزداد بزيادة التركيز وتعتمد بصورة رئيسية على تركيز الصبغة والطول ألموجي المستخدم .

الهدف الرئيسي هو تقدير العمر الزمني من خلال عدة مؤشرات وهي (زمن الضخ ,التردد,الشدة ,وزمن التكامل) من خلال تسجيل طيف الفلورة وطيف النفاذ بجهاز Spectra Academy متصل بدائرة الكترونية خاصة مع استخدام مصدر للضخ وهو اللد الازرق لصبغة (MO) واللد الاخضر لصبغة (R6G) وبترددات من Hz (150000 -10000) مع Duty Cycle حوالي 50%. تم ملاحظة أعلى قمة لطيف الفلورة عند الطول الموجي حوالي (513nm) لصبغة MO و (561nm) لصبغة R6G . كذلك تم ملاحظة إن هنالك العديد من الأطوال الموجية (القمم)تظهر بالإضافة للقمة الأعلى (الأصلية) تبدأ من (220nm) إلى (882nm) وهذه الأطوال الموجية ناتجة عن الانتقالات التي حدثت في مستويات الطاقة وهذا بسبب تقنية الضخ التي تم استخدامها في هذه الدراسة . حيث يمكن أجراء تطابق بين التردد وزمن الضخ للحصول على الكمية المناسبة من الطاقة للمستوى, وبالتالي فان التطابق الذي سنحصل عليه هو نفس

مقدار الزيادة في الكفاءة .تم ملاحظة وجود قمم بطول موجي (882.403,800.304,) nm لصبغة MO مع (882.11 and 799.973) nm لصبغة(R6G) وهذه الأطوال الموجية غير موجودة في الدراسات السابقة ولكن تم إيجادها وفقا لطريقة الضخ المستخدمة في هذه الدراسة .

تم قياس شدة الضوء النافذ أيضا عن طريق تسجيل طيف النفاذ للعينات بوجود الدائرة الالكترونية وتحليل العينة عند الترددات (f=10000,50000,80000,120000,150000)Hz و% (Duty Cycle=10,30,50,70,and 90) لصبغة (MO) و (R6G) مع تغير في زمن الضخ والترددات عند زمن تكامل بحدود (30ms) .فقد لوحظ إن أعلى شدة سجلت لطيف النفاذ لصبغة MO هي (I=15844.6) عند تردد (f=80000 Hz) وزمن الضخ (T_{ON}=0.01125ms)(Duty Cycle = 90 %) وهذا يعني إن % 10من الزمن كان النظام مغلقا و90% النظام كان في وضع التشغيل, بينما أعلى شدة سجلت لطيف النفاذ لصبغة (R6G)هي (I=15943.4) عند تردد (80000 Hz) وزمن ضخ (T_{ON}=0.00375 ms),(D.C=30%) وهذا يعني إن 70%من الزمن كان النظام مغلقا و30% النظام كان في وضع التشغيل ,لذلك في زمن الضخ هذا والتردد ,الجزيئات انتقلت إلى المستوى الأعلى ووصلت حد الإشباع ومستوى الطاقة مملوء بالالكترونات في هذا الزمن وبالتالي في هذه الحالة ممكن إن تعمل كمفتاح بصري من خلال هذه التقنية .

كما قمنا بدراسة تأثير زيادة زمن التكامل من (60,30,الى 90) ms على شدة الضوء النافذ مع أزمان ضخ مختلفة من خلال ملاحظة الزيادة في شدة النفاذ عند تغير زمن التكامل و التي تثبت مدى التطابق الحاصل ما بين التردد وزمن التكامل وهذا من المؤشرات التي تؤثر على زمن الفلورة أيضا.

Abstract

In this work, it will (construct) designing a Special Electronic Circuit (TTL) that can control through it the frequency and pumping time and from that it is possible to estimate the fluorescence lifetime ,with study the spectra properties of dyes that used by measure the absorption and fluorescence spectra for Rhodamine 6G dye (R6G) dissolved in Ethanol and Methyl Orange (MO) Dye dissolved in distilled water for different concentrations .

The used concentrations were ($1x10^{-4}$, $3x10^{-4}$,$3x10^{-5}$, $5x10^{-5}$, and $7x10^{-5}$) M for R6G dye and ($1x10^{-4}$,$5x10^{-5}$, $1x10^{-5}$, and $1x10^{-6}$) M for MO dye. It is noticeable that they have a red shift only at high concentrations.

The absorption and fluorescence spectra of the prepared solutions were studied before and after adding particles Silver nanoparticles (AgNPs) to solution of organic MO dye for two concentration ($1x10^{-5}$ and $1x10^{-6}$) M, it was observed increase in absorption intensity and quench of the fluorescence spectra. In addition, the nonlinear optical properties of the two dyes (R6G and MO) were studied using Z-Scan technique within the visible spectrum using four continuous-wave lasers with wavelengths (405,473,532, and 650) nm.

The main objective is to estimate the fluorescence lifetime from the indicators such as pumping time ,frequency ,intensity and integration time by measuring the fluorescence and transmittance spectra with Spectra Academy device connected with a Special Electronic Circuit ,with using Methyl Orange (MO) Dye at concentration (1×10^{-5} M) ,Rhodamine 6G Dye at Concentration (5×10^{-5} M) and pumping sources (Blue ,Green) LED with frequencies from (10000-150000) Hz, and install the duty cycle at D.C = 50 %.

It can observed the maximum peak of Fluorescence spectra occurs, at wavelengths around (513 nm) for MO dye and (561 nm) for R6G dye. Also have been notice there is many wavelengths (peaks) appear addition to the maximum (original) peak start from (220 nm) to (882nm) and these wavelengths (peaks) result from transitions that occurred in the energy level and this due to the mechanism that used and then can make a match between frequency and pumping time and get the appropriate amount of energy for the level, therefore the match that we will get is the same amount of increase in efficiency.

It is possible that can notice a peaks at a wavelengths (800.304 and 882.403) nm for MO dye with (799.973, and 882.11) nm for R6G dye and these wavelengths are caused by transitions in energy levels and these do not present in previous studies ,but it is present according to the pumping method used in this research. The transmitted light intensity was also measured by recorded the transmittance spectrum of samples with using Electronic Circuit and analyze the sample at frequencies (f = 10000, 50000, 80000 ,120000 and ,150000) Hz and duty cycle (D.C = 10%, 30%, 50% ,70% ,and 90%), for (R6G and MO) with change in pumping time and frequencies at Integration time(t) =30 ms .

Also notice the maximum intensity recorded in transmittance spectra of MO dye is (I=15844.6) at frequency =80000 Hz and pumping time (T_{ON} = 0.01125 ms) (Duty Cycle = 90%) that mean 10% of time the system was OFF and 90% was ON , while the maximum intensity recorded in transmittance spectra of R6G dye is (I=15943.4) at frequency =80000 Hz and pumping time (T_{ON} = 0.00375 ms) (D.C = 30%) that mean 70% of time the system was OFF and 30% was ON, therefore at this pumping time and frequency ,the molecules transitions to upper level and has reach to saturation limit and energy level filled with electrons at

this time, in this case the processes leading to optical limiting through this technology.

Also study The influence of different integration time (30ms ,60ms and 90 ms) on the intensity of transmitted light with different pumping times ,then also studied the effect of the integration time on the intensity of transmitted light with different pumping time .it is observe the increase in intensity at some point when change in the integration time ,which prove the extent of the match between the frequency and integration time and this is one of indicators that affect on the fluorescence lifetime.

1.1 Introduction

Organic dyes are known as hydrocarbons, Organic dyes are composed of large molecules that have a complex structure and have a wide absorption and fluorescence spectrum in the visible and ultraviolet regions of the electromagnetic spectrum with a large molecular weight. Because it contains conjugate chains composed of carbon atoms linked by alternating single and double bonds, which is called the chromophore system [1],also the fast technological progress in optics have placed great demand on the development of Nonlinear Optical Materials (NLO)with prominent applications in optoelectronic devices such as optical limiting and all optical switching, optical data storage devices [2-4]. Nonlinear optics is the investigation of how intense light like the laser interacts with matter. Laser is one of the great inventions of the second half of the last century. Lasers brought about a revolution in optical technology and had an extensive influence in various fields of science and technology. Normally, only the laser light is adequately exceptional to alter the optical properties of a material. The optical reaction of a material typically scales straightly with the amplitude of the electric field, at high powers, however, the material properties can change more quickly. This leads to nonlinear effects consisting of self-focusing, saturated absorption, polarization and high-harmonic generation [5,6]. Z-scan technique is the simplest and highest in sensitivity, it has been created by Mansoor Sheik Bahae et al.[7,8] for computing nonlinear optical properties of materials [9-12]. It also utilized to computing Nonlinear Refraction (NLR), Nonlinear Absorption (NLA) for solution, film models and then studying the optical limiting effect. Some nonlinear optical impacts can be utilized for the designing and showing the optical limiter[13-15], which is utilized to protect the human eye and the sensors by taking care of the laser output [16]. Since 1960, dye lasers have been considered both attractive sources

of coherent tunable visible radiation and effective media on the account of their unique operational flexibility [17,18] . The first dye laser utilized in 1966 by Sorken and Lankard [19] utilizing Phthalocyanine to produce a dye laser, followed by a Rhodamine 6G laser by the same scientists in the following years[20]. Hundreds of dyes covering the range from the ultraviolet to the near infrared, and versatile to a wide range of various field. From basic science like chemistry, physics, and spectroscopy to industry and medicine [14,15].

1.2 Literature Survey

In (2005) ,Nur Farizan Binti Munajat studied and characterize the suitable material to be saturable absorber for passive Q-switching laser. The dye laser was utilized as a source of Q-switching laser. As a preliminary, the laser was calibrated to determine the best performance of laser beam. Various materials including 3, 3'- Diethyloxadicarbocyanine Iodide (DODCI), 1,3'-Diethyl-4, 2'-quinolyloxacarbocyanine Iodide (DQOCI) and 1,1'-Diethyl-4, 4'-carbocyanine Iodide (Cryptocyannine) and Chromium-doped Yttrium Aluminium Garnet (Cr^{4+}: YAG) crystal are employed as a saturable absorber material. The pulse width, the single pulse energy and the peak power of the Q-switched laser output are measured. Two of the tested materials namely1 ,3'- Diethyl-4, 2'-quinolyloxacarbocyanine Iodide (DQOCI) and Chromium-doped Yttrium Aluminium Garnet (Cr^{4+}: YAG) crystal demonstrate a good performance to be a saturable absorber [16].

In (2008) , Hassan H. Hammud and his group studied the effect of solvents on the absorption and fluorescence emission spectra of six purine derivatives. The effects of solvent and pH on the positions of λ_{max} (absorption) and λ_{max} (emission) of these compounds were determined and studied, the results showed the dependence of these spectral properties on the interactions between the solvent and solute ,it was also noted that there are spectral displacement resulting from the arrangement of solvent molecules around the excited solute molecule [17] .

In (2008) , Sahib Nimma Abdul-Wahid studyied the optical properties for BDN-I dye solutions which are used to Q-switch the Nd:YAG laser the BDN-I dye was prepared and dissolved in different

pure organic solvents such as (carbon-tetra-chloride , chloroform, Acetone, Dioxane , and pyridine) and in a mixture of carbon–tetra-chloride with another polar organic solvent. The giant laser pulse power , and the dye solution transmittance (T) have been measured. The (T) values are utilized in calculation of the optical properties such as (Reflectance (R), Absorptance (A) and refractance (r)), some indices as optical density (d) , refractive index (n), relative refractive index (n_r).The effect of the variation Of the BDN-I molar concentration dye solution and mixing ratios have been studied on the optical properties firstly , the effect of the optical properties on each other secondly ,and finally , the effects of the BDN-I dye solutions optical properties on the giant laser pulse characteristics. It can be concluded that the relative refractive index (n_r) has an important role in controlling the passive Q-switching process by specifying the optical properties of the BDNI solution [18].

In (2010) , R. Krishnamurthy and R. Alkondan they studied the effect of concentration on the properties of nonlinear refraction of a Mercurochrome dye in a liquid and solid medium . The dye exhibited a negative (defocusing) nonlinearity and large nonlinear refractive index of the order of 10^{-7} cm^2/W. The nonlinear refractive index was found to vary with concentration, and The third-order nonlinearity of the dye was dominated by nonlinear refraction, which leads to strong optical limiting of laser. Optical limiting characteristics of the dye at various concentrations in solution and film were studied. The result reveals that Mercurochrome dye can be a promising material for optical limiting applications[19] .

In (2014) , Mahmoud E. M, Sakr. Maram T. H.Studied Lifetime, Efficiency and Photostability Enhancement of Pyrromethene Laser Dyes

by Metallic Ag Nanoparticles ,by Complexation of metallic silver nano particles (NPs) with Pyrromethene laser dyes (PM567, PM597) has significant effect on lifetime, photostability and the fluorescence efficiency. These enhancement of optical properties of the complex in solution due to surface Plasmon resonance (SPR) have been promised higher efficiencies in case of [40% Ag NPs: PM dye] complexes for dye laser systems. The fluorescence lifetimes of PM dyes in optimum complex concentration are significantly shorter than the pure dye revealing a decrease of non-radiative decay rate of the dyes. Also, the optimum complex concentration show higher photostabilities and fluorescence efficiencies of the PM dyes than the dyes itself [20].

In (2014) , Hassan A.F. et al. studied the spectral properties (absorption and fluorescence) for Fluorescein Sodium dye at different concentrations (5×10^{-5}, 7×10^{-5} , 1×10^{-4} , 5×10^{-4} , 7×10^{-4}) M at room temperature, the results showed that the increase in concentration leads to shift the peak of the spectral properties to long wavelength for all models, and the overlapping between spectral properties decreases with increasing the concentration, the value of quantum efficiency increases with decreasing the concentration as follows (88%, 85%,70%, 55%, 53%) . In addition, they calculated the radiative life time and the fluorescence life time for all models[21].

In (2014) , Florian M. Zehentbauer and group study a series of eight different organic solvents are investigated at constant dye concentration. Relatively small changes of the fluorescence spectrum are observed for the different solvents; the highest fluorescence intensity is observed for methanol and lowest for DMSO. The shortest peak wavelength is found in methanol (568 nm) and the longest in DMSO (579 nm). Concentration

effects in aqueous R6G solutions are studied over the full concentration range from the solubility limit to highly dilute states. Changing the dye concentration provides tunability between ~550 nm in the dilute case and ~ 620 nm at high concentration, at which point the fluorescence spectrum indicates the formation of R6G aggregates[22].

In (2015) , Duanduan Wu and his group studied that Gold nanoparticles (GNPs) can be used to build a saturable absorber (SA) for (635 nm) Q-switched pulse generation. When the SA was used in a Pr^{3+}-doped ZBLAN fiber laser, stable passively Q-switching was achieved for a tunable repetition rate range from (285.7 to 546.4 kHz) and the pulse duration can be as narrow as (235 ns). The results exhibit that the GNPs film has good saturable absorption ability in the visible spectral region [23].

In (2017) , Shavakandi S.M. et al. studied the linear and nonlinear optical properties of FSS doped droplet. Raman spectroscopy, fluorescence, absorption and emission spectra measurements of the FSS were evaluated by utilizing Uv-Visible spectrophotometer and spectrofluorimeter. The nonlinear optical properties includes (NLR) Nonlinear Refractive index and (NLA) Nonlinear Absorption coefficient were calculated by utilizing Z-scan method with a continuous laser at 532 nm with a power of 80 mW, all the models were taken at room temperature. The results showed that the absorption, fluorescence and emission show red shift, the (NLR) and (NLA) indicate to negative sign and rely on droplet mass fraction and increase by dye concentration [24].

In (2019) , Husam Sabeeh study the effect of adding (Silver, Titanium dioxide, and Silica) nanoparticles to the (Fluorescein and Rhodamine 6G) dyes on the absorption and fluorescence spectra of these dyes, then estimating theoretical models for selected samples to ensure

that these models fits with the experimental behavior of adding used nanoparticles to the xanthene dyes. After that this work show that the photostability of Fluorescein dye can be enhanced from adding these nanoparticles to the dye [25] .

In (2019) , S Jeyaram, S. Hemalatha, T Geethakrishnan they study Nonlinear refraction, absorption and optical power limiting properties of an anthraquinone dye (disperse blue 14) in water have been investigated using (635 nm) diode laser by Z–scan technique. Disperse blue 14 dye shows a negative nonlinear index of refraction of (-2.96×10^{-7} cm^2/W) and an efficient reverse saturable absorption characteristics with a nonlinear absorption coefficient of (2.04×10^{-3} cm/W) in the present experimental conditions. Optical power limiting characteristics are observed for disperse blue 14 dye with a low limiting threshold of (1.77×10^2 KW/cm) [26].

In (2020) , Hiroki Tanaka and his group they investigated the saturation characteristics of the visible absorption in oxide crystals doped with Cr^{4+} or Co^{2+}. These transition-metal-doped crystals were found to exhibit useful properties as saturable absorbers to *Q*-switch visible lasers [27].

In (2021) , Afrah M. Al Hussainey , Ban A. Naser they study The non-linear refraction index and the non-linear absorption coefficient for solution of (Acriflavine) organic laser dye in ethanol solvent at (10^{-5} M) concentration and thin films of this dye doped with polymer and (Ag) nano material have been measured,using the Z-Scan technique with (457 nm) of (CW) laser with different laser power (56,70,84 and 102 mW). The results showed that increasing the nonlinear refractive index when

increasing powers but decreasing of nonlinear absorption coefficient, when increasing powers for all prepared samples. Thin films of dye doped with the polymer and Ag nano material have shown better nonlinear properties and optical limiting as compared with samples of pure dye .The result imply that all samples can be used as a potential medium for various optoelectronic applications including that in optical power limiting [28].

1.3 Aims of the Study

The aim of this work, is spectroscopic study and Non-linear optical properties of the (Rhodamine 6G and Methyl Orange (MO) dyes) and observed the effect of adding Silver nanoparticles to dyes on the properties (Absorption and Fluorescence spectra) in different concentrations of dyes, Adding the appropriate nano material to the dye and re-measuring the difference between the two cases because addition nanomaterial will increase the absorption cross section so that can improve the efficiency of dye absorption , then After that this work must show that the photostability of dye can be change after adding nanoparticles to the dyes , to investigate the possibility of using these dyes as optical switches. Finally the aims of work is building a technological pathway by designing a special electronic circuit to keep the laser parameters under control and has the ability to change the frequency of laser and pumping time ,by this optical system design can be used to limit the amplitude of an optical signal .when this two parameters (frequency ,and pumping time) changed we can observed the time of filling and discharge of excited state, and it is possible to calculate the Fluorescence lifetime for this dye.

2.1 Introduction

This chapter includes the descriptions of the background relate to this study such as the physical concepts, mathematical relationships.

2.2 Laser Dyes

The active material of laser dyes are large organic molecules, when one of these natural organic molecules is dissolved in an appropriate liquid dissolvable (for example ethanol, methanol, or an ethanol-water blend) it can be used as laser medium in a dye laser. Generally, laser dyes are complex molecules containing a number of ring structures which lead to complex absorption and emission spectra, the laser dyes can be classified into various classes by prudence of their structures that are chemically similar. Common examples are the coumarins, xanthenes and pyrromethenes as appeared in figure(2-1). The structure and composition of the molecules have an important influence on spectral emission. Nonetheless, there are many laser dyes that can be utilized to span continuously the emission spectrum from the near ultraviolet to the near infrared [29]. Laser dyes, either as solutions or solid are the active medium in pulsed and CW dye lasers as well as ultrafast shutters for Q-switching and passive mode-locking, thus a variety of dyes is important to cover the entire spectral range [30]. Dye molecules are utilized for the most part to produce tunable laser, the essential absorption processes in laser dyes could be divided into linear absorption. Saturation of absorption and reverseable saturable absorber. Saturation of absorption is vital for utilize of the dyes in mode locking. The most essential practical usage of reverse saturable absorption is for optical limiting devices that protect sensitive optical components, including human eye from laser induced damage [31]. Laser dyes are

promising compounds for nonlinear optical applications since they display strong nonlinear optical conduct [32].

For effective performance laser dyes molecules should have the following properties [33].

1. Strong absorption at excitation wavelength and minimal absorption at lasing wavelength.
2. High quantum yield .
3. A short fluorescence lifetime.
4. Good photochemical stability.
5. Laser dyes have to be very pure since impurities frequently quench the laser output.
6. Low probability of intersystem crossing to the triplet state.

By appropriate dye chosen it is possible to make coherent light of any wavelength from 320 to 1200 nm[33] .

The approximate working ranges of various laser dyes are demonstrated schematically in figure (2-1).

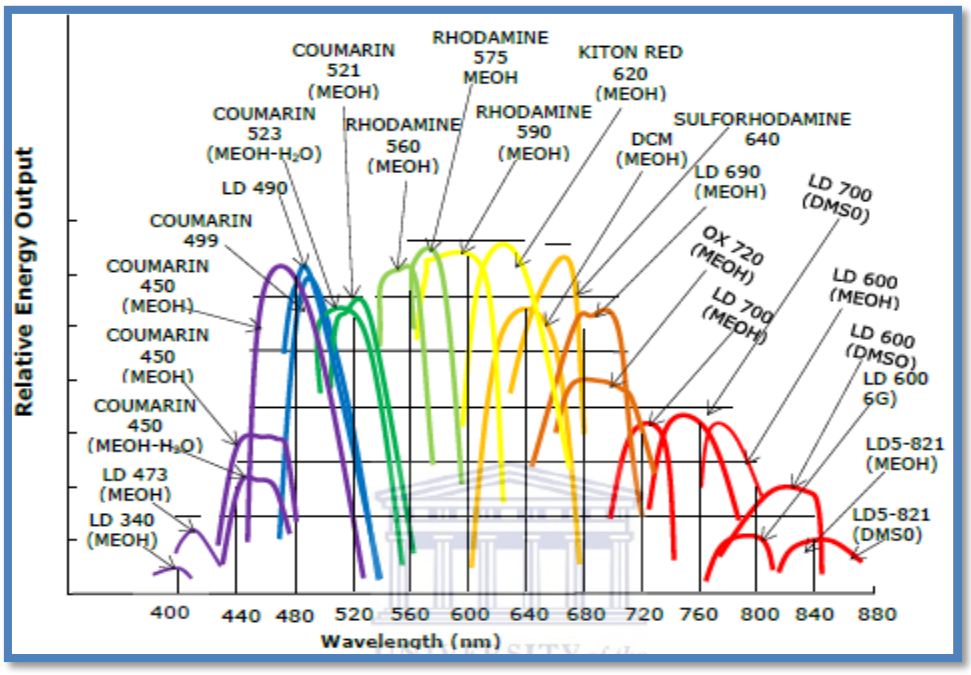

Figure (2-1) : Dye Spectral Emission Characteristics of some Common Laser Dyes [34]

2.2.1 Types of Laser dyes

Laser dyes are classified into four groups based on the wavelength they emit [34]:

1- Polymethine Dyes: such as Cyanines dye, emit in the red and near-infrared region of the spectrum between (700-1000) nm.

2- Xanthine Dye: such as Rhodamine dye, emits light in the visible region of the spectrum between (500-700) nm.

3- Coumarin Dye: such as Coumarin and Methyl orange dye emit light in the green and blue area between (400-500) nm.

4- Scintillator dyes: such as Y11 dye, emit in the UV area between (320-400) nm.

2.2.2 Applications of Laser Dyes

There are many applications for laser dyes, including [35] :

1- Industrial applications of laser dyes include separation of isotopes of important radioactive elements such as Uranium. Uranium is used as fuel in the nuclear power reactors to generate electricity.
2- Medical applications of laser dyes include skin treatments, including tattoo removal, diagnostic measurements, lithotripsy and activation of photosensitive drugs for photodynamic therapy, etc.
3- Optical communications.
4- Image processing .
5- Switching.
6- 3D data storage and optical limiting.

2.3 Nanoscience and Nanotechnology

Nanoscience and nanotechnology are recent revolutionary developments of science and technology that are evolving at a very fast pace since a decade. They are motivated us to formulate materials with renowned and enhanced characteristics they are likely to influence almost all areas of physics, chemistry, biology, medicine and other interdisciplinary fields of science and technology [36,37]. Nanoscience and nanotechnology refer to the control and manipulation of matter at nanometer dimension. Particles with sizes in the range of (1–100) nm are called nanoparticles. Nanoscience has impacted our lives with innovations inspired by nanoscale features, computer hard drives, which store information. Researchers from the numerous disciplines which include physics, chemistry, biology and substances science employ nanoscience principles for superior packages in energy , medicine, data garage, computing and some place else [38,39]. Despite the fact that step forward in any research field are hard to expectation, the destiny of nanoscience will possibly contain scaling up from the atomic assembly and individual nano devices to macroscopic systems and structures with development properties and severally capabilities.

The metallic nanoparticles have vast applications in medicine [40], energy storage [41] and dye-sensitized solar cells [42] etc.. Metallic nano particles possess specific optical, electronic, chemical and Magnetic properties which are strikingly exclusive from those of the character atoms in addition to their bulk counterparts. Nano (10^{-9} m) sized metallic particles exhibit optical residences of exceptional aesthetic, technological and intellectual values. Colloidal solutions of the noble metals namely, silver and gold show feature colours that have obtained full-size attention to the researchers.

2.4 Nanoparticles

Nanoscience is the study of the basic principles of molecules and compositions with at leastwise one dimension approximately between 1 and 100 nano meters. At this science, a particle is described like a tiny object which behaves like a whole unit regarding its properties . The term "nanoparticles" isn't typically applicatively to individual molecules; it generally indicates to inorganic materials [43] .

At the nanoscale size, dependent properties are usually observed. Hence, the properties of materials vary as their size approaches the nanoscale and as the percentage of the surface in relation to the percentage of the volume of a material becomes important [44].
Nanoparticles frequently have specific optical peculiarities as they're small sufficiently to confine their electrons and create quantum effects. the nano material used in the study is: Nano Silver (Ag).

2.4.1 Silver Nanoparticles (AgNps)

The chemical element known as silver has the symbol Ag (derived from a Greek word, which means "shiny" or "white"). A white, softened metal, Pure silver as known has the better electrical and thermal conductivity than most metals and alloys [45] .

The silver is found in the Earth's crust in the pure, free elemental shape (native silver), like an alloy with gold and other metals, and in minerals such as argentite. Most silver is produced as a byproduct of gold, lead, copper, and zinc refining [46].

Silver nanoparticles can be synthesized and prepared experimentally using several different techniques such as chemical reduction laser ablation photochemical sol-gel and electrochemical methods [47]. Nano

particles, of silver metal (AgNPs) are widely increasingly used in several fields involving health care medical and industrial chemical and biological properties. These targets include different application for instance optics, magnetic, thermal, electrical conductivity, and biological application [48,49].

Silver NPs are interest due to their unique properties which can be incorporated into antimicrobial applications composite, fibers, cryogenic, superconducting ,materials, biosensor materials, cosmetic products, and electronic, components. Devices, such as air conditioners or refrigerators, have a silver nano coating upon their internal surfaces with a total anti - bacterial and anti-fungal impact. As air moves, the coated surfaces interact with the silver ions that can withstands any aerial bacteria, which in turn suppress the respiration of bacteria, negatively affects bacteria's cellular metabolism and prevents cell growth [50].

2.4.2 Properties of AgNPs

The properties of silver nano particles, including surface activity shape of particles, size distribution, particle composition, agglomeration and particle reactivity are critical factors for classification of nano silver particles [51,52,53]. It is expected that silver nano size can be fabricated in different shapes and sizes, spherical, hexagonal and rod are a common shapes appeared during synthesis. Figure (2-2) presents different shape and size of synthesis particles. More studies stated the assertions that smaller size particles may be more toxicity than larger particles due to their surface area [54].

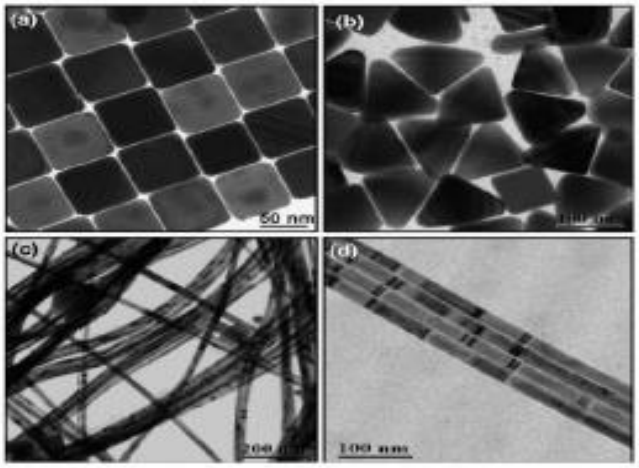

Figure (2-2): Various shapes of AgNPs (a) Cubes ;(b) Triangles;(c)Wires;(d) An alignment of wires [55]

2.5 Synthesis of Nanoparticles

Synthesis techniques to generate metal nanoparticles depend on the isolation of small amounts of material. There are two general, strategies mechanism to obtain materials on the nanoscale; I-the top-down method (dispersion method) is where material is removed from the bulk material leaving only the desired nanostructures. II-the bottom up method (reduction method) is one where the atoms produced from reduction of ions are assembled to generate nanostructures [56,57].

2.5.1 Dispersion Methods (Top down method)

The Top down method typically, starting from bulk involves laser ablation [58] arc discharge [59], etc. Nucleation, takes place starting from the plume and continues till a solid substrate comes in its way. Control of particle size is achieved by tuning the fluence wavelength irradiation time ,etc. The above crude method may, be modified by altering, the design, of the cluster. Top down techniques suffer from the need to remove large amounts of material.

2.5.2 Reduction Methods (bottom up method)

The bottom up methods starting from atoms, include chemical[60], electrochemical [61], sono-chemical [62]. thermal and photochemical reduction, [63-65] etc, have been used to generate nanoparticles. Bottom up synthesis techniques usually employs an agent to stop the growth of the particle at the nanoscale. Capping materials such as a surfactant or polymer are used to prevent aggregation and precipitation of the metal nanoparticles out of solution. Choice of the reduction technique time and capping material determine the size and shape of the nanoparticles generated. Spheres, rods, cubes, disks, wires, tubes branched triangular prisms and tetrahedral. In this work, pulsed laser ablation in liquids method was used to generate nanoparticles [65].

2.6 The Photophysics Properties of Laser Dyes

The significant properties of organic dyes which make them very attractive in the photonics world of application are the large absorption and emission cross sections which they exhibit in the visible part of the spectrum over a wide range of wavelengths. They constitute a large class of polyatomic molecules containing long chains of conjugated double bonds.

The large absorption cross section (σ_a) is due to the presence of large dipole moment (μ) originating from the π electrons of carbon. These π electrons are free to move over a distance roughly equal to the chain length L.

Since the chain length L is quite large, correspondingly μ is also large. The absorption cross section σ_a which is proportional to (μ^2) is of the order of ($l0^{-16}$ cm ^{2}) [66]. Compounds with conjugated double bonds absorb light at wavelengths above 200 nm. The large number of

conjugated double bonds present in organic dyes also increases the absorption in the visible part of the spectrum [1]. The dyes display strong broadband fluorescence spectra under excitation by visible or UV light. With different laser dyes the overall spectral range extends from (300 nm to 1200 nm).

2.6.1 Energy Levels and Transition in Organic Dye Molecules

A dye molecule contains a large number of atoms and will have a number of possible energy states due to electronic, vibration and rotational motions. Therefore, the complete energy level diagram will be complicated. The electronic transitions of large complex molecules can be represented by Jablonski diagram as shown in Figure (2-3) , which gives the configuration of the state in terms of one coordinate only.

The energy levels of the organic molecules are named as single when the total spin becomes zero and an triplet states when the total spin is unity. In general, dye molecules have pairs of electrons in the ground state and the total spin is zero. And due to this, there exists only singlet ground states (S_o). When the molecule is excited, one of the electrons in the π electrons cloud goes to the higher electronic state. In the excited state, the electrons may have its spin either parallel or anti-parallel to the ground state. Due to this both the singlet and triplet states exist in the excited states are designated as S_1, S_2,…, S_n and T_1, T_2,…, T_n respectively.

The triplet state is lower in energy than the corresponding singlet state [67]. Each electronic state has many vibrational and rotational states, which are represented by horizontal lines in each electronic state.

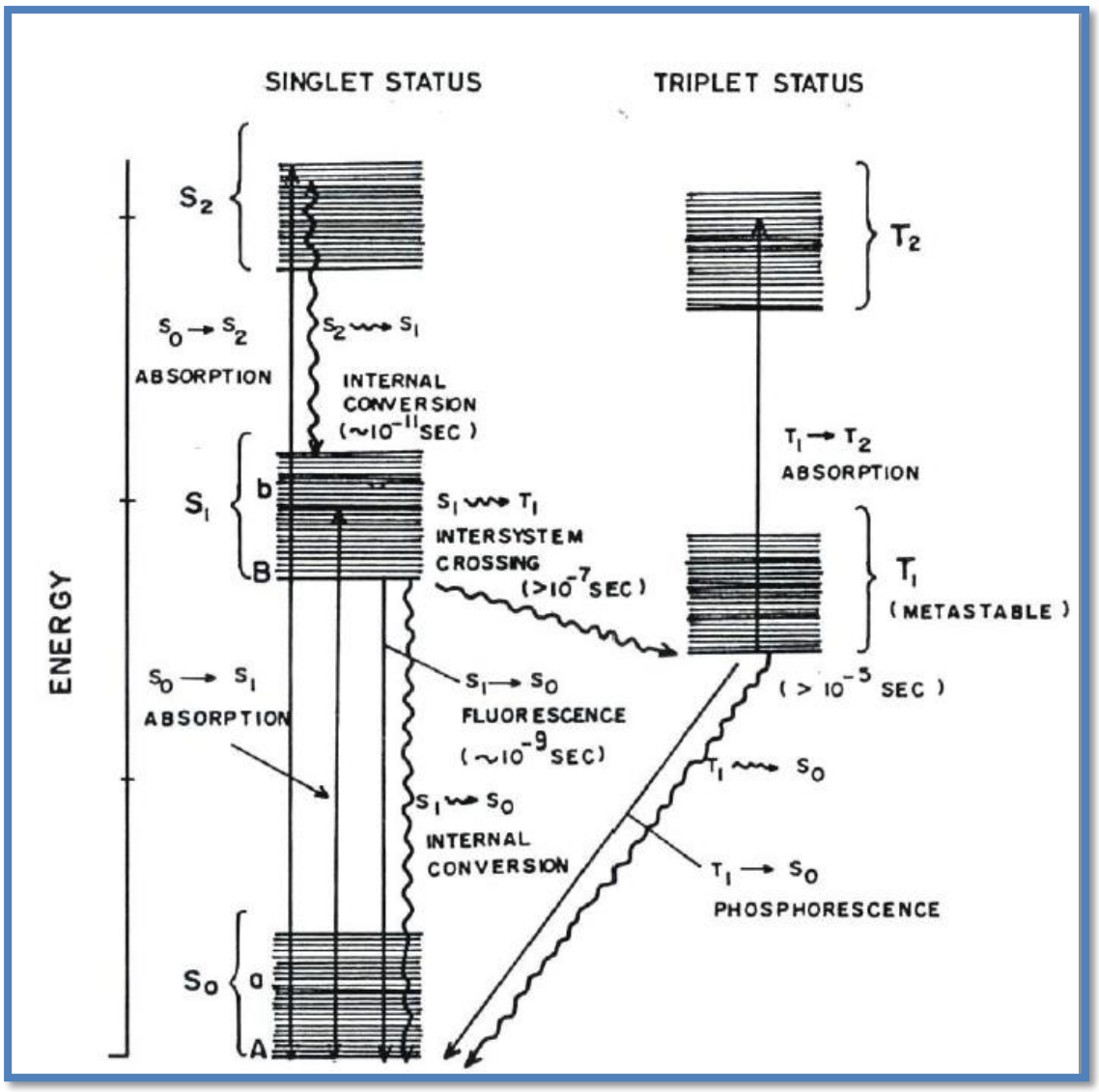

Figure (2-3) Energy level diagram of a dye molecule

Electronic transition between the singlet- singlet or triplet-triplet states are allowed, but between singlet and triplet are forbidden. The energy gap between S_1-S_2 or S_2-S_3 or T_1-T_2 excited states is less. As a result, vibrational levels of one state (S_1) overlap with those of the other (S_2). This leads to a strong non-radiative decay to lower states by vibrational relaxation, when the molecules are excited to higher energy states such as S_2, S_3 etc. This takes place in time duration of the order in pico seconds. The non-radiative process between the singlet-singlet or triplet-triplet states is termed as internal conversion.

For a dye molecule, the energy gap between S_1 and S_2 will be high compared to those between other higher states and internal conversion is weak. A radiative transition occurs between them. This emission is termed as fluorescence.

The transition from singlet to triplet or vice-versa is termed as intersystem crossing. Some of the molecules in S_1 may decay non-radiatively to the triplet state T_1. This tripping of spin of the molecules in the excited states due to the perturbation arising out of spin-orbit coupling which increases with the number of atoms in the molecule and also with the atomic number of the atoms constituting the molecule.

The radiative transition between T_1 and S_0 states is termed as phosphorescence, which is forbidden and weak. Hence, T_1 is usually a metastable state. The lifetime of the triplet state T_1 is in the range of milli seconds to seconds depending upon the environment of the molecule. However, in liquid media, the molecule in T_1 decays to S_0 non-radiatively in (l00 ns) due to collisions with solvent molecules at room temperature.

The absorption and emission spectra of dyes are broad bands. The broad band characteristics are due to the vibrational structure and the change in the inter nuclear distances on excitation. The minima of S_1 and S_2 states have different configuration coordinates. This causes the emission peak to be shifted to the longer wavelength side of the absorption peak. This shift is called the Stoke's shift. A number of factors can influence the absorption and emission processes between S_0 and S_1 states by causing changes in the magnitude of the various competing processes [67-71].

2.6.2 Absorption and Fluorescence Spectral Characteristics

The absorption spectra of organic dyes have a large spectral Width which usually covers several tens of nanometers. In the general case of a dye molecule which consists of a large number of atoms, many normal vibrations of different frequencies are coupled to the electronic transition. The collisional and electrostatic perturbations caused by the surrounding solvent molecules further broaden the individual lines of such vibrational series. Every vibronic sublevel of electronic state has been further superimposed by rotationally excited sublevels. These are highly broadened by the frequent collisions with the solvent molecules and there is a quasi-continuum of states superimposed on every electronic level. Thus the absorption is practically continuous all over the absorption band. The same is true for the fluorescence emission corresponding to the transition from the electronically excited state of the molecule to the ground state. This results in a mirror image of the absorption band displaced towards higher wavelengths [72].

2.6.3 Fluorescence Lifetime

The lifetime of the excited state is defined by the average time the molecule spends in the excited state prior to return to the ground state which is denoted by τ . The lifetime of the fluorophore in the absence of nonradiative processes is called intrinsic lifetime or natural lifetime and is given by [73] :-

$$\tau_0 = \frac{1}{K_r} \qquad \text{.....(2-1)}$$

This leads to the relationship for quantum yield [73] :

$$\Phi = \frac{\tau}{\tau_0} \qquad \text{.....(2-2)}$$

The quantum yield is the fraction of the excited fluorophores which decay by emission(k_r) relative to the total decay ($k_r + k_{nr}$).The lifetime of a fluorophore is determined by the sum of the rates which depopulate the excited state. In the absence of other quenching interactions, the lifetime is given by [74,75]:

$$\tau = (K_r + K_{nr})^{-1} \quad \text{.....(2-3)}$$

The lifetime of fluorophore is increased or decreased by the change in the value of k_{nr} .Almost invariably, the lifetimes and quantum yields increase or decrease together. The lifetime τ alone is insufficient to distinguish changes in radiative rates from changes in non-radaitive rates. Measurements of fluorescence quantum yields are coveted to distinguish the two contributions . The radiative rate (k_r), and the non-radiative rate (k_{nr}) are calculated by the equations [76]:

$$K_r = \frac{\Phi}{\tau} \qquad \text{.....(2-4)}$$

$$K_{nr} = \frac{(1-\Phi)}{\tau} \qquad \text{.....(2-5)}$$

Naturally (k_{nr}) , indicates the sum of various processes.

2.6.4 Solvent Effect on Fluorescence Spectra

Solvents have been shown to play an important role in laser dye photo physics. The dye laser active medium consists of a typical organic dye concentration of ($l0^{-2}$ -$l0^{-5}$) M dissolved in a specific solvent. Due of this, dye solvents play have an important role in the design of dye lasers. Choosing the right solvents can have a big impact on Lasing wavelength

and energy. The energy difference between the ground state and the excited states is influenced by the solvent and the fluorophore molecules interaction [72]. This energy difference is attributed to the refractive index *n* and the dielectric constant (ε) of the solvent

Most of laser dyes are polar ones and excitation into their low lying excited singlet state will be accompanied by an increase in the dipole moment. The solvent polarity have a decisive role in shifting the lasing wavelength. In most of the cases, increasing the solvent polarity will shift the gain curve towards the longer wavelength side which is known as the Stoke's shift. In high polar solvents the shift can be as high as (20-60) nm. Some solvents cannot be used in the longer wavelength side due to vibrational overtones of the solvents which will interfere with the lasing process. Solvents like water, methanol and ethanol which would appear optimal solvents for many dyes are not useful for the near-IR and IR dyes [77].

2.6.5 Solvent Effects On Energy of Electronic States

The natures and the energy of the electronically excited states of a dye molecule limiting the photo-physical & photochemical properties of a dye molecule. The impact of solvent media on the energies of electronic states of solute molecule i.e., an electrostatic interaction between solute & solvent particles, known as "solvation", is of substantial importance in photo-physics and photo-chemistry .

When a dye is dissolved in a solvent, the solvent molecules arrange themselves around the dye molecule in such a way as to minimize the energy of the system. The dye molecule undergoes interactions with these

solvent molecules and attains thermal equilibrium. The interaction between the dye molecule and the solvent molecule can be broadly divided into two types. They are the long-range and short- range(specific) interactions [78] .

2.7 Fluorescence Quenching

Intensity of fluorescence spectrum can be reduced by a broad variety of processes. This reduction in spectrum intensity is named quenching. Quenching can occur through altered mechanisms. Collisional quenching occurs when the excited-state fluorophore is disabled upon contact with some other molecule in solution, which is termed the quencher. Away from collisional quenching, quenching of the fluorescence can happen by a variety of other processes. Fluorophores can form nonfluorescent complexes with quenchers. This process is called static quenching because it occurs in the ground state and does not depend on molecular collisions [79,80].

2.8 Linear Optical Properties

The interaction between the nature and distribution of charges inside the material (electronic, molecular or ionic) and the electromagnetic radiation leads to the appearance of the optical properties of materials [81].

When the electromagnetic radiation falls on the material and interacts with it, many processes occur as part of the electromagnetic radiation is absorbed by the material and the other part is called the transmitting ray because it passes through the material while another part of the electromagnetic radiation is reflected from the surface of the material called the reflected part [82].

In order to obtain information about the interference composition of the material and the nature of its bonds, it is necessary to know the transmittance, absorption and reflectivity of the electromagnetic radiation falling on the material. For example, the energy packets and the quality of transitions within the material are identified by studying the ultraviolet spectrum, but to know the field of practical applications in which materials are used, the visible spectrum must be studied ,and one of the most important linear optical properties [83]:-

2.8.1 Absorbance(A)

The mathematical quantity that relates the particle density (concentration) in a sample and sample thickness (optical path length) is the absorbance (A) or optical density [83].

$$A = \log(\frac{I_o}{I}).....(2-6)$$

where I: is the intensity of the light at wavelength λ that passes through the sample (the intensity of the transmitted light), I_0 : is the intensity of the light before entering the sample, (the intensity of the incident light).

The absorption of the incident rays by the material causes an electronic activity that may lead to the disintegration of its molecules if the value of the absorbed energy is greater than the value of the dismantling of one of the bonds or its transfer to a higher energy level, as the possibility of absorption increases, with the increase in the concentration of the material in the lower energy level and with the increase in the number of photons of the incident rays [84].

The probability of photon absorption is directly proportional, to the concentration of the absorbed particles in the sample and the thickness

of the sample (the length of the optical path), according to Beer-Lambert Law, which is an empirical relationship that links the absorption of light with the properties of the material through which the light passes, the law states that the number of absorbing molecules in a substance is proportional to the portion, of the absorbed ray passing through it. If the rays pass through a specific solution, the amount of absorbed or transmitted light is an exponential function of the concentration of the solute. And as in the following equation [85] :

$$I = I_0 e^{-\alpha_{op} C_m L} \ldots\ldots (2-7)$$

As α_{op} : represents the optical absorption coefficient, L: the optical path, length, and C_m: the molar concentration.

The equation can be written as follows [85]:

$$Ln \frac{I_0}{I} = \alpha_{op} C_m L = A \ldots\ldots\ldots (2-8)$$

Beer-Lambert's law can be applied in different spectral regions such as ultraviolet, visible, and others, provided that the radiation used is monochromatic [86].

2.8.2 Transmittance (T)

The transmittance of the medium, is defined as the percentage ,of the intensity of the transmitted light (I) to the intensity of the incident light (I_0). Also it can define the energy of the radiation transmitted from the medium to the energy, of the radiation falling, on it. It is given by the following relationship [87] :

$$T = (\frac{I}{I_0}) \ldots\ldots\ldots (2-9)$$

According to, the Beer-Lambert law the transmittance decreases with the increase in the molar concentration (C_m) and the length of the optical path (L) through which the light passes.

Regarding permeability of the medium ,it is related to the absorbance of the solution (A) that given in the equation [87] :

$$A = -\log(\frac{1}{T}) = -\log(\frac{I}{I_0}) = \log(\frac{I}{I_0}).....(2-10)$$

From this relationship, we notice that the permeability (T) increases as the absorbance of the medium (A) decreases.

2.8.3 Reflectivity (R)

Reflection in light is the reflection of light falling on the separating two media of different optical density, and reflectivity is defined as the energy of the reflected light as given in the following equation [84]:

$$R = (\frac{n-1}{n+1})^2.....(2-11)$$

2.9 Nonlinear Optics

2.9.1 The Concept of Nonlinearity in Optics

The birth of nonlinear optics occurred at the same time as that of laser, in early 1960's. Nonlinear optics is an important branch of science which took birth with the advent of highly intense laser systems. It is concerned with the study of the phenomena that result from highly intense light induced modifications in the optical properties of the materials. The field of nonlinear optics (NLO) explores the coherent coupling of two or more electromagnetic fields in a nonlinear medium [88-90] . The discovery of the important nonlinear effect, the second harmonic generation (SHG) introduced a new branch of experimental

investigation in the area of laser-matter interaction. Later on many interesting nonlinear optical effects are discovered which have significant applications in the field of telecommunication, optical storage, optical switching, optical power limiting etc [91-94].

Study of nonlinear effects leads us to a new understanding of fundamental light-matter interaction. Implementation of the various NLO effects in the appropriate areas of technologies like optical communication, optical switching, optical data storage demands a detailed knowledge of the NLO processes and their dynamics.

Nonlinear optics is observed with lasers which have high degree of spectral purity, coherence and directionality with which atoms and molecules can be irradiated with an electric field that is comparable to interatomic field.

Nonlinearity is a property of the medium through which light travels rather than a property of the light itself.

Nonlinear optics deals with interaction of light of high intensity with matter, resulting a considerable alteration of the properties of matter itself.

2.10 Nonlinear Optical Properties

Nonlinear optics is the study of phenomena that occur as consequence of the modification of the optical properties of materials on interaction with intense light. Nonlinear phenomena has been studied extensively. The particles of the medium are displaced from their equilibrium positions, so that positive charged particles move in the direction of the electric field, while the negative charged particles move in the direction opposite to the direction of the applied electric fields. Dipole moments are created because of the displacement between

positive and negative charged particles, and the dipole moment per unit volume describes the induced polarization of the medium.

When the applied electric fields are sufficiently small, the electric polarization is approximately linearly proportional with the applied electric field E [95]:

$$P = \varepsilon_o \chi . E \quad \ldots\ldots\ldots\ldots (2\text{-}12)$$

Where(ε_o) is the permittivity of free space, (χ) is the electric susceptibility tensor. This is the case of linear optics .However, when the applied electric fields are high enough, the induced polarization has a nonlinear dependence on these electric fields and can be expressed as a power series with respect to the electric field [96]:

$$P = \varepsilon_o(\chi^{(1)}.E + \chi^{(2)}.EE + \chi^{(3)}.EEE+\ldots) \quad \ldots\ldots \quad (2\text{-}13)$$

$$P = P^{(1)} + P^{(2)} + P^{(3)} \quad \ldots\ldots\ldots \quad (2\text{-}14)$$

Where $\chi^{(1)}$is the linear susceptibility, $\chi^{(2)}$ is the second order nonlinear susceptibility, and $\chi^{(3)}$ is the third order nonlinear susceptibility .The term $\chi^{(1)}$ is responsible for linear absorption and refraction, and is the only term that reflects the linearity between the induced polarization and the incident electric field. The term $\chi^{(2)}$is present only in non-centrosymmetric materials, i.e. materials that do not have inversion symmetry. The third order nonlinear optical interactions, which are described by the term $\chi^{(3)}$[97].The field of nonlinear optics (NLO) has been developing for a few decades as a promising field with important applications in the domain of photo electronics and photonics. Organic materials are considered as one of the important classes of third order NLO materials because they exhibit large and fast nonlinearities.

Various types of organic compounds have been studied to obtain materials with large third order nonlinearity. On the other hand, a wide range of techniques has been used to measure third order nonlinearity e.g.

degenerate four waves mixing, third harmonic generation and Z-Scan technique. Among all these techniques Z-Scan is a simple for the measurement of the nonlinear refractive index and nonlinear absorption coefficient. It provides not only the magnitudes of the real and imaginary parts of the nonlinear susceptibility but also the sign of the real part. Both nonlinear refraction and nonlinear absorption in solid and liquid samples can be rapidly measured by the Z-Scan technique, which utilizes self-focusing or self-defocusing phenomena in optical nonlinear materials. There are two methods of Z-Scan ,the closed -aperture and open -aperture system [98]:

2.10.1 Closed-aperture Z-Scan

A closed aperture Z-Scan measures the change in intensity of a beam, focused by lens (L) in Figure (2-8), as the sample passes through the focal plane. Photo detector (PD) collects the light that passes through an axially centered aperture (A) in the far field. The change on axis intensity is caused by self-focusing or self-defocusing by the sample (S) as it will create a change in index of refraction forming a lens in a nonlinear sample as shown in Figure (2-4) [99].

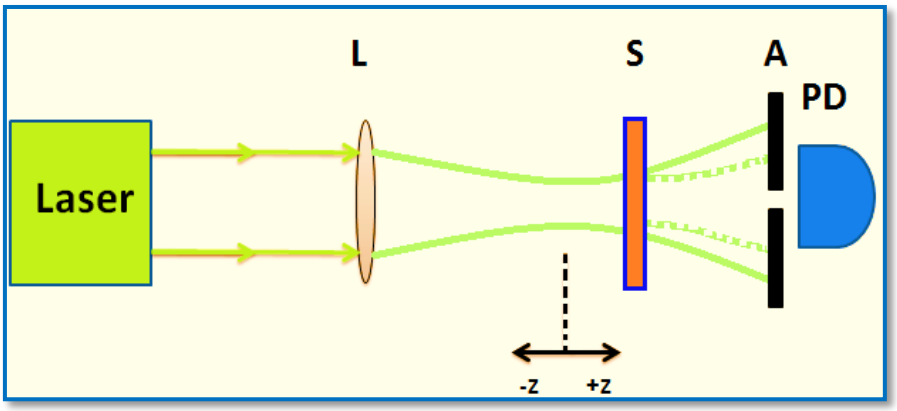

Figure (2-4): Closed aperture Z-Scan[99].

To show how the Z-Scan transmittance as a function of (Z) is related to the nonlinear refraction of the sample, if a medium with a negative

nonlinear refraction index and a thickness smaller than the diffraction length of the focused beam. This can be considered as a thin lens of variable focal length. Beginning far from the focus (Z<0), the beam irradiance is low and nonlinear refraction is negligible. In this condition, the measured transmittance remains constant (i.e., Z-independent). As the sample approaches the beam focus, irradiance increases, leading to self-lensing in the sample. A negative self-lens before the focal plane will tend to collimate the beam on the aperture in the far field, increasing the transmittance measured at the iris position [100].

After the focal plane, the same self-defocusing increases the beam divergence, leading to a widening of the beam at the aperture and thus reducing the measured transmittance. Far from focus (Z >0), again the nonlinear refraction is low resulting in a transmittance Z-independent. A transmittance maximum (peak), followed by a transmittance minimum (valley) is a Z-Scan signature of a negative nonlinearity. An inverse Z-Scan curve (i.e., a valley followed by a peak) characterizes a positive nonlinearity. Figure (2-5) depicts these two situations [100].

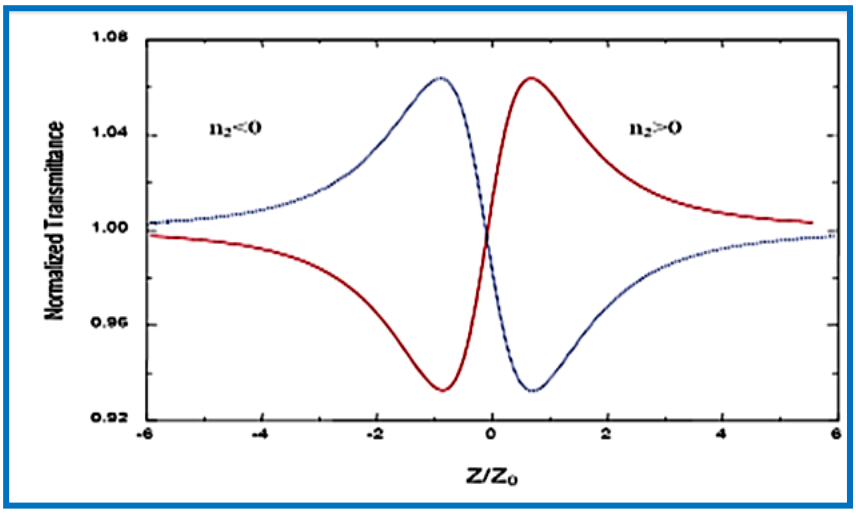

Figure (2-5): Calculated Z-Scan transmittance curves for nonlinearity[100].

The nonlinear refractive coefficient is calculated from the peak to valley difference of the normalized transmittance by the following formula [101]:

$$n_2 = \frac{\Delta\Phi_o}{I_o L_{eff} k} \quad (2\text{-}15)$$

Where, $k = 2\pi/\lambda$, (k) is wave number, (I_o)is the intensity at the focal spot and ($\Delta\Phi_o$)is the nonlinear phase shift [101]:

$$\Delta T_{p-v} = 0.406|\Delta\Phi_o| \quad (2\text{-}16)$$

(ΔT_{p-v}) the difference between the normalized peak and valley transmittances, (L_{eff}) is the effective length of the sample, determined from [102]:

$$L_{eff} = \frac{(1-exp^{-\alpha_o L})}{\alpha_o} \quad (2\text{-}17)$$

Where (L) is the sample length and(α_o)is linear absorption coefficient which is given as[102]:

$$\alpha_o = \frac{\ln(\frac{1}{T})}{t} \quad (2\text{-}18)$$

Where (T) is the transmittance, (t)is the cuvette thickness .The linear refractive index(n_o) obtained from equation [102]:

$$n_o = \frac{1}{T} + \left[\left(\frac{1}{T^2} - 1\right)\right]^{1/2} \quad (2\text{-}19)$$

The intensity at the focal spot is given by[98]:

$$I_o = \frac{2P_{peak}}{\pi {\omega_o}^2} \quad (2\text{-}20)$$

Is defined as the peak intensity within the sample at the focus,

Where(ω_o)is the beam radius at the focal point.

2.10.2 Open-aperture Z-Scan

An open-aperture Z-Scan analyzes the change in intensity of a beam in the far field at photo detector PD, which captures the full beam, as focused by lens (L)in Figure (2-6), in the far field at photo detector (PD), which captures the entire beam. The change in intensity is caused by two photon absorption in the sample S as it travels through the beam waist [103].

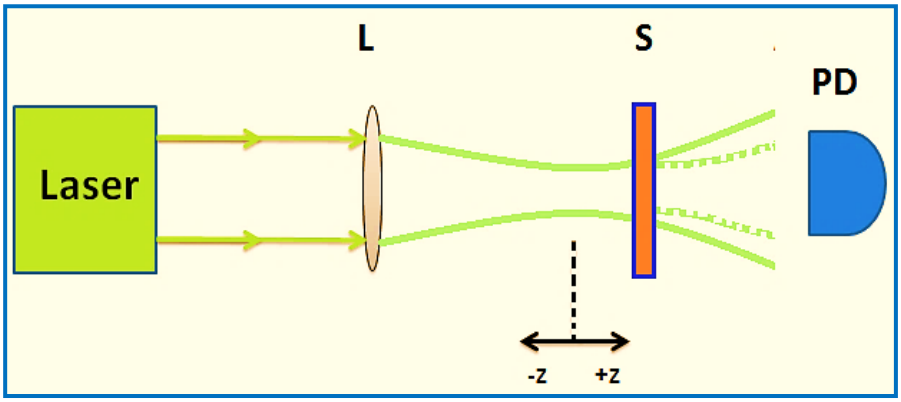

Figure (2-6): Open-aperture Z-Scan[103].

Clearly, even with nonlinear absorption, a Z-Scan with a fully open aperture is insensitive to nonlinear refraction (thin sample approximation). The Z-Scan traces with no aperture are expected to be symmetric with respect to the focus (Z = 0) where they have a minimum transmittance (e.g., two photon absorption)or maximum transmittance (e.g., saturation of absorption).In fact, the coefficients of nonlinear absorption can be easily calculated from such transmittance curves. Nonlinear absorption coefficient (β),can be easily calculated by using following equation [104]:

$$\beta = \frac{2\sqrt{2}\,T(z)}{I_o L_{eff}} \qquad (2\text{-}21)$$

Where T(z):The minimum value of normalized transmittance at the focal point, at (Z=0). It should be clear that the transmittance versus sample

position graph of such an open aperture Z-Scan should be symmetric around the focus as shown in Figure (2-7).

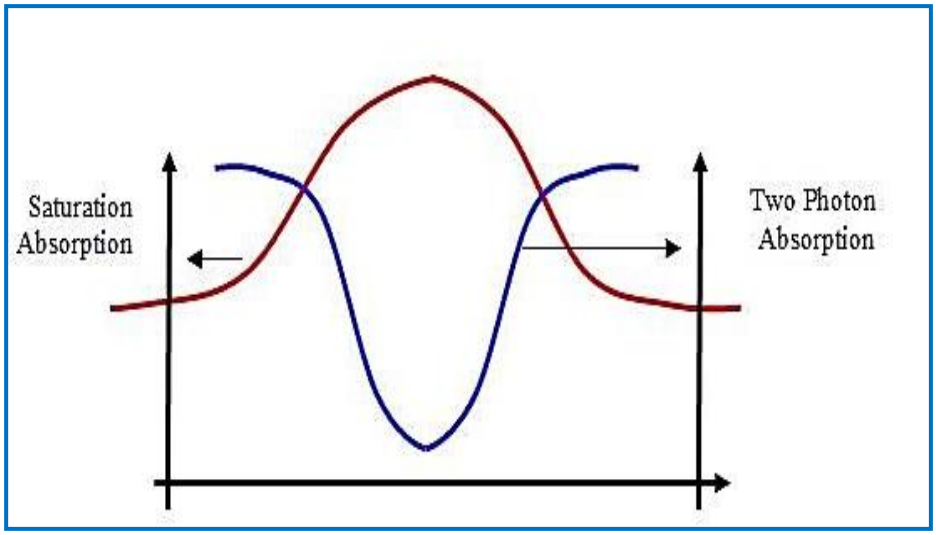

Figure (2-7): Open aperture Z-Scan curve[104].

2.10.3 Nonlinear Absorption and Nonlinear Refraction

The basic optical properties involved in the light matter interaction are absorption, which is defined by the absorption coefficient(α), and refraction, which is defined by the index of refraction (n). When the material is irradiated, the energy of the absorbed photons makes it possible for the transition from the ground state to the excited state .There is also a change in the refractive index when a material is placed in a strong electric field. In fact, the index of refraction becomes dependent on the intensity of the electric field. At high intensity, the refractive index is given by [105]:

$$n = n_o + n_2 I \qquad (2.22)$$

Where (n_2)is the nonlinear refractive coefficient related to the intensity. The absorption of the material is also intensity dependent given by [105]:

$$\alpha = \alpha_o + \beta I \qquad (2.23)$$

Where,(α_o) is the linear absorption coefficient and (β) is the nonlinear absorption coefficient related to the intensity. The coefficients (n), and (α) are related to the intensity of laser.

2.10.4 Saturable Light Absorption

A nonlinear process that can be associated with real (rather than virtual) energy levels and population changes in those levels is that of saturable absorption. This process occurred when the nonlinear absorption coefficient ($\beta < 0$), which can be appeared when a strong light absorption between two levels causes saturation (bleaching) of the corresponding electronic transition. The two levels involved surface resonance ground and excited state. On the other hand, this is a process in which a material can be highly absorbing at a specific wavelength when a low-intensity beam is incident upon the material, yet an extremely intense beam (at that same wavelength) will pass through the medium with little change in intensity [106].

2.10.5 Reverse Saturable absorption (RSA)

Reverse saturable absorption (RSA) is an excited state absorption process, manifested as a decrease in optical transmission with increase in incident optical intensity. RSA occurs when the excited state, which is populated by optical excitation, has an absorption cross-section larger than the ground state absorption cross-section [106], leading to a reduction in transmission under intense laser fields. RSA due to ESA is the dominant process leading to nonlinear absorption in organic materials.

2.10.6 Two Photon Absorption (TPA)

Two-photon absorption (TPA) is the simultaneous absorption of two photons of identical or different frequencies in order to excite a molecule from one state (usually the ground state) to a higher energy electronic state. The energy difference between the involved lower and upper states of the molecule is equal to the sum of the energies of the two photons, as in the case of a saturable absorber, is the process of two-photon absorption. This process occurred when the nonlinear absorption coefficient $\beta > 0$. This effect is shown in Figure (2-8). The two-photon transition rate can be significantly enhanced if an intermediate level (2) is located near the virtual level shown by the dashed line in Figure (2-8) [107].

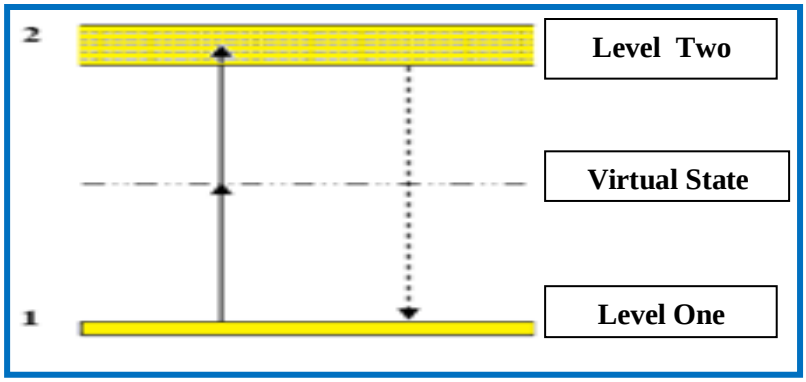

Figure (2-8): Energy levels for two-photon absorption process [107].

2.10.7 Kerr Effect

A nonlinear interaction of light in a medium related to the nonlinear electronic polarization, which can be described as modifying the refractive index. For high-intensity laser beams, the Kerr effect can create a local change in the refractive index that causes the laser material to act as a lens. This can result in self-focusing of laser beams[108].

2.10.8 Self-Focusing and Defocusing

A nonlinear process that causes a spatial variation of the laser intensity, in which an intense beam of light modifies the optical properties of a material medium in such a manner that the beam is caused to come to a focus within the material. The material acts as a positive lens, because the laser beam induces a refractive index variation within the material with a larger refractive index at the center of the beam than at its periphery. Self-focusing can be obtained when the nonlinear refractive index is positive in sign while self-defocusing it work to increase the divergence in the laser beam which leads to expand of the beam and thus leads to a decrease in transmittance and the material acts as a negative lens. Both self-focusing and self-defocusing materials will refract the light away from the optical sensor and thus act as an optical limiter. A self-defocusing material has the advantage of leading the light away from the beam axis and thus is regarded as self-protecting, in contrast to a self-focusing material which will suffer risk of damaging. On the other hand, a self-focusing material will be able to activate itself at lower energy input compared to a self-defocusing material [109].

2.11 Optical Power Limiting (OPL)

Optical limiting influences and devices are becoming more interesting in the field of non-linear optics and optoelectronics because of their special application possibility. Optical limiters are material or devices which are transparent to light at low intensities and gets opaque at higher intensities. Various approaches have been developed towards better optical limiting based on, e.g., electro-optical [110], magneto-optical [111], and all optical [112] mechanisms. The all-optical limiters rely on materials that exhibit one or more of the nonlinear optical mechanisms: Two-photon absorption (TPA), Excited State Absorption (ESA), Free

carrier absorption. Thermal defocusing and scattering, photorefraction, nonlinear refraction, induced scattering, Most of the above mentioned processes would give rise to the phenomenon of optical limiting, whereby a material limits the transmission of optical energy at high fluencies [113].

Optical limiters display a decreasing transmittance as a function of intensity or fluence, so that the potentially damaging high intensity radiation is effectively suppressed, while permitting high transmission at normal light intensities, thereby providing protection to sensitive optical components and devices against radiation-induced damage [114]. They can be used to protect laboratory researchers from high-intensity laser radiation, safeguard military personnel from being blinded by the enemy light sources, or protect components in the devices that make use of laser light.

Laser damage protection of eyes and sensitive components is not only a scientific subject but also a potential public safety issue nowadays, as lasers have become common in daily life: they are even being incorporated into toys. Significant progress has been made over recent decades in the development of optical limiters with large NLO response, which include small π-electron systems such as fullerenes, phthalocyanines, porphyrins, graphitic systems such as carbon black suspensions (CBS), single-walled and multiwalled carbon nanotubes(CNTs), inorganic nanoparticles and, metal complexes and clusters [115-119]. For over a decade now, the optical-limiting benchmark for broadband (wide spectrum) limiting has been held by CBS and CNT suspensions [115,116].

The rapid development of nanoscience and nanotechnology not only gave rise to new opportunities into the synthesis of optical limiting

materials, but also facilitated the research and design of practical optical limiters. Practical thin films with broadband optical-limiting characteristics can now be fabricated . These NLO materials are referred to as smart materials due to the fact that the sensing, processing and actuating functions required for optical limiting action are inherent in them which are otherwise separate in dynamic devices [120].

The ability to control the propagation and intensity of light in predetermined and predictable manner is one of the key challenges in the development of modern optical devices. Optical limiters are one of the most important types of devices used to control the amplitude of high intensity optical pulses. They have been demonstrated for use in pulse shaping and pulse compression, in addition to their potential use in the protection of human eyes and optical sensors from radiation damage. Desirable properties for optical limiting (OL) candidates include a high linear transmittance, a low limiting threshold, a broad spectral response and a large dynamic range [121].

In addition to the above mentioned processes, different mechanisms such as molecular re-orientation, photo induced scattering, photo refraction etc. can bring about optical limiting effect.

Optical limiting based on nonlinear absorption mechanisms (ESA, TPA, MPA etc) relies on the fact that the transmission of the nonlinear absorbing media decreases when the input laser intensity increases. Nonlinear absorber materials which possess large optical nonlinearity, fast response time, high linear transmittance and good optical transparency are extensively investigated for passive mode OPL applications.

This is because nonlinear absorption (NLA) renders the possibility to make devices that are transparent under non harmful conditions, but become opaque as the intensity exceeds some threshold [121]. The

principle behind this type of optical limiting is the intensity dependent nonlinear absorption.

2.11.1 Materials for Optical limiting

Varieties of materials are studied for optical limiting purposes based on different processes. Improved nonlinear materials with more sensitivity and less linear loss are being developed to incorporate them into optical systems and their ability to protect real sensors. More attention focuses around pulsed lasers in the visible and near infrared bands, in view of the importance and vulnerability the eye . In the UV-near IR transmission band, suspensions lead to optical limiting using scattering mechanism . Dyes lead to OL in selected portion of the visible band because of nonlinear absorption and refraction.

The most extensively studied materials are the macrocyclics including phthalocyanines and naphthalocyanines , porphyrins and fullerenes and their derivatives in which long-lived triplet excited state can be produced copiously. Liquid crystals are another class of materials studied in the visible to mid IR region via refraction and TPA [122]. Various other materials like, photorefractive materials, photonic band gap materials , nanomaterials and nanotubes, nonlinear absorbers doped in xerogels and sol-gel films, glasses , filters, organic/inorganic clusters, layered systems and bacteriorhodopsin are studied for their optical limiting properties.

List of Contents

List of Tables

List of Figures

List of Abbreviations

Abbreviation	*Meaning*
LED	Light Emitting Diode
AgNPs	Silver nano particles
Nd:YAG	Neodymium YAG laser
PLAL	Pulsed laser ablation
UV-Vis	Ultraviolet –visible spectroscopy
AFM	Atomic Force Microscope
LIF	Laser induced fluorescence
IR	Infrared radiation
R6G	Rhodamine 6G Dye
MO	Methyl Orange Dye
DW	Distilled water
TTL	Transistor – Transistor Logic
OL	optical limiting
NLO	Nonlinear optics
NLR	Nonlinear Refraction
NLA	Nonlinear Absorption
TPA	Two-photon absorption
ESA	Excited State Absorption
CNTs	carbon nanotubes
CBS	carbon black suspensions
SNR	Signal-to-Noise Ratio

List of Symbols

Symbol	*Meaning*
λ	Wavelength
I	Light Intensity
I_0	Incident Light Intensity
A	Absorbance
$\alpha_{\circ p}$	Linear absorption coefficient
L	Optical path length
R	Reflectivity
μ	Dipole moment
σ_a	Absorption cross section
T	Transmittance
n_2	Nonlinear refractive index
β	Nonlinear absorption coefficient
f	Frequency
D.C	Duty Cycle
t	Integration time
K_r	The radiative rate (k_r)
K_{nr}	Non-radiative rate (k_{nr})
τ	The lifetime
Φ	Quantum yield
$\Delta\Phi_\circ$	Nonlinear Phase Variation at the Focus
L_{eff}	Effective Length
ΔT_{p-v}	The Variance of the Aperture Transmittance
S	The Linear Transmittance of the Aperture
χ	Electric susceptibility tensor
r_a	Aperture Radius

w_a	Beam Radius at the Aperture
W	Weight
C_m	Molar concentration
M_w	Molecular Weight
(η)	Quantum efficiency

3.1 Introduction

This chapter shows the material chosen for the present investigation. The dyes were selected after making an inventory of dyes which located within the same ranges of sources available in the laboratory and the most common and used . The samples preparation include two dyes were studied; the first one is Rhodamine 6G dye solution in ethanol solvent, the second is Methyl orange dye solution in Distilled water solvent, synthesis of silver nanoparticles by Pulsed laser ablation (PLAL) ,in addition to nanomaterials prepared to dyes solution and test the solution before and after adding nanomaterials with noting any change.

It presents building a technological pathway by designing a special electronic circuit to keep the (Laser , LED) parameters under control. Also ,it connects the circuit to spectra academy device to test the samples and description of the measuring devices used to the present work .So, several samples tests were used including the absorption, transmission, fluorescence spectra measurement, Laser induced fluorescence(LIF), Z-scan technique ,and atomic force microscope measurement. These measurements were made at room temperature, and included a complete description of the equipment utilized in the present work.

3.2 Materials Chosen for the Present Study

3.2.1 Rhodamine 6G Dye is a synthetic organic compound available as a dark reddish purple, brown, or red crystalline solid [25].It belongs to xanthene family with molecular formula ($C_{28}H_{31}N_2O_3Cl$), molecular mass (479.02 g / mol) , solubility in Ethanol at (27 ºC) and the structural formula which is shown in the Figure (3-1), with the properties of dye shown in the Table (3-1).

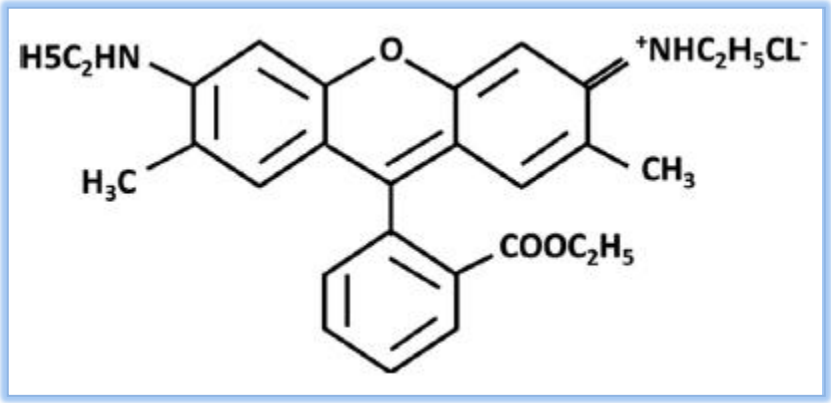

Fig: (3-1) Structure of Rhodamine 6G [25].

Table (3-1): properties of Rhodamine 6G dye

Chemical formula	($C_{28}H_{31}N_2O_3Cl$)
Appearance	red, crystalline solid
Molar mass	(479.02 g / mol)
Solvent	Ethanol
Absorption maximum	530 nm
Fluorescence maximum	556 nm

3.2.2 Methyl Orange (MO) Dye

It is a high intense coloured compound and also named as Acid Orange 52, Orange III, Helianthin, and 4- [(4-imethylamino) Phenylazo] benzenesulfonic acid sodium salt [123]. The structure of Methyl Orange is shown in the Figure (3-2), with the properties of Dye shown in the table (3-2). The molecular formula of MO dye is $C_{14}H_{14}N_3NaO_3S$ and a molar mass of (327.33g/mol).

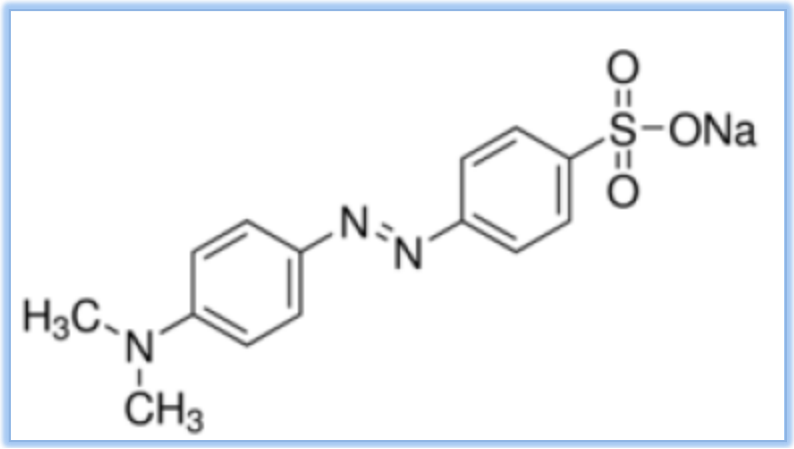

Fig:(3-2) Structure of Methyl Orange dye[123]

Table (3-2): Properties of Methyl Orange Dye

Chemical formula	$C_{14}H_{14}N_3NaO_3S$
Appearance	red, crystalline solid
Molar mass	327.33 gm/mol
Solvent	distilled water (DW)
Absorption wavelength	460 nm

3.3 Samples Preparation

3.3.1 Methyl orange dye and Rhodamine 6G dye solutions preparation

A concentration of ($1x10^{-3}$ M) Methyl orange dye solution in DW solvent and Rhodamine 6G dye in ethanol solvent was prepared, according to the following equation [83].

$$W = \frac{M_w \times V \times C}{1000} \quad \text{..... (3-1)}$$

Where

W : weight of the dissolved dye, (g), M_w : the molecular weight of the dye (g/mol),

V : the volume of the solvent (ml), and

C : the dye concentration (mol/l)

The prepared solution were dilution, according to the following ,equation [83]:-

$$C_1 \times V_1 = C_2 \times V_2 \quad \text{..... (3-2)}$$

where

C_1 : primary concentration,

C_2 : new concentration,

V_1 : the volume before dilution, and

V_2 : the volume after dilution

Methyl orange dye solution were prepared concentrations .The concentrations used are ($1x10^{-4}$,$5x10^{-5}$, $1x10^{-5}$, and $1x10^{-6}$) M.

Rhodamine 6G dye solution were prepared concentrations .The concentrations used are ($1x10^{-4}$, $3x10^{-4}$,$3x10^{-5}$, $5x10^{-5}$, and $7x10^{-5}$) M.

Figure (3-3 (a ,b ,c)) shows Methyl orange dye solution and Rhodamine 6G dye solution at different concentrations and dye on magnetic stirrer.

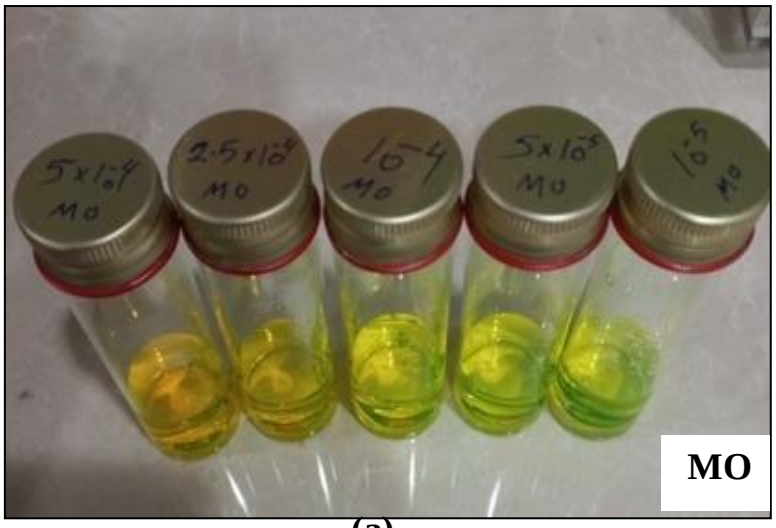

(a)

(b)

(c)

Fig (3-3): (a) Methyl Orange (MO) dye solution ,(b) Rhodamine 6G dye solution at different concentrations, (c) Dye on magnetic stirrer

3.3.2 Synthesis of Silver Nanoparticles (AgNPs)

A pure (99.995%) bar of silver metal was immersed in a glass beaker, containing distilled water (DW) ,after washing the metal by alcohol to remove contamination and any other impurities. Then silver plate target was irradiated by the Nd:YAG (1064 nm) laser, whose beam was focused on the bottom of the beaker on the target surface via a convex lens. The energy of the laser is (60 mJ) with a repetition frequency of (6 Hz) and (300) pulses, which is sufficient to ablate silver particles due to a laser shot.

Figure (3-4) (a) shows a photo of the Nd: YAG laser used and (b) illustrates the process of silver, ablation in liquid. This device was available at University of Babylon - College of Science for Women - Department of Laser Physics .

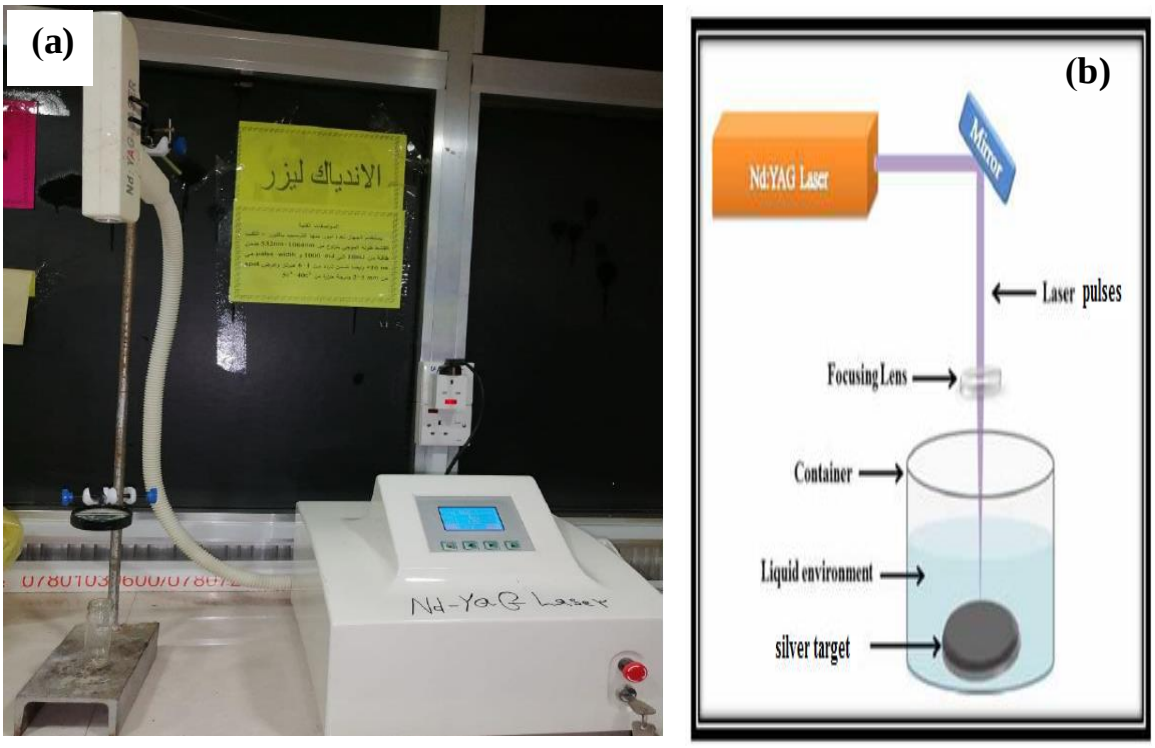

Figure (3-4): (a) Nd: YAG laser device . (b) Schematic diagram of the experimental PLAL setup.

3.4 Electronic Circuit Design

The dyes were selected after making an inventory of the dyes which located within the same absorption ranges of sources and available in the laboratory. There are commonly used in important application . The samples preparation include two dyes, the first is Rhodamine 6G dye solution in ethanol solvent, the second is Methyl orange dye solution in Distilled water solvent. In addition to nanomaterials prepared to dyes solution and test the solution before and after adding nanomaterials (Ag), by spectra academy device with noting any change in absorption and emission spectra. Building a technological pathway by designing a special electronic circuit (TTL) to keep the laser parameters under control and has the ability to :

-Changing the frequency at which the LED operates from (1Hz -200KHz)

-Duty cycle control for each frequency above from (10% to 100%)

-The freedom to change the parameters above allows to obtain direct and decisive results for each change in them on the performance of the dye in terms of an increase or decrease in the absorption or emission beams and thus for the efficiency of filling and unloading the energy levels included in the laser action in the dye)

-It is fed from an external circuit (9 volts or 12 volts) and has an output connected to the laser system (through which the laser frequency and pulse duration are controlled, which is the crucial point in knowing the best frequency and pulse duration when obtaining the best output parameters from the dye).The experiment set up of electronic circuit with spectra academy device can show in Figure (3-5).

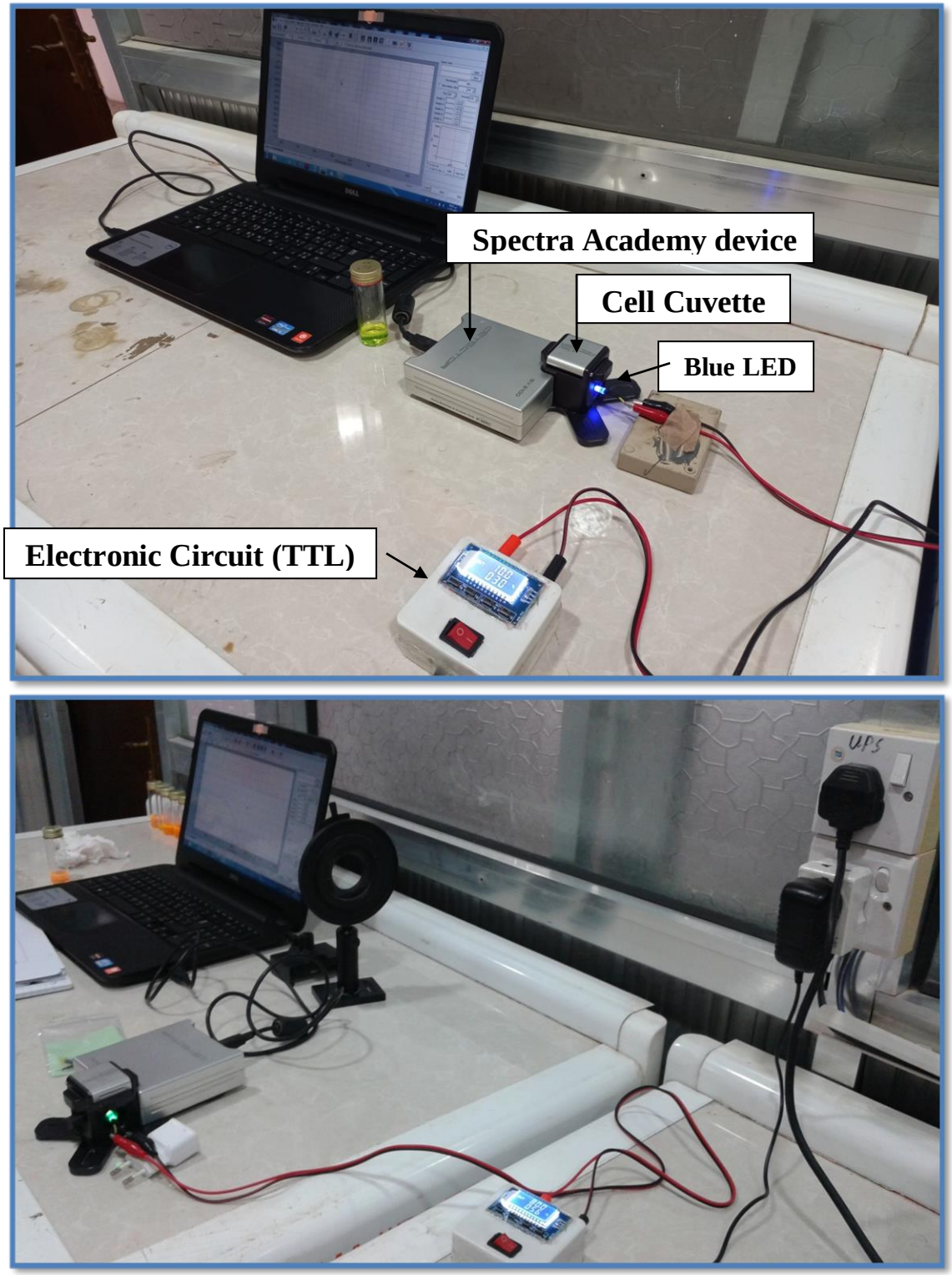

Figure (3-5): Experiment set up of Electronic Circuit with Spectra Academy device

3.5 Frequency/Duty Cycle Module Adjustable Square Wave Signal Generator NE555

Features:

– As a square wave signal generator, generates a square wave signal used for experimental development.

– Used to drive a stepper motor for generating a square wave drive signal.

– Generate adjustable pulse for MCU.

– Generate adjustable pulse, to control circuitry associated.

– Size: 31mm x 22mm

– Main chip: NE555

– Input Voltage: 5V-15V DC. When power supply is 5 V, the output current can be 15 mA around; when 12V power supply, the output current can 35 mA around.

– Input current: >=100 mA

– Output amplitude: 4.2V V-PP to 11.4V V-PP. (Different input voltage, the output amplitude will be different).

– Maximum output current: >=15mA (5V power supply, V-PP greater than 50%), >=35mA (12V power supply, V-PP greater than 50%).

– Output with LED indication (low level, LED will on; high level, LED will off; low frequency, the LED flashes) .

– The output duty cycle can fine-tune; duty cycle and frequency is not separately adjustable; adjusting the duty cycle will change the frequency.

The output frequency range is selectable:

– LF file: 1Hz ~ 50Hz

– IF file: 50Hz ~ 1 kHz

– High-frequency file: 1 kHz ~ 10 kHz

– HF file: 10 kHz ~ 200 kHz

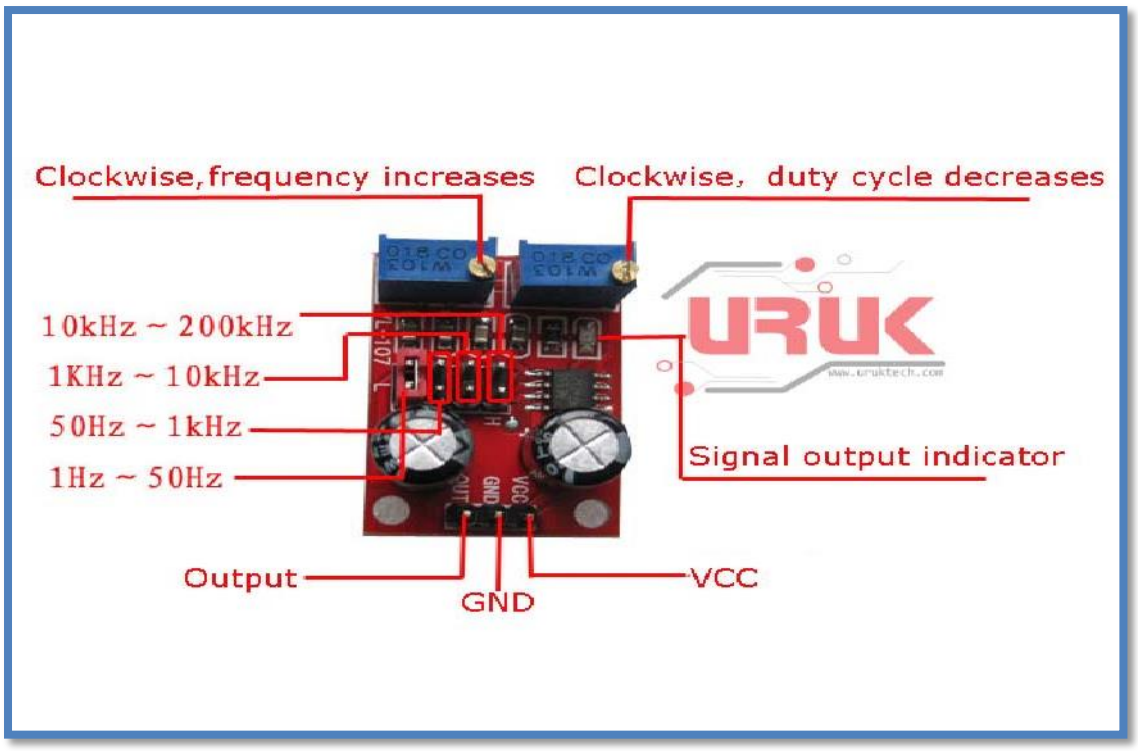

Figure (3-6): Schematic diagram of Electronic Circuit

3.6 The Optical Testing

3.6.1 Absorption Spectrometry

The absorption spectrum was, measured using (UV-Visible-Spectrophotometer) In this study, spectrometer was used the (CECIL CE 7200(ENGLAND)) this spectrometer, covers a wide area of the electro-magnetic spectrum from the, ultraviolet region to the near-infrared region. This device was available at University of Babylon - College of Science for Women -Department of Laser Physics .

Figure (3-7) shows a picture of the used device, with specification of the UV-Visible Spectrophotometer show in Table (3-3) and the device includes, two sources :

a- The deuterium lamp covers the region within, the wavelengths (360-190) nm.

b- The Tungsten Lamp, which covers a spectral distribution, within the region of the wavelengths (360-1100) nm.

Table (3-3) Specification of the UV-Visible Spectrophotometer

Wavelength range	190 nm – 1100 nm
Wavelength scan rate	Maximum 1000 nm /min
Detector	Silicon photodiode
Power requirements	220-240 V.AC

Figure (3-7): UV-Visible Spectrophotometer

3.6.2 Spectra Academy Device (UV-Visible Spectrometer)

Spectra Academy comprises of a spectrometer (detector), light source, cuvette holder, and other extensions. This miniature spectrometer can measure different modes (absorbance, transmittance, fluorescence, reflectance, and irradiance) by switching the light source location. CCD array installed detector uses a Czerny Turner monochromator, and easily interfaces with a PC via USB. Lamp and lens unified light source makes it possible to conduct the experiments without any external additional component required. However, using an external light source is also a possible by using the SAM connector for an external optical fiber ,figure (3-8) shows the Spectra Academy Device.

Some of applications of spectra academy device with different modes are : -

-Absorbance / Transmittance mode

Absorbance & Transmittance intensity measurement Property transition monitoring according to concentration DNA / RNA ratio analysis
Quantitative analysis
Photoelectric chemistry measurement

-Reflectance mode

Film thickness measurement Materials characterization Reflectometry

-Irradiance mode

Relative irradiance measurement
LED analysis using integrated sphere
Diverse light source measurement, using external optical fiber

-Fluorescence mode

Fluorescence measurement (biochemistry) Environmental material analysis (water, soil) Fluorescence spectrum measurement
(Additional light source needed for Fluorescence measurements)

To test the emission spectra of organic dyes , with using laser induced fluorescence method by shed a laser beam at specific wavelength on the sample and measure by spectra academy device

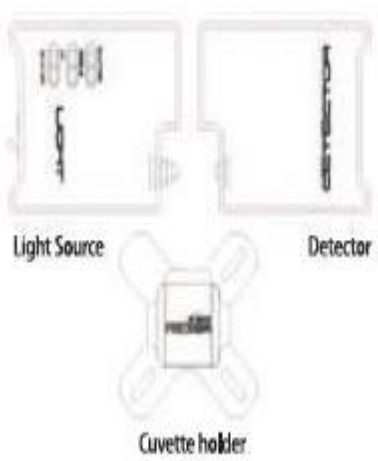

Figure (3-8): Spectra Academy Device

3.6.3 Photoluminescence Spectroscopy (PL)

Photoluminescence spectroscopy works in a non- contact mode. It is a non-destructive technique of examining the materials electronic structure. When light strikes a sample ,it gets absorbed by imparting its excess energy to the material by the phenomenon known as photo-excitation. One manner method in which sample dissipates this excess energy is through light emission, i.e., luminescence. In case of photo-excitation, this luminescence is known as photoluminescence , figure (3-9) shows the Photoluminescence Spectroscopy .

Figure (3-9) : Fluorescence Spectrometer

A spectrofluorometer is an analytical instrument used to measure and record the fluorescence of a sample. While recording the fluorescence, the excitation, emission or both wavelengths may be scanned. With additional accessories, variation of signal with time, temperature, concentration, polarization, or other variables may be monitored. This device was available at University of Babylon - College of Science for Women -Department of Laser Physics .

3.7 Atomic Force Microscope (AFM)

Atomic force microscope device is used in the field of nanotechnology to find out and draw the topography of surfaces with nano and macro dimensions. The atomic force microscope consists of a Cantilever at the end of a probe, consisting of a sharp tip used to scan, and the surface of the sample. This Cantilever is made of silicon nitride (Si_3N_4) with a radius of Within a few nanometers. Figure (3-10) shows a picture of the device that used and the Topography of the Ag NPs in 3-D . The test of the AFM carried out in the Ministry of Science and Technology.

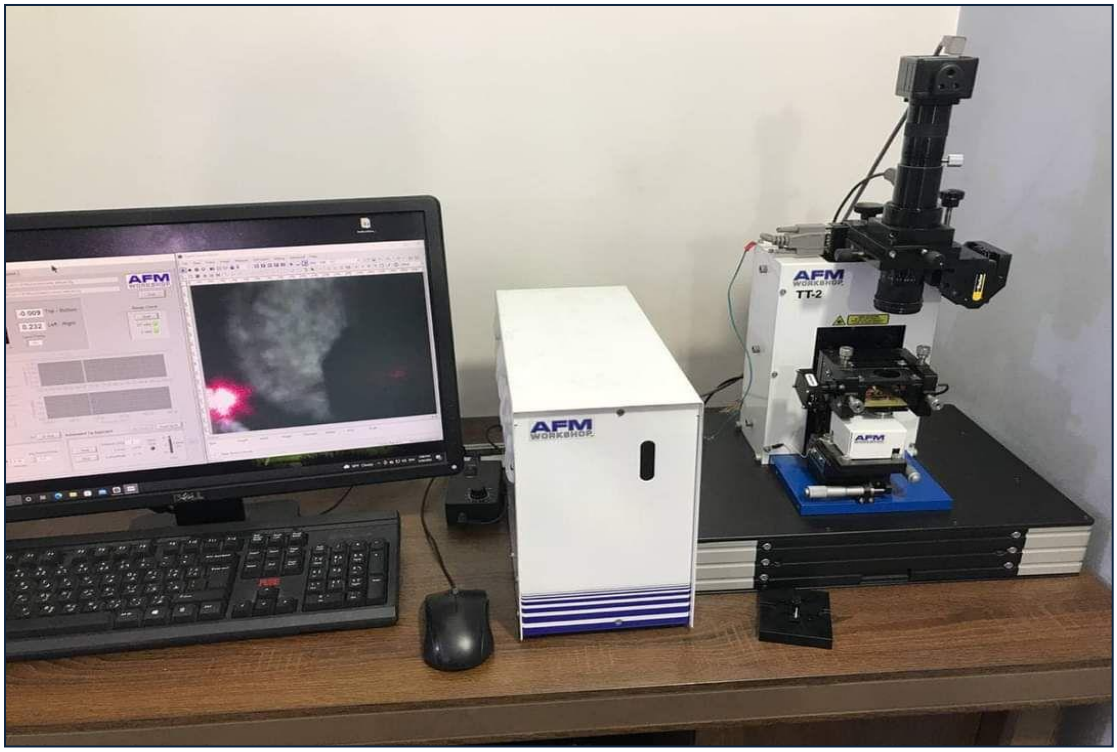

Figure (3-10): Atomic Force Microscopy Device

3.8 Z-scan Technique

Z-scan measurements were performed in the work of both two common parts, closed and open aperture. the closed-aperture z-scan is used to measure the nonlinear refractive index, while the open-aperture is used to measure the nonlinear absorption coefficient by using CW lasers. Figure (3-11(a ,b)) shows the pictures of the Z-scan system with diagram for Z-scan, This device was available at University of Babylon - College of Science for Women -Department of Laser Physics, this experience (ZSCAN-VER-8) is equipped by a company (MAHFANAVAR) and consists of :

-Lasers of continuous pattern (CW) and with different wavelengths (405 ,473 ,532 ,and 650) nm, power of lasers (1.49 ,4.35,11.56, and 5) mW respectively.

-Different optical filters to control the intensity of the laser beam that flowing onto the model.

-Optical lenses with different focal lengths (8.5, 5 cm)

-Beam Spliter to split the beam between the detectors

- The first detector is directly Beyond the beam bisector and equipped with a (1 mm) hole to detect nonlinear refraction and a post-beam mediator detector for the detection of nonlinear absorption

-A lens before the nonlinear absorption detector to collect the equilibrated laser beam on it

-Connecting wires to transmit signals from the detectors to the Controller, and in turn it is connected to a wire (USB) to a computer

-The controller device (contains two ports to connect to the detectors and the regulator) from through it we control by increasing or decreasing the

sensitivity and gain of the reagents according to the transmittance of the model.

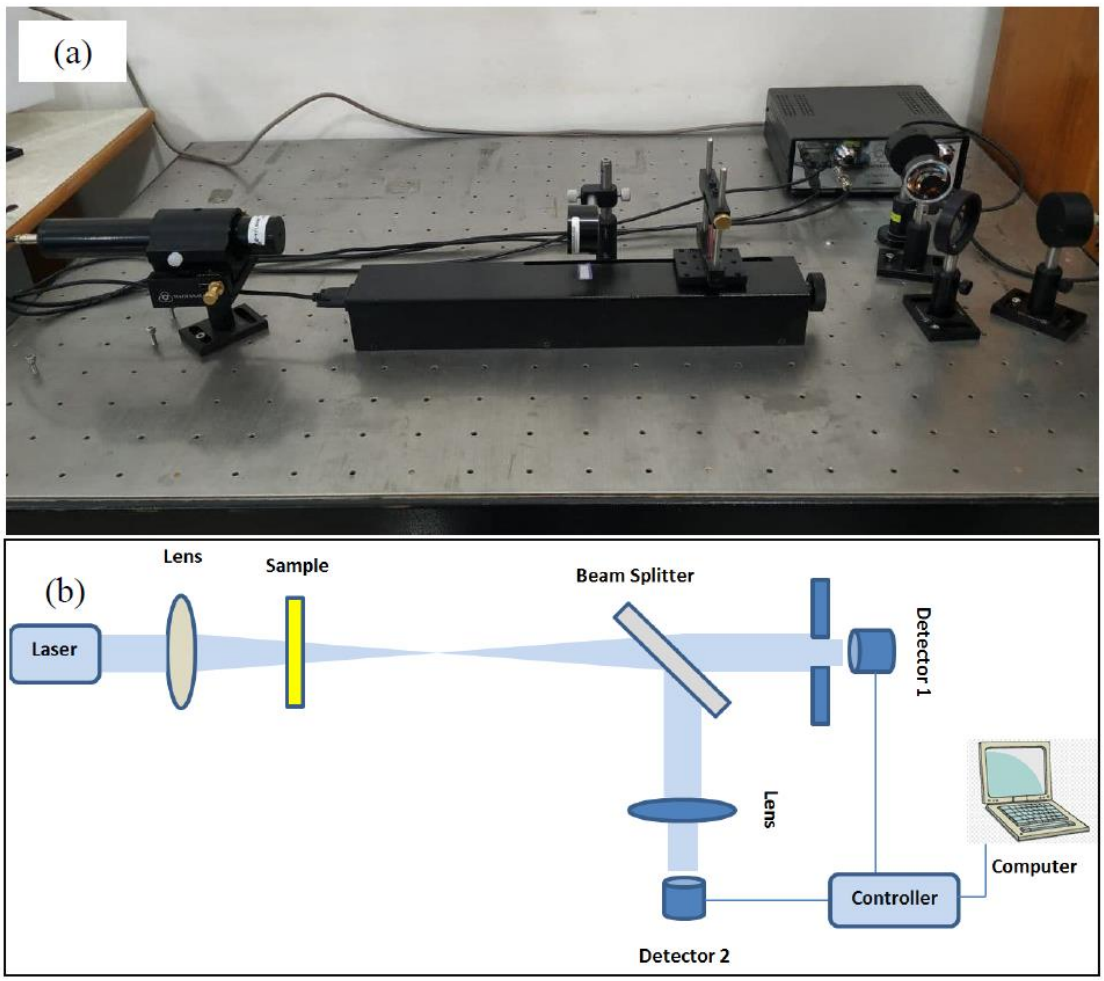

Figure (3-11): (a) Experimental setup for Z-scan, (b) Schematic diagram for Z-scan.

4.1 Introduction

This chapter deals with study of the absorption and fluorescence spectra and estimate the lifetime from some indicators are studied .The spectral characteristics of the dyes were studied by recording the absorption and fluorescence spectra by Spectra Academy device. The spectral parameters such as wavelength peak of absorption and fluorescence spectra .The full width at half maximum (FWHM) were calculated from the absorption spectra. The wavelength peaks of fluorescence, the full width at half maximum (FWHM) and area under the curve were calculated from the fluorescence spectra with analyze all data by using origin program ,also will added nano particles to dyes to enhancement the spectrum ,and this studies is important for the next step. The main body which is the most important step in the search , is designing a special electronic circuit (TTL) that we can control through it the frequency and pumping time and from the pumping time it is possible to know how much energy the level will needs .

Through this Electronic Circuit (TTL) will hope to achieve the following goals :-

1-The main objective is to estimate the lifetime from the indicators such as pumping time ,frequency ,intensity and integration time

2-Enable the material (dyes) to act as an optical switches or active medium

3-Increased pumping efficiency

4-Release a new transitions that did not appear in previous studies

5-From experience, we want to achieve the principle from adding nano particles to the dyes also, this addition can affect on the transition time

,through the spectral changes in absorption bands of this organic material these organic materials of dye are very efficient and have high fluorescence line .

4.2 Photophysical Properties of Laser Dyes

There are many approaches had been used to measure Absorption and Fluorescence Spectra. First one is UV-Vis spectrophotometer, Spectra Academy, and Photoluminescence Spectroscopy (PL) to get more accurate data .

4.2.1Absorption and Fluorescence Spectra of Rhodamine 6G and Methyl Orange (MO) Dyes

The Absorption and Fluorescence spectra of Rhodamine 6G and Methyl Orange (MO) Dye were studied in different concentrations. Following figures (4-1) and (4-2) show the absorption and fluorescence spectra of Rhodamine 6G dye (Rh6G) dissolved in Ethanol for different concentrations ($1x10^{-4}$, $3x10^{-4}$,$3x10^{-5}$, $5x10^{-5}$, and $7x10^{-5}$) M.

While figures (4-3) and (4-4), show the absorption and fluorescence spectra of Methyl Orange (MO) dye dissolved in distilled water for different concentrations ($1x10^{-4}$ M, ,$5x10^{-5}$ M, $1x10^{-5}$ M, and $1x10^{-6}$ M). In this work, the maximum peak of the absorption is (491) nm for Methyl Orange (MO) and (531) nm for Rh6G) and maximum peak of fluorescence spectra is (520.4 nm) for Methyl Orange (MO) Dye and (571.7) nm for Rh6G Dye.

It can observe the optical absorption spectra show two major absorption spectra regions, the Soret band at about (300-400nm) due to π-π^* transition and Q- band at 600-750nm region which is also due to π-π^* transitions . The Q- band is broader and split into two components with absorption peaks located at around 600 and 635nm respectively.

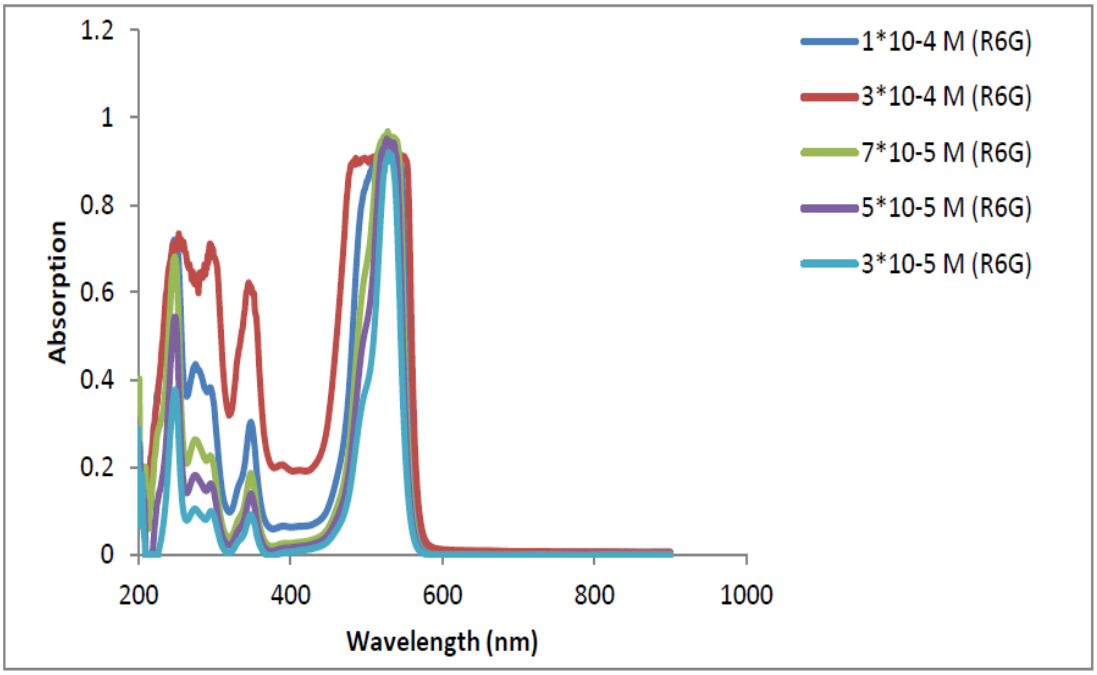

Figure (4-1) Absorption spectra of Rhodamine 6G Dye in different concentrations

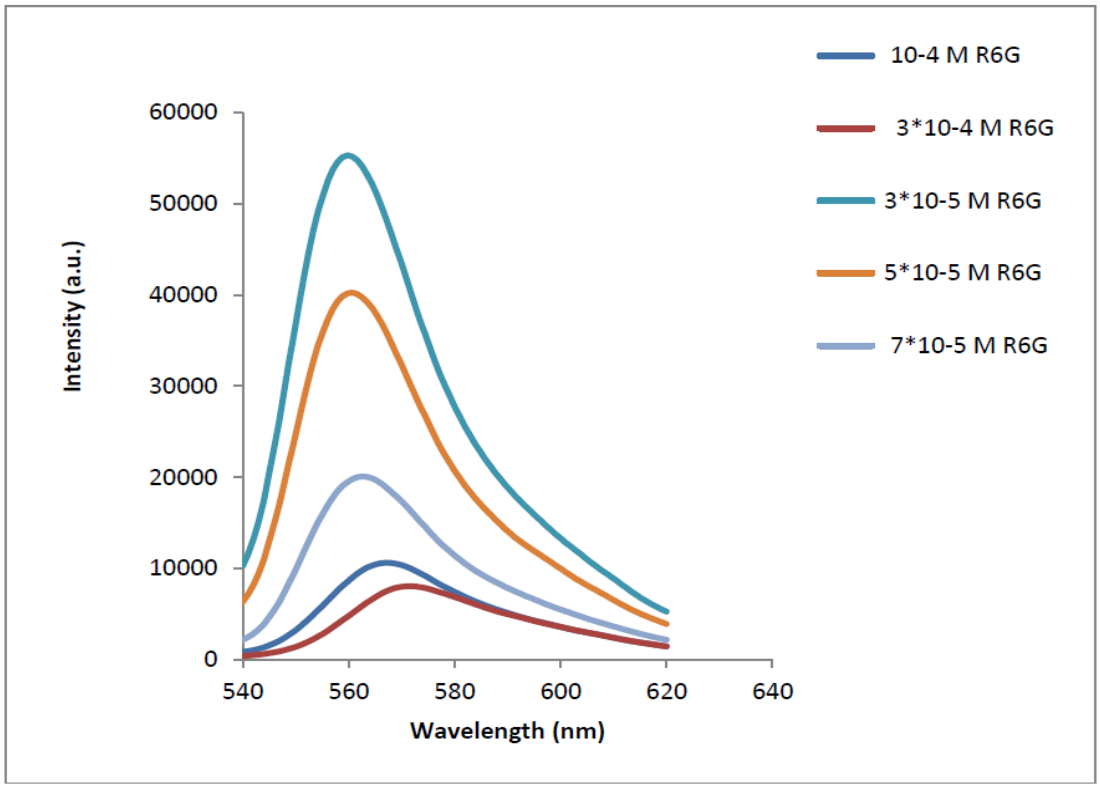

Figure (4-2) Fluorescence spectra of Rhodamine 6G Dye in different concentrations

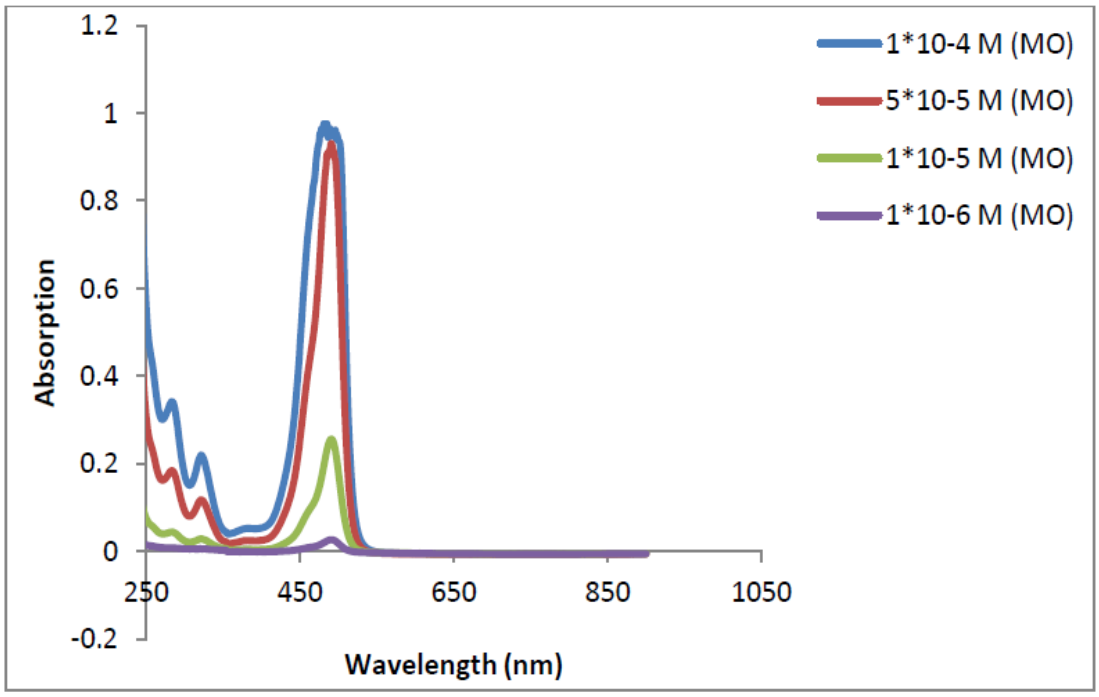

Fig. (4-3) Absorption spectra of Methyl Orange (MO) Dye in different concentrations

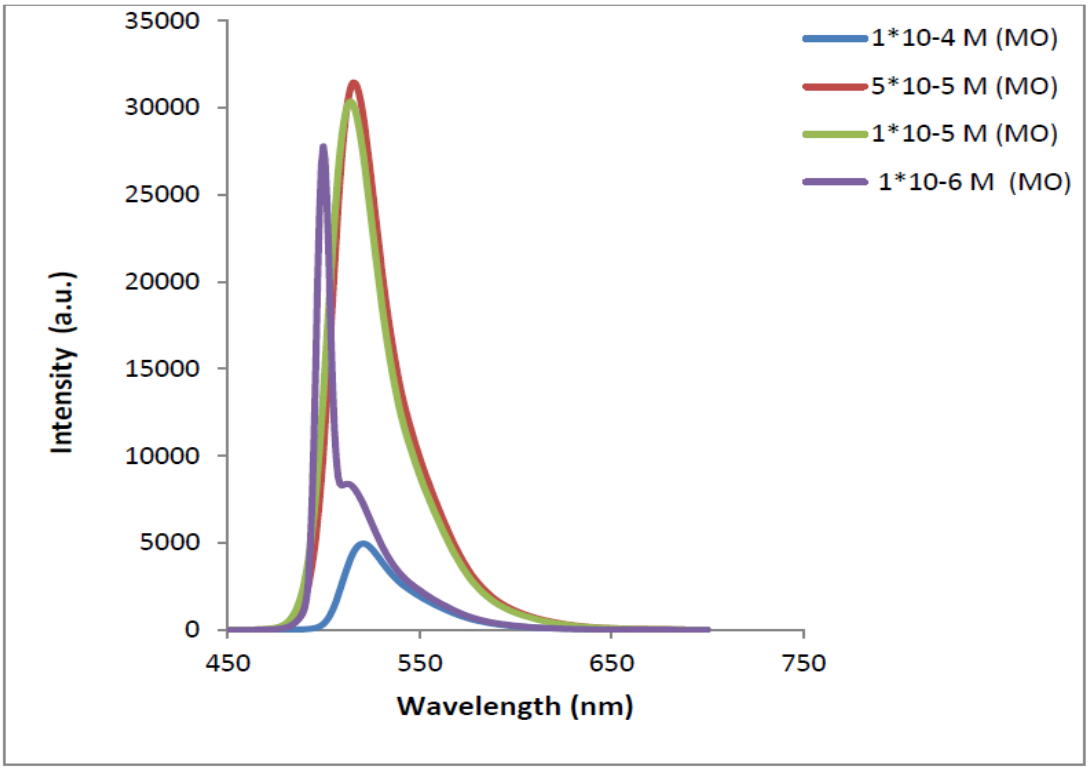

Fig (4-4) Fluorescence spectra of Methyl Orange (MO) Dye in different concentrations

Table (4-1) The Rhodamine 6G Dye with Different Concentrations without Nanomaterials

R6G Dye	λ_A(nm)	Absorption Intensity	λ_f (nm)	Fluorescence Intensity
3×10^{-4} M	531	0.92	571.7	8042.9
1×10^{-4} M	529	0.91	567.1	10614.1
7×10^{-5} M	528	0.96	562.5	20096.8
5×10^{-5} M	527	0.95	560.7	40259.8
3×10^{-5} M	529	0.91	559.8	55327.2

Table (4-2) The Methyl Orange (MO) Dye with Different Concentrations without Nanomaterials

MO Dye	λ_A(nm)	Absorption Intensity	λ_f (nm)	Fluorescence Intensity
1×10^{-4} M	485	0.97	520.4	4961
5×10^{-5} M	490	0.92	515.4	31463.7
1×10^{-5} M	491	0.25	514.4	30364.4
1×10^{-6} M	491	0.02	499.8	2779.8

From figures (4-1 and 4-2), it is clear that increasing the concentration of dyes lead to increase the absorption intensity and lead to lowering the fluorescence intensity in R6G dye as shown in table (4-1) , they have a red shift only at concentrations (1×10^{-4} M and 3×10^{-4} M) for Rh6G dye. This is because the high concentration of dye , due to red shift that happened because increasing the concentration ,lead to increases the opportunity to form dimmers that are pairs of dye molecules and formation of excimers (excited dimmers) at high concentrations.

On the other hand, figures (4-3 and 4-4), explain that increasing the concentration of dyes led to increase the absorption intensity while the maximum peak unchanged for Methyl Orange (MO) Dye, they had maximums fluorescence intensity at concentrations (1×10^{-5} M,5×10^{-5} M) for MO dye and minimum fluorescence intensity at concentrations (1×10^{-4} M ,1×10^{-6} M) as shown in table (4-2).

Also, there is increase in the fluorescence intensity when the concentration of dye increase ,but this increase does not continue at the high concentration (1×10^{-4} M)MO as the fluorescence intensity will decreases at highest concentration because of the effect of dimmers formation (molecular aggregation) of dye molecules which leads to restrain the fluorescence intensity ,because there is a damping in the emission spectrum and in this case the rate of non-radiative decay increases, that mean these aggregation lead to decrease in the emission spectrum ,that is at low concentration (1×10^{-5} M ,5×10^{-5} M) MO will be the fluorescence intensity is the best possible.

4.2.2 The Measurement of Silver (Ag) Nanoparticles By Using AFM Analysis

Silver Ag nanoparticles was studied by AFM analysis to determine size of nanoparticles .It was done by putting a drop of solution was dried on glass plate .The atomic force microscope is perfect for quantitatively measuring the surface coarseness in the nanoscale range and for seeing the surface nano-texture on many different kinds of material surfaces by using this technique to measured the particles size of silver Ag nanoparticles . The particle size disruption histogram of Silver (Ag) nanoparticles and a topography of AgNPs in 3D image of nanoparticles shows in figure (4-5) with The average particle size obtain from the corresponding diameter distribution was about 37 nm .

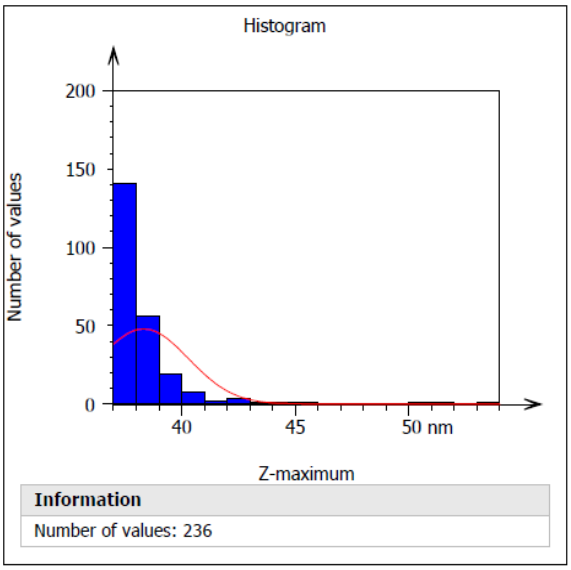

Statistical summary					
Parameters	Unit	Mean	Std dev	Min	Max
Projected area	nm²	563.1	5168	1.081	64808
Z-maximum	nm	38.34	1.965	37.09	53.01

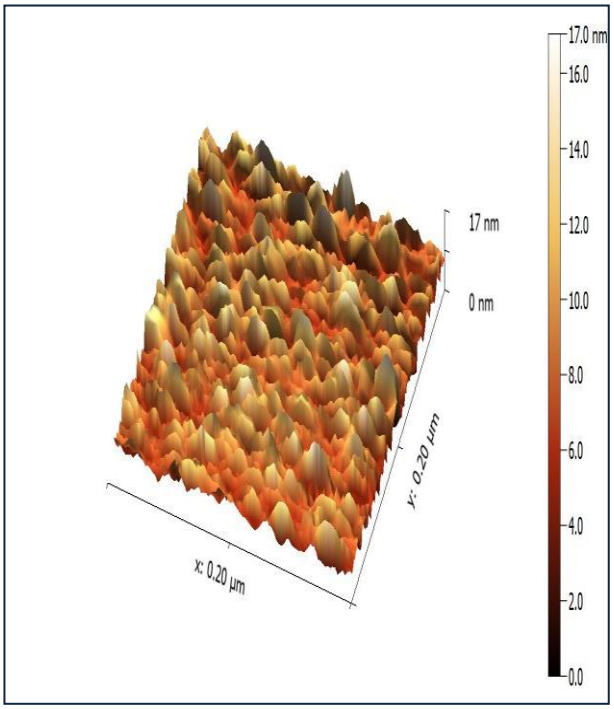

(a) **(b)**

Fig (4-5) (a) Particle size distribution histogram of Silver (Ag) nanoparticles from atomic force microscope (AFM) analysis (b) A Topography of AgNPs in 3D image of nanoparticles

4.2.3 Absorption and Fluorescence Spectra of (MO) Dye with Added Silver (Ag) Nanoparticles

Selected two concentration of Methyl Orange (MO) Dye, which was (1×10^{-5} M and 1×10^{-6} M) with (2mL) of AgNps solution. A different amounts of nanoparticles with each dye according to the response of each dye with each nanoparticles type. Absorption spectra of MO dye, that measured by using UV-Vis spectrophotometer and fluorescence spectra of MO dye are measured using Photoluminescence Spectroscopy (PL) at an excitation wavelength (500 nm).

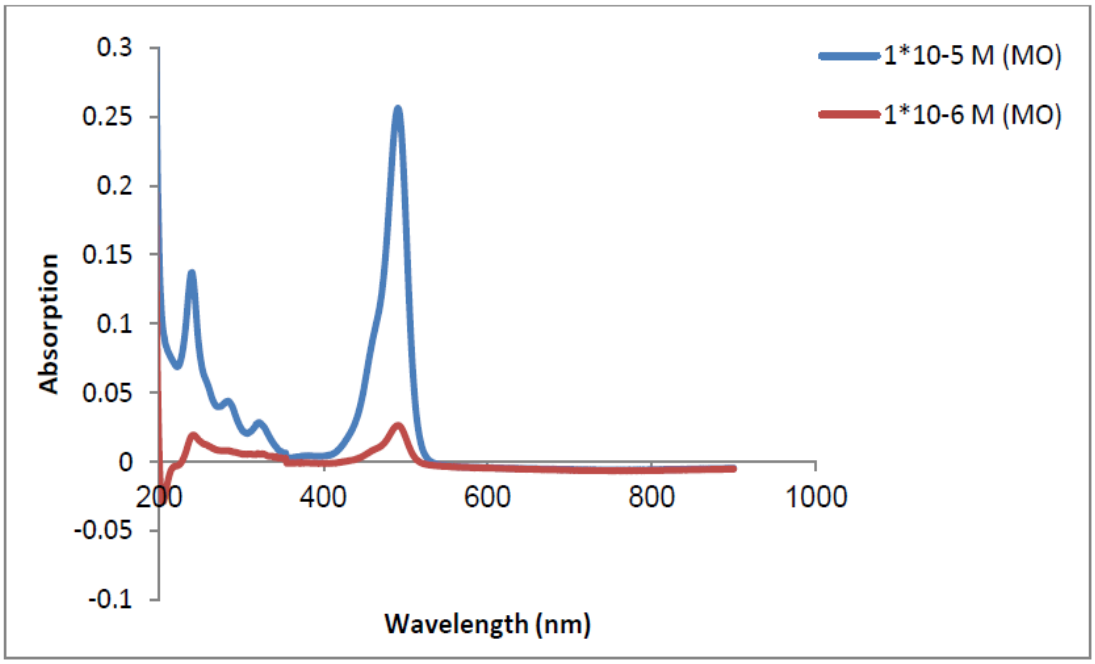

Figure (4-6) Absorption spectra of Methyl Orange (MO) Dye in different concentrations without Ag Nanoparticles

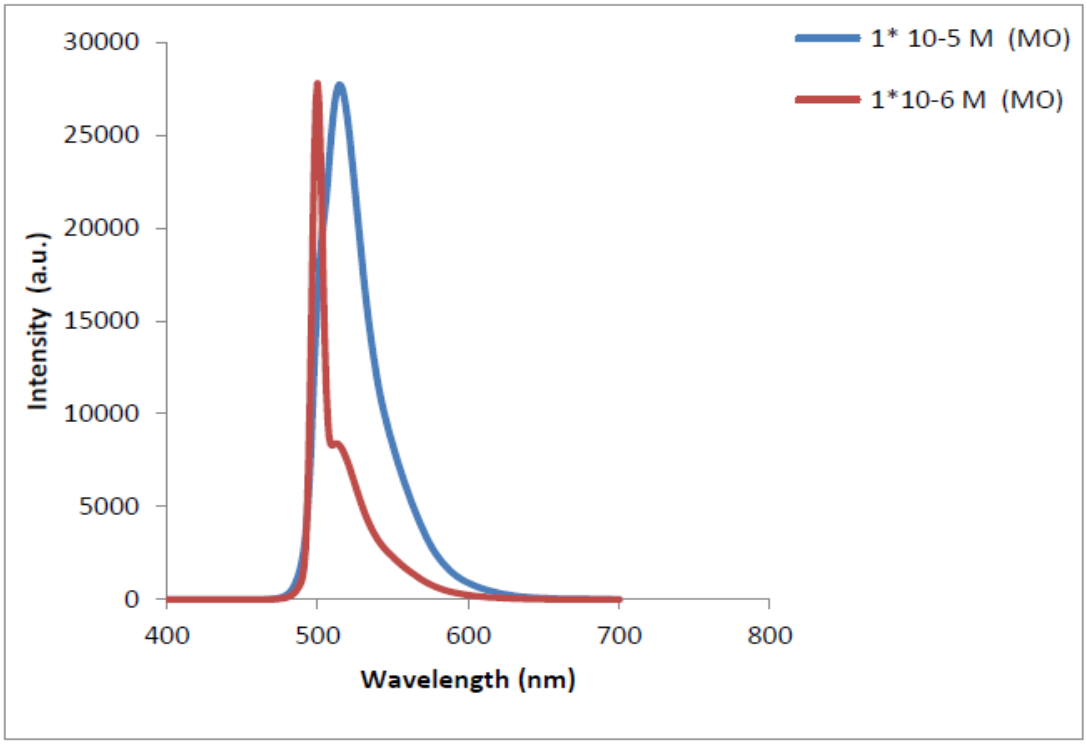

Fig (4-7) Fluorescence spectra of Methyl Orange (MO) Dye in different concentrations without Ag Nanoparticles

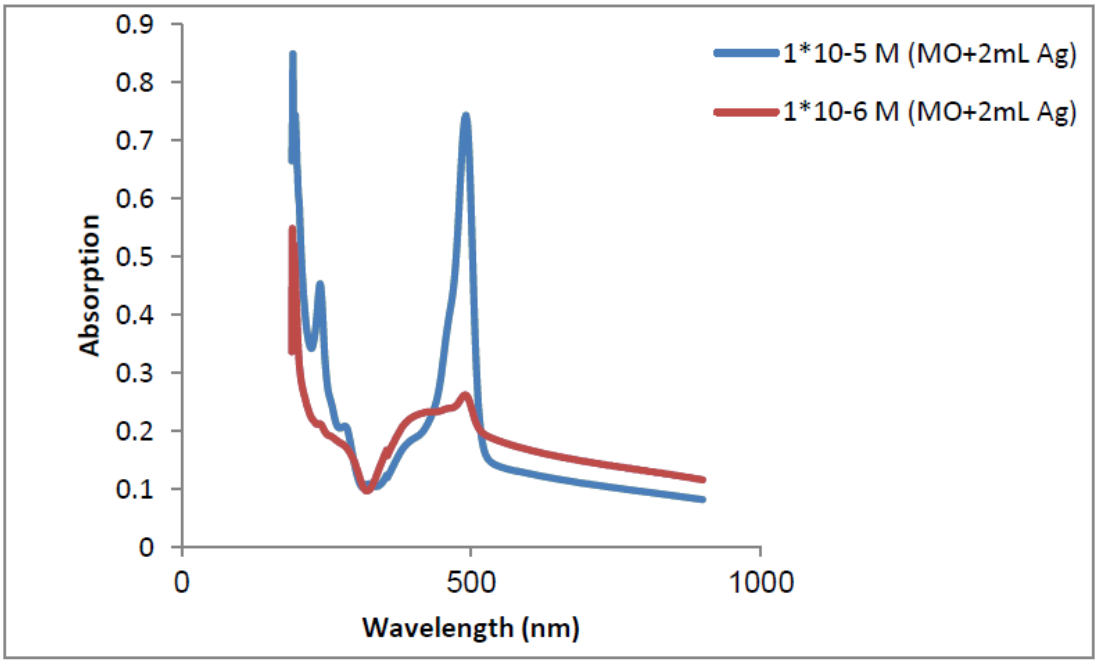

Fig (4-8) Absorption spectra of Methyl Orange (MO) Dye with Ag Nanoparticles

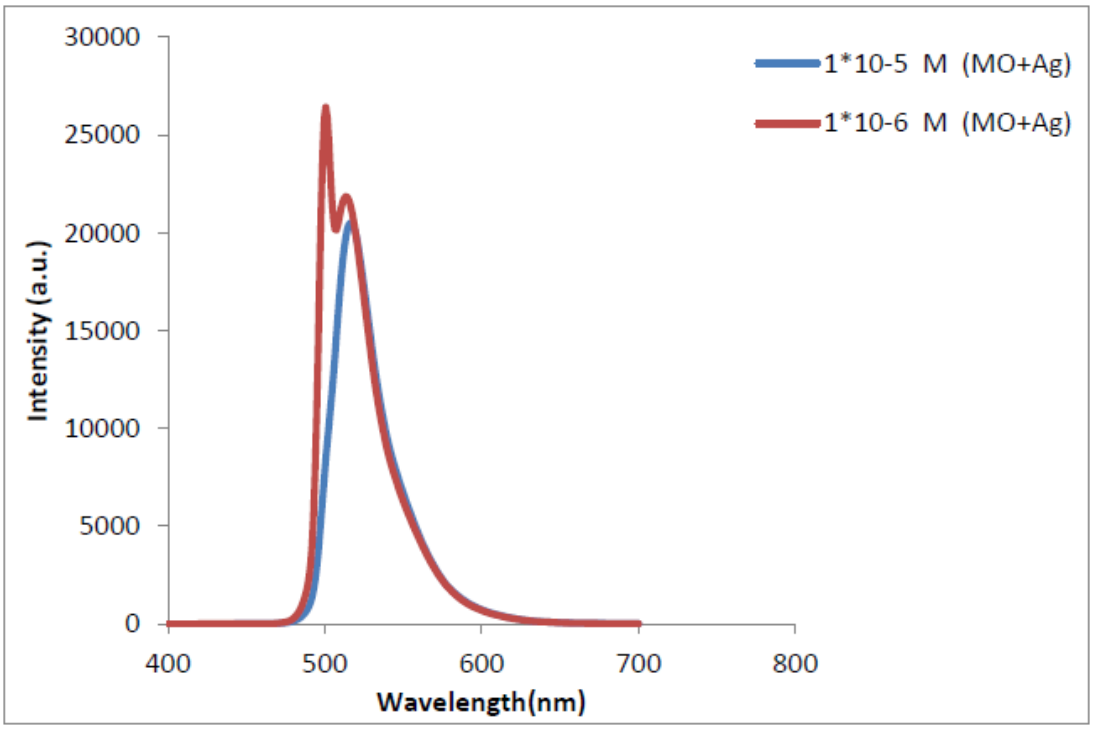

Fig (4-9) Fluorescence spectra of Methyl Orange (MO) Dye with Ag Nanoparticles

Figures (4-6) and (4-7), shows the absorption and fluorescence spectra of Methyl Orange (MO) Dye without Ag nanoparticles and figures (4-8) and (4-9) shows the absorption and fluorescence spectra of Methyl Orange (MO) Dye with Ag nanoparticles. Also note from Adding Ag nanoparticles to the (MO) Dye at concentration (1×10^{-5} M and 1×10^{-6} M) had led to increase in absorption intensity and quench the fluorescence intensity of these dye.

Adding AgNPs to the dye solution may cause either enhancement or quenching of the fluorescence intensity of the dye, depending on the distance between the dye molecules and the metal surface.

The enhancement of the fluorescence spectra can be from either local field enhancement of surface plasmon or from high scattering of electromagnetic field by dielectric nanoparticles. The quenching of the

fluorescence spectra can be from electron transfer (AgNps) nanoparticles), or from Förster Resonance Energy Transfer (FRET) or other non-radiative energy transfer (Silver nanoparticles)

When metallic NPs are in close proximity to fluorophores, quenching of the luminescence occurs because the non-radiative decay of the excited molecules will increase due to energy transfer from the dye molecules to the AgNPs, whereas when metallic NPs are located at a greater distance, enhancement of the luminescence is observed due to a decrease in non-radiative decay .

4.3 Solvent Effect On Absorption and Fluorescence Spectra of Methyl Orange (MO) Dye

Solvent effects play a key role in many chemical and physical processes in solutions , we study the effect of solvent on spectra of Methyl orange (MO) dye at the dye concentration (1×10^{-5} M) has been prepared and dissolved in water and ethanol for comparison. Figure (4-10) shows the spectra of the absorption of the MO dye dissolved in water and ethanol, and it can be see the effect of solvent on the spectral properties of dyes.

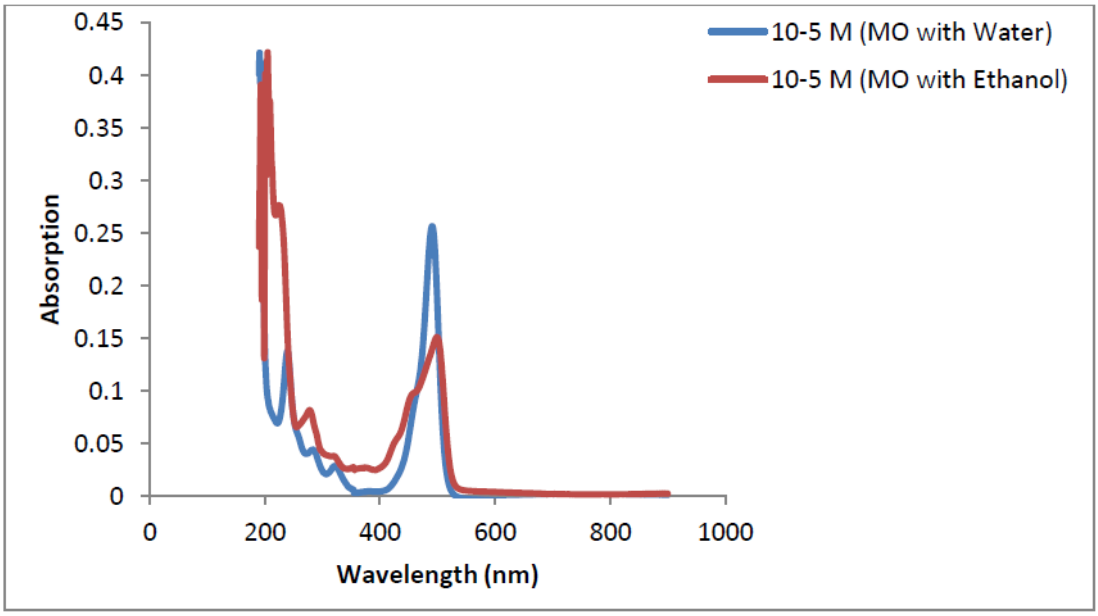

Figure (4-10) The Absorption spectra of pure MO dye dissolved in Water and Ethanol

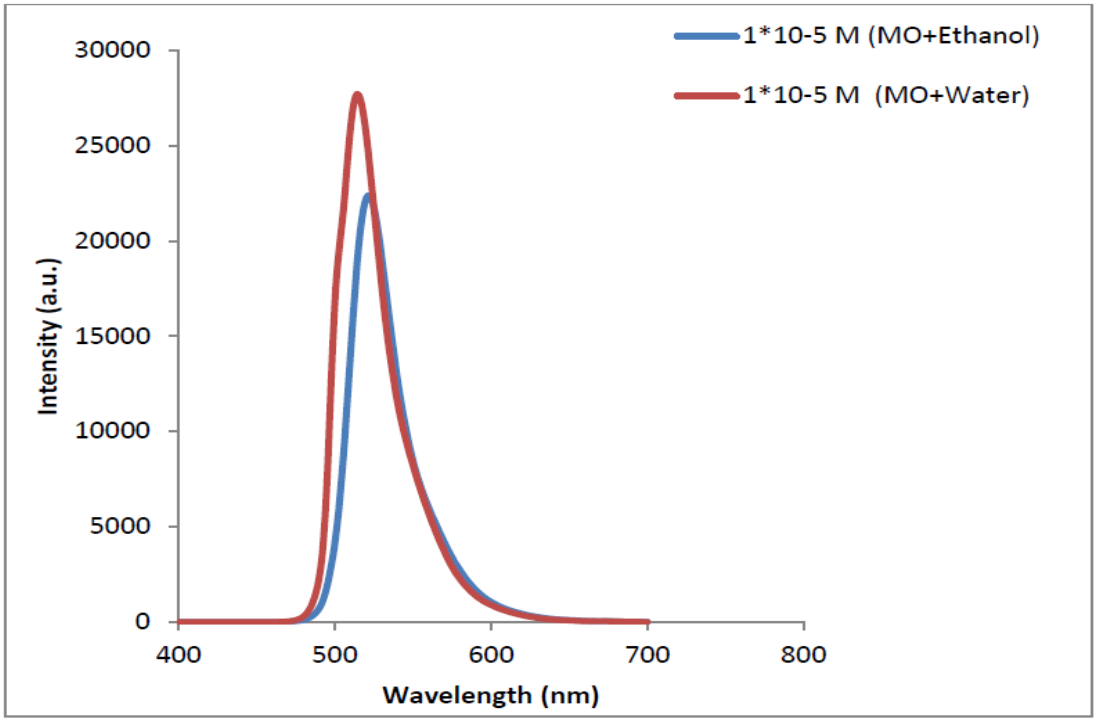

Figure (4-11) The Fluorescence spectra of pure MO dye dissolved in Water and Ethanol

And to clarify the effect of the medium (the solvent) on the spectral properties of the dye dissolved in both water solvent and ethanol, the absorption and fluorescence spectra of both solvents were compared, as shown in Table (4-3). The reason for the differences in the absorption

spectra of the dye for both solvents ,it is known that both solvents, is polar .Note that the polarity of water is approx (80) and ethanol is (25).

This could be due to the fact that the polarity of water is much higher than that of ethanol and also that water has the potential to bond its molecules and the formation of hydrogen bonds allows more bonds with dye molecules, which can change the order of the energy levels of the dye molecule.

The form of absorption peak MO clearly affected as the solvent using water leads to slightly shift the absorption curve toward the long wavelengths side relative to the absorbance curve of the dye dissolved in ethanol. This shift indicates that the energy value of the ground state level changed due to the polarity of the solvent . In general, not only the polarity of the solvent that can affect the linear properties of the solute but also the other properties of the solvent such as the ability of the solvent of denoting and accepting a hydrogen bond.

Table (4-3) Comparison between the Absorption and Fluorescence spectra properties of solution of MO dye dissolved in ethanol and water at Concentration (1×10^{-5} M)

Concentration	**(1×10^{-5} M) MO Dye**	
λ_A max (nm)	Water	491 nm
	Ethanol	499 nm
Absorption Intensity	Water	0. 25
	Ethanol	0. 15
λ_f max (nm)	Water	514.5 nm
	Ethanol	521.4 nm
Fluorescence Intensity	Water	27720.9
	Ethanol	22396.7

4.5 The Measurements of Absorption and Fluorescence Spectra of the Dyes (R6G , MO) by using Spectra Academy device

1- Absorption Spectra measurement for (R6G,MO) dyes by using Spectra Academy device

The spectra academy device using to measured the absorption spectra of the R6G dye dissolved in ethanol for different concentrations (10^{-4}, 3×10^{-4} ,3×10^{-5} ,5×10^{-5}) M as shown in figure (4-16) .Also measured the absorption spectra of the MO dye dissolved in distilled water for different concentrations ($3x10^{-4}$ M, $1x10^{-4}$ M ,$5x10^{-5}$ M, $1x10^{-5}$ M, and $1x10^{-6}$ M) with and without AgNPs as shown in figures (4-17) and (4-18). The stable (best) spectra observed at low concentrations, because there is saturation at high concentrations that happened because formation of excimers (excited dimmers) at high concentrations as shown in figures .

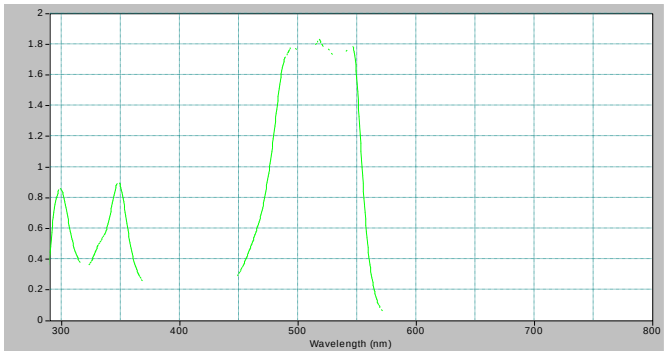

(10^{-4} M) R6G

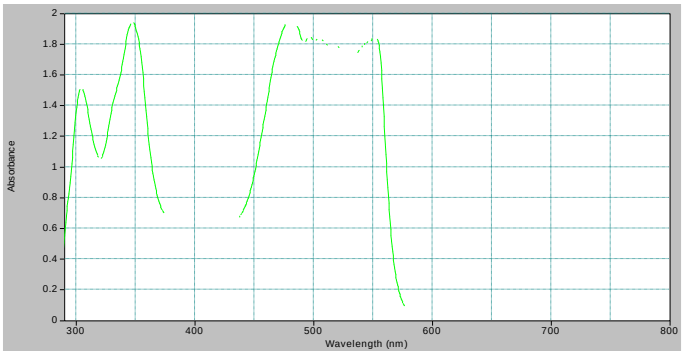

(3×10^{-4} M) R6G

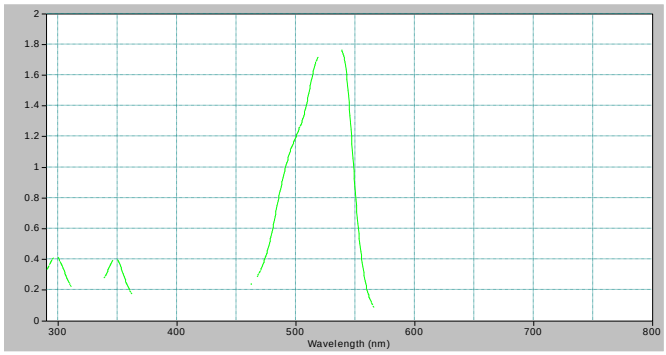

(3×10^{-5} M) R6G

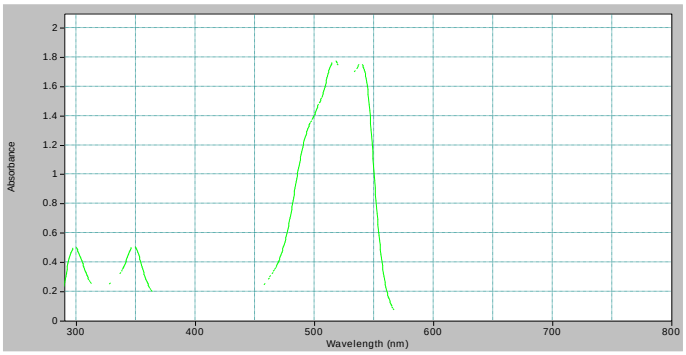

(5×10^{-5} M) R6G

Fig (4-16) Absorption Spectra of R6G Dye at concentrations (10^{-4}, 3×10^{-4}, 3×10^{-5} ,5×10^{-5}) M by using Spectra Academy device

2- Absorption Spectra for MO Dye by using Spectra Academy device

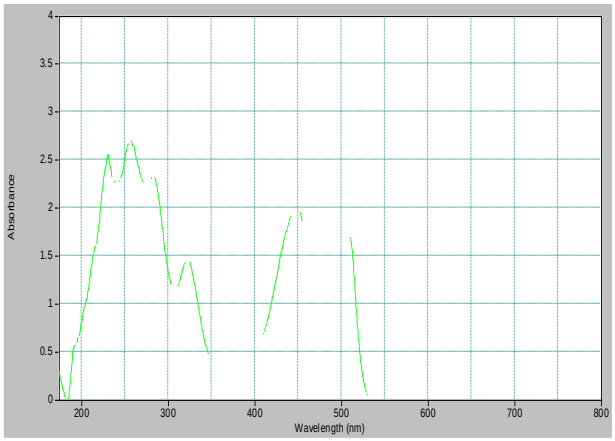

(3×10^{-4} M pure MO in Water)

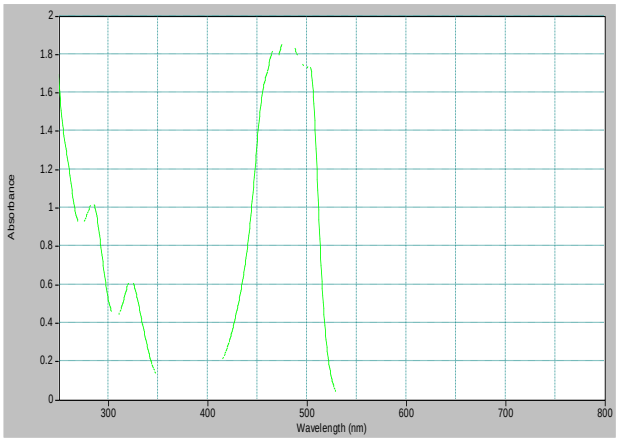

(1×10^{-4} M pure MO in Water)

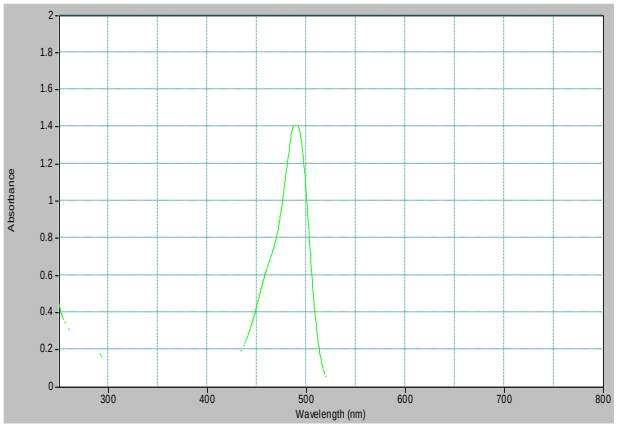

(5×10^{-5} M pure MO in Water)

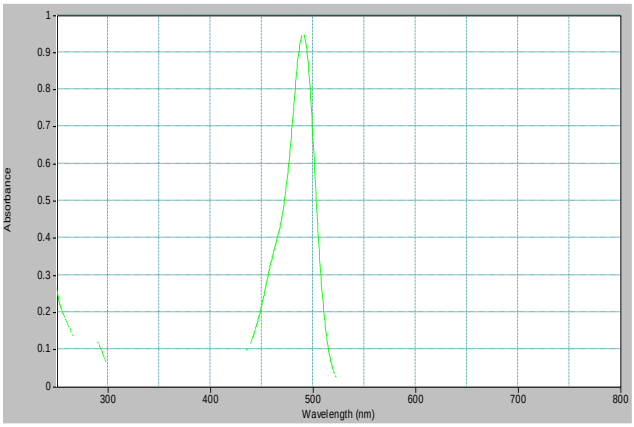

(1×10^{-5} M Pure MO in Water)

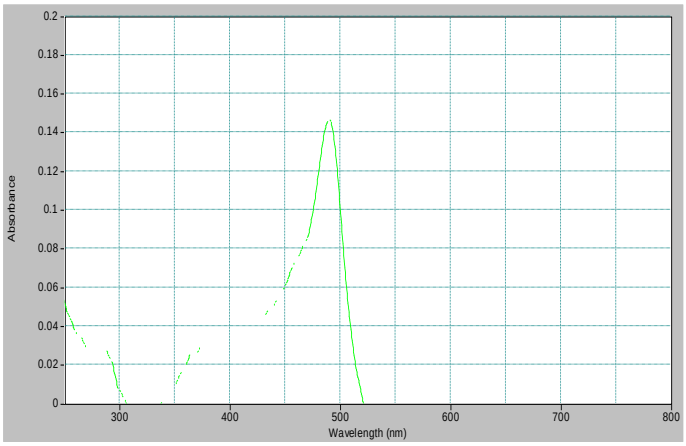

(1×10^{-6} M Pure MO in Water)

Fig (4-17) Absorption Spectra of MO Dye at concentrations ($3x10^{-4}$ M, $1x10^{-4}$ M ,$5x10^{-5}$ M, $1x10^{-5}$ M, and $1x10^{-6}$ M) by using Spectra Academy device

3-Absorption Spectra for MO Dye with added Ag nanoparticles by using Spectra Academy device

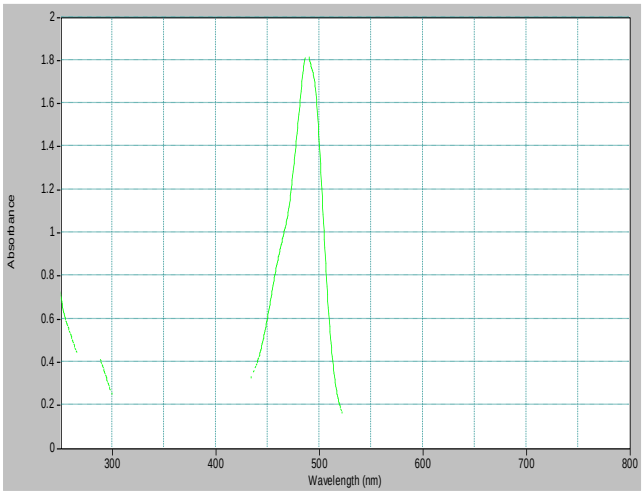

(1×10^{-5} M (MO+2mL Ag) in Water)

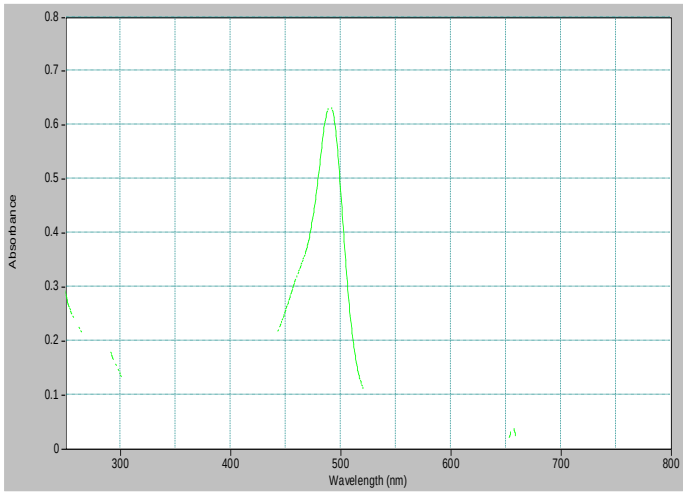

(1×10^{-6} M (MO+2mL Ag) in Water)

Figure (4-18) Absorption Spectra of MO Dye with AgNPs at concentrations ($5x10^{-5}$ M, $1x10^{-6}$) M

4-Fluorescence Spectra for R6G Dye measured by using LIF technique in spectra academy device

The fluorescence spectra of the R6G dye dissolved in ethanol for different concentrations (10^{-4}, 3×10^{-4} ,5×10^{-4},7×10^{-4}, 3×10^{-5} ,5×10^{-5},7×10^{-5})M by using LIF technique with (λ=405 Blue , λ=532 Green , λ=650 Red)lasers as pump source of dyes as shown in figure (4-19). There is the best emission at pumping by green laser (λ=532) because R6G dye have emission peak located inside this region .But there is no peak emission when pumping by red laser (λ=650) and can see just the peak of source (Red laser) because it is the dye's is outside the absorption region. there is saturation in high concentration that happened because formation of excimers (excited dimmers) at high concentrations.

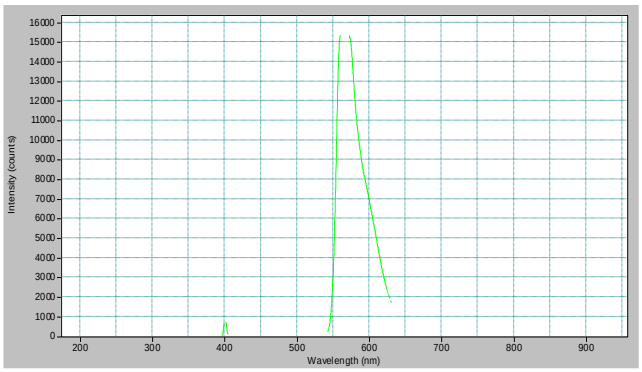

(1×10^{-4} M R6G –Blue Laser)

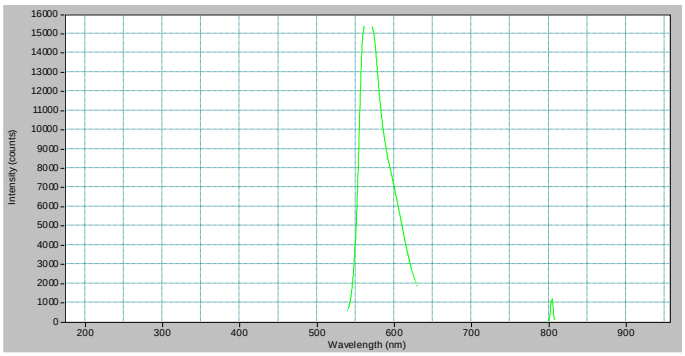

(1×10^{-4} M R6G –Green Laser)

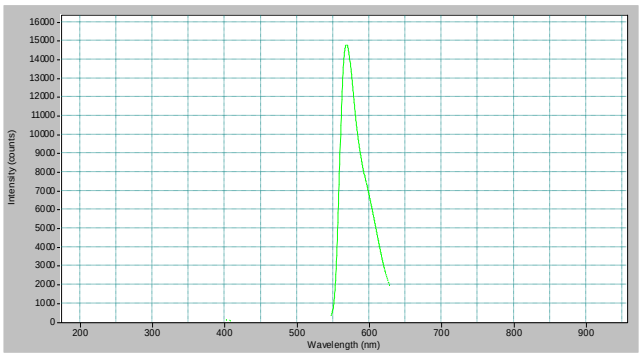

(3×10^{-4} M R6G –Blue Laser)

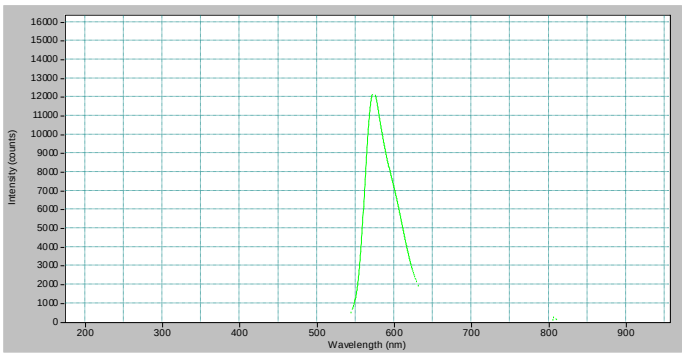

(3×10^{-4} M R6G –Green Laser)

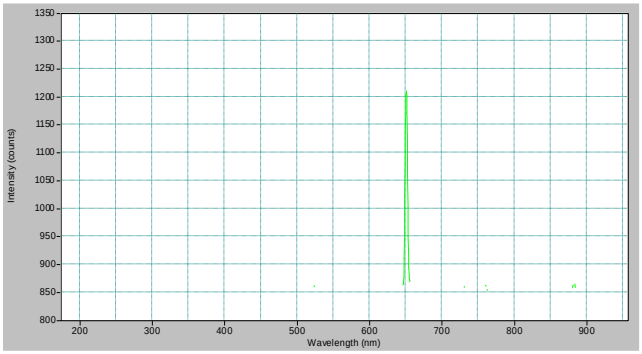

(3×10^{-4} M R6G –Red Laser)

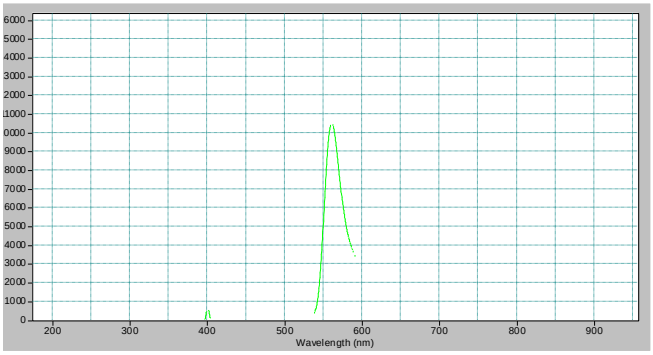

(3×10^{-5}M R6G –Blue Laser)

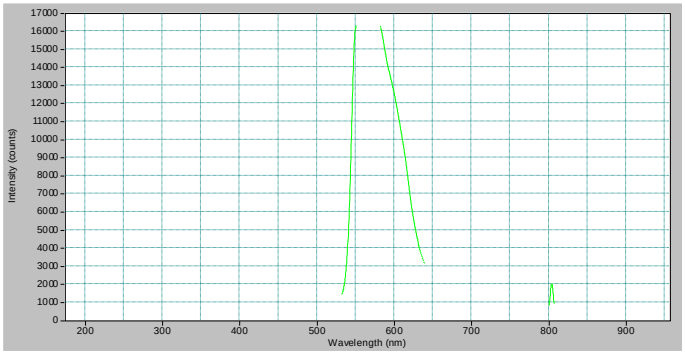

(3×10^{-5} M R6G –Green Laser)

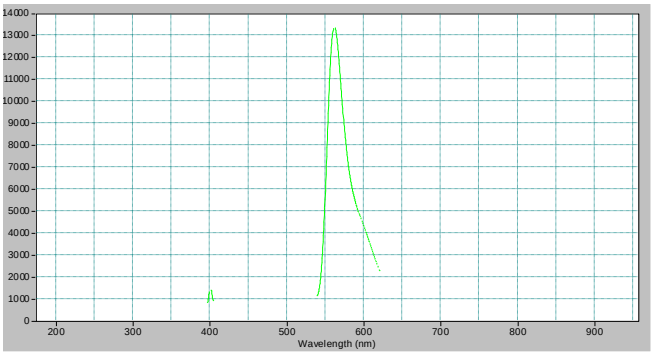

(5×10^{-5} M R6G –Blue Laser)

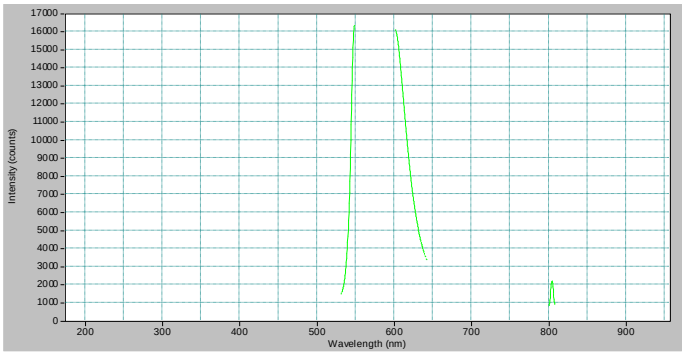

(5×10^{-5} M R6G –Green Laser)

Fig (4-19) Fluorescence Spectra of R6G Dye by using (Blue ,Green ,Red) lasers as pump source at concentrations (10^{-4}, 3×10^{-4} , 3×10^{-5} ,5×10^{-5}) M

5-The Fluorescence Spectra of MO Dye by using LIF technique in Spectra Academy device

The fluorescence spectra of the MO dye dissolved in distilled water for different concentrations (5×10^{-5} ,1×10^{-5},1×10^{-6}) M by using LIF technique with (Blue ,Green ,Red) lasers as pump source of dyes as shown in figure (4-20). There is a best emission spectra at pumping by blue laser (λ=405) because MO dye have emission peak located inside this region.

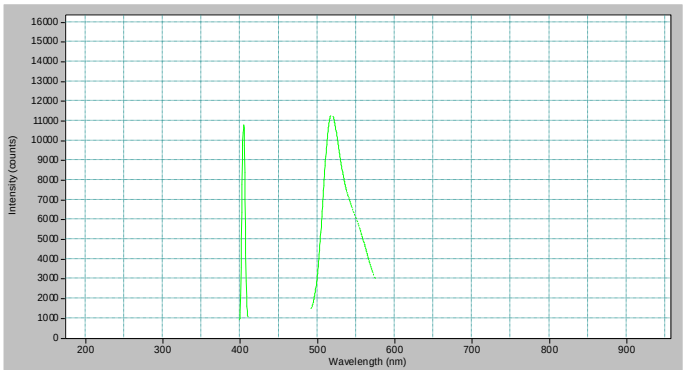

5×10^{-5} M (MO –Blue Laser)

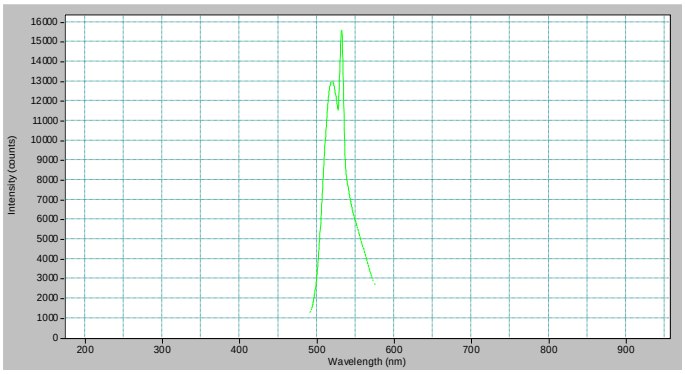

5×10^{-5} M (MO –Green Laser)

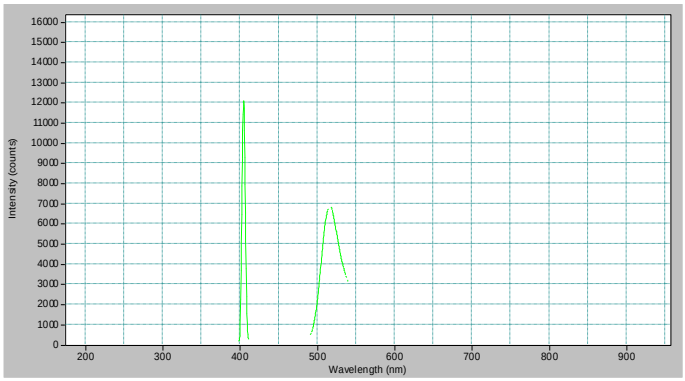

1×10^{-5} M (MO pure –Blue Laser)

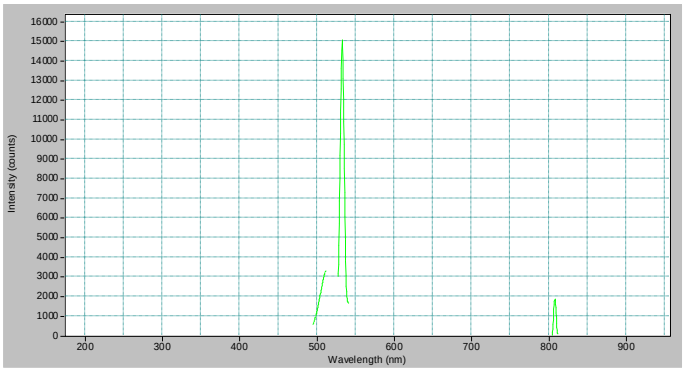

1×10^{-5} M (MO pure –Green Laser)

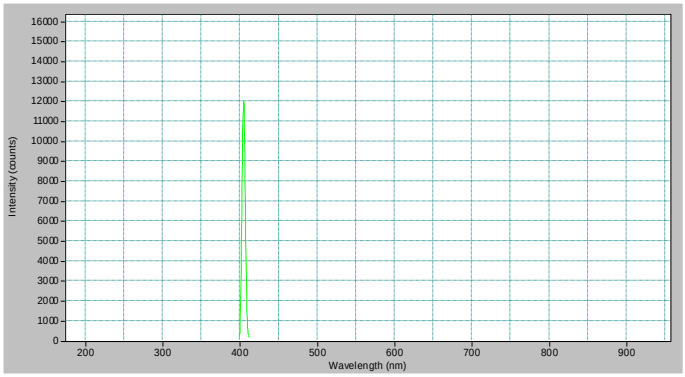

1×10^{-6} M (MO pure –Blue Laser)

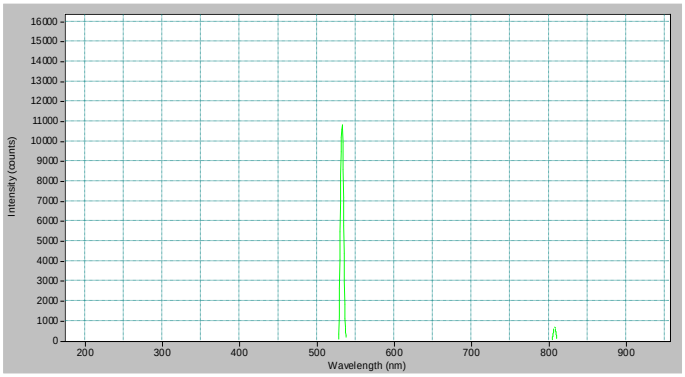

1×10^{-6}M (MO pure –Green Laser)

Fig (4-20) Fluorescence Spectra of MO Dye at concentrations (5x10^{-5}, 1x10^{-5}, and 1x10^{-6})M by using LIF technique

6-The Fluorescence Spectra of MO Dye with added Ag Nano particles measured by LIF with using Spectra academy device

Added Ag nanoparticles to MO dye at concentrations (1x10^{-5} M, and 1x10^{-6} M) .The nanoparticles have a big effect on Fluorescence spectra. There is increase in spectra intensity because the effect of nanoparticles on dyes molecules. It noticeable that the big effect of Ag nanoparticles when pump the dye by blue laser (λ=405 nm) because of MO dye spectra is located within region of pump .While when pump by Green laser there is little effect because it is outside the absorption band of the dye. as can show in figure (4-21).

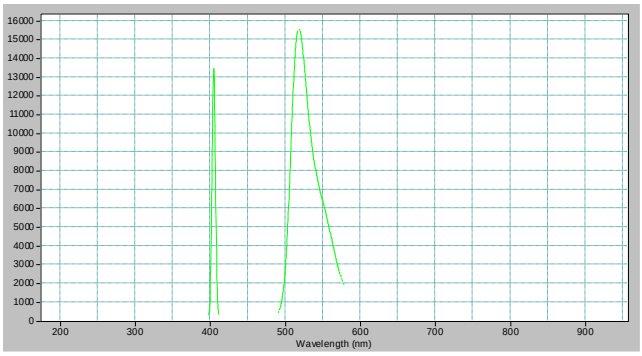

1×10^{-5} M (MO +2mL Ag) – Blue Laser

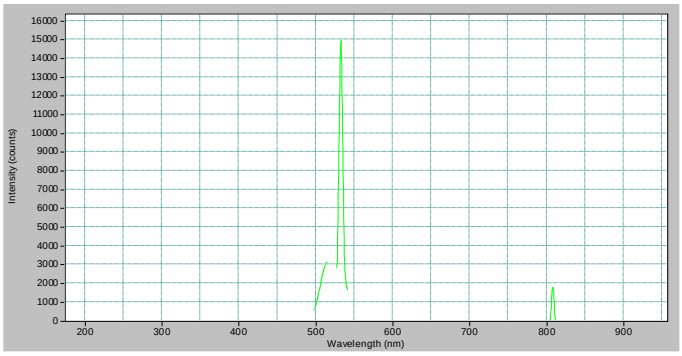

1×10^{-5} M (MO +2mL Ag) –Green Laser

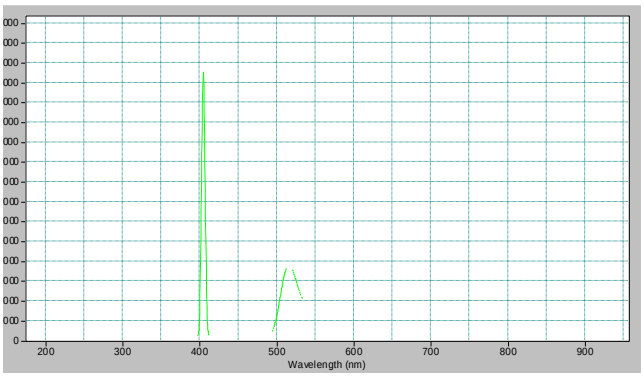

1×10^{-6} M (MO+2mL Ag) –Blue Laser

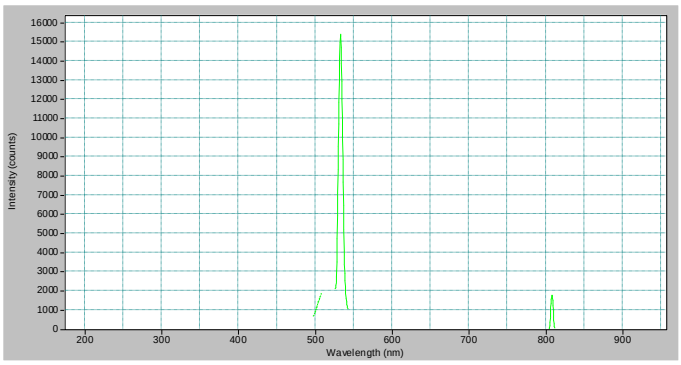

1×10^{-6} M (MO +2mL Ag) –Green Laser

Fig (4-21) Fluorescence Spectra of MO Dye at concentration ($1x10^{-5}$, and $1x10^{-6}$) M with Ag Nanoparticles

4.6 Analysis of the Absorption and Fluorescence Spectra by Origin Program for (R6G , MO) Dyes

1-Analysis The Data of Absorption spectra for MO Dye by Origin Program

The data of Absorption spectra measured by UV-VIS spectrometer will be used to apply it in origin program to find FWHM and area under the curve of R6G and MO dyes for different concentrations .

It can noticeable from the table (4-8) the absorption peaks at concentrations (5×10^{-5} M,1×10^{-5} M, 1×10^{-6} M) MO Dye ,the maximum peak of MO dye at 490 nm and there is increase in absorption intensity when concentration increase and also more peaks can note at high concentration (5×10^{-5} M) because of the high dye molecules concentration.

After adding nanomaterial to concentrations (1×10^{-5} M, 1×10^{-6} M) for MO dye as can be shown in table (4-9) and noting the change in the absorption and emission spectra (which is a function of the change in energy levels as a result of the addition)

It is observed increase in area under the curve and FWHM (The larger FWHM value describes a wider beam spread, corresponding to more light diffusion) and also increase in absorption intensity after adding Ag nano particles .

There are many bands appear after adding Ag nano particle additional to original peak of MO dye that because the scattering effect and the particles of Ag causing more reflecting between particles and molecules of dye due to the increase in resonance and optical path broadness that due to increase in absorption cross section

Table (4-8)Analysis the Data of Absorption spectrum for MO Dye by Origin Program

Dyes	Area under the curve	FWHM	λ(nm)	Intensity
MO ($5x10^{-5}$M)	46.21425	21.73951	199	2.34584
	52.42205	28.88226	239	1.80918
	27.88616	30.0186	283	0.57382
	74.87237	463.8217	485	2.74235
	61.02037	20.50322	490	2.81168
MO ($1x10^{-5}$M)	20.72269	30.96465	239	0.43006
	34.56552	32.21162	491	0.78715
MO ($1x10^{-6}$M)	6.46666	6.28598	192	0.99472
	8.80306	69.53457	491	0.16612

Table (4-9) Analysis the Data of Absorption spectra for MO Dye by Origin Program with Added Ag nanoparticles

Dyes	Area under the curve	FWHM	λ(nm)	Intensity
MO+Ag ($1x10^{-5}$ M)	9.88378	4	192	2.30186
	35.28888	17.21109	196	1.98444
	44.05297	29.18623	239	1.11416
	148.9763	40.65487	491	1.98444
MO+Ag ($1x10^{-6}$ M)	27.35039	12.63309	191	1.34211
	17.87497	59.80852	238	0.34678
	27.96881	68.33721	426	0.40834
	2.45056	5	431	0.40908
	2.04354	4	437	0.40901
	92.6971	119.4849	490	0.49585

2-Analysis The Data of Absorption spectra for R6G Dye by Origin Program

The data of UV-VIS spectrometer (Absorption spectra) and apply it in origin program to find FWHM and area under the curve for R6G dyes at different concentrations we can see from the table (4-10) the absorption peaks at concentrations (1×10^{-4}, 3×10^{-4} ,3×10^{-5}, 5×10^{-5} ,7×10^{-5}) M for R6G Dye ,the maximum absorption peak of R6G dye at (530 nm) . There is increase in intensity absorption when concentration increase and also more peaks can be noted at high concentration (3×10^{-4} M) because of high dye molecules at this concentration , there is increase in FWHM and area under the curve together at different region and concentrations but in the same range of R6G dye ,also observe at every concentrations they have a different behavior

Table (4-10) Analysis the Data of Absorption spectra for R6G Dye by Origin Program

Dyes	Area under the curve	FWHM	λ(nm)	Intensity
R6G ($1x10^{-4}$M)	72.94563	38.13772	247	2.14059
	32.14956	26	275	1.28719
	20.87127	16.80368	295	1.12824
	26.02064	26.85155	348	0.891
	112.7139	33.01263	513	2.6876
	13.45228	4	518	2.70161
	16.19995	5	524	2.72351
	18.96706	6	527	2.73107
	10.85772	3	534	2.72351
	51.69887	17.48557	538	2.72351
R6G ($3x10^{-4}$M)	50.68413	20.81006	245	2.11548
	4.21269	1	248	2.12291
	12.70412	5	253	2.1852
	6.33396	2	256	2.14597

	16.34809	7	259	2.12856
	15.30242	7	267	1.97518
	9.21871	4	276	1.87667
	3.75923	1	280	1.91437
	5.7246	2	283	1.92019
	7.68787	3	287	1.97385
	52.21756	26.81152	294	2.11548
	73.67259	44.30833	345	1.84891
	5.89769	9	387	0.60022
	8.69224	14	390	0.601
	8.96711	15	411	0.56298
	87.12496	25.51847	483	2.68222
	5.36865	1	486	2.70307
	8.02676	2	489	2.68905
	8.04697	490	493	2.696
	18.88974	6	497	2.70307
	8.06733	2	502	2.696
	5.38528	503	505	2.70307
	8.11279	505	508	2.71025
	16.26547	5	512	2.71754
	8.12768	2	516	2.72497
	27.19131	9	525	2.74021
	24.53492	8	531	2.74803
	13.57745	4	540	2.73252
	57.29062	19.26902	543	2.73252
R6G ($3x10^{-5}M$)	2.35284	2	195	1.01761
	4.9592	5.78915	199	1.10055
	3.09982	3.94163	205	0.77557
	73.75584	19.1666	248	1.3649
	127.839	26.2421	529	2.99165
	78.67184	14.72356	533	2.97641
R6G ($5x10^{-5}M$)	3.42708	3	192	0.98788
	4.23217	2.92155	195	1.21572
	4.02482	4	201	1.03856
	3.69451	5.22219	206	0.71428
	48.96412	21.77504	248	1.90695
	20.63774	26	274	0.82003
	16.03195	21.88692	295	0.76115
	25.72979	41.93578	348	0.69298
	126.2227	490.5507	522	3.06426

	18.53099	5	527	3.12705
	12.38779	3	530	3.10817
	115.655	17.11959	534	3.09903
R6G ($7x10^{-5}M$)	3.17659	3	192	0.92022
	2.90326	2.93121	196	1.12213
	6.15483	3.19827	201	1.20683
	1.73135	2.6754	209	0.60629
	55.75847	23.07166	248	2.04676
	18.78096	25	274	0.79257
	26.95676	16.84694	295	0.68231
	99.77451	487.8556	520	2.8464
	8.55386	520	523	2.87569
	81.6048	26.96603	528	2.9071

3-Analysis the Data of Fluorescence spectra for MO Dye by Origin Program

After measured the Fluorescence Spectra of MO dye by using LIF technology and applying the measurement data in origin program to find area under the curve and the full width half maximum (FWHM) at different concentration of MO dye (5×10^{-5},1×10^{-5},1×10^{-6}) M and with using blue and green laser as pump source as shown in table (4-11).

The increase in area under curve and FWHM and Fluorescence intensity ,after adding Ag nano particles, without any change in number and positions peak ,the increase intensity happened because the particles of Ag causing more reflecting between particles and molecules of dye due to the increase in resonance between the collective oscillations of conduction electrons with incident electromagnetic field .

Table (4-11) Analysis the Data of Fluorescence spectra for MO Dye by Origin Program

Dyes	Area under the curve	FWHM	λ(nm)	Intensity
MO ($5x10^{-5}$M) Blue laser	823095.3	43.21227	516.027	15706.63
	8449.596	4.94561	404.934	1663.327
MO ($5x10^{-5}$M) Green laser	246603.3	23.64936	516.447	10479.418
	226716	7.63362	531.932	11926.5
	1047.158	3.80278	807.229	264.7
MO ($1x10^{-5}$M) Blue laser	67694.97	5.17735	404.491	12112.15
	301487.5	33.44749	515.606	6895.354
MO ($1x10^{-5}$M) Green laser	85564.53	23.21733	515.606	3580.764
	138700.7	6.35248	532.348	15072.71
	7406.663	3.75991	807.558	1913.873
MO ($1x10^{-6}$M) Blue laser	66778.67	5.16866	404.491	12024.86
	33885.66	34.50931	513.923	754.182
MO ($1x10^{-6}$M) Green laser	52235.19	4.71817	532.348	10849.06
	2901.352	3.93599	807.229	706.063

Table (4-12) Analysis the Data of Fluorescence spectra for MO Dye by Origin Program with Added Ag nanoparticals

Dyes	Area under the curve	FWHM	λ(nm)	Intensity
MO+Ag ($1x10^{-5}$M) Blue laser	82908.84	5.46507	404.491	13478.92
	695369.4	35.61097	517.707	15593.29
MO+Ag ($1x10^{-5}$M) Green laser	73374.1	21.4666	516.867	3285.555
	139548.3	6.14182	532.348	14993.43
	6992.111	3.77026	807.886	1809.555
MO+Ag ($1x10^{-6}$M) Blue laser	80340.16	5.5475	404.047	13550.58
	162042.2	32.43578	515.606	3837.082
MO+Ag ($1x10^{-6}$M) Green laser	185526.1	6.88122	532.348	15405
	6699.157	3.65721	807.886	1816.773

4-Analysis the Data of Fluorescence spectra for R6G Dye by Origin Program

-Measurement of Fluorescence Spectra of R6G Dye by using LIF technology and Applying Measurement in origin program to find Area under the curve and full width half maximum (FWHM) at different concentration of dye and with using blue and green laser as pump source is shown in table (4-13).

Table (4-13) Analysis the Data of Fluorescence spectra for R6G Dye by Origin Program

Dyes	Area under the curve	FWHM	λ(nm)	Intensity
R6G ($1x10^{-4}$M) Blue laser	753765.4	42.29753	560.033	15393.69
	4216.19	5.05462	400.495	764.773
R6G ($1x10^{-4}$M) Green laser	779916.1	42.91638	562.08	15438.23
	5062.728	3.97326	803.939	1209.154
R6G ($3x10^{-4}$M) Blue laser	1.01E+06	59.1078	561.671	15489.84
	3188.441	5.1	400.495	567.272
R6G ($3x10^{-4}$M) Green laser	5276.037	3.95687	803.939	1259.373
	503948.5	40.11168	569.838	10816.18
R6G ($3x10^{-5}$M) Blue laser	408042.2	28.47421	560.443	10506.75
	3069.163	5.05939	400.495	575.009
R6G ($3x10^{-5}$M) Green laser	1.19E+06	71.97926	550.993	15600.2
	5298.19	3.96267	803.61	1269.164
R6G ($5x10^{-5}$M) Blue laser	492415.2	28.5859	561.262	12612.45
	3547.128	5.08668	400.495	633.445
R6G ($5x10^{-5}$M) Green laser	1.33E+06	76.63245	549.344	15596.2
	6124.067	3.92061	803.939	1462
R6G ($7x10^{-5}$M) Blue laser	372743.7	28.95561	562.899	9401.137
	1619.306	5.2588	400.495	234.937
R6G ($7x10^{-5}$M) Green laser	583696.2	30.00122	562.49	14315.96
	5886.151	3.87627	803.939	1439.191

4.7 Measurements of the Fluorescence Spectra for MO And R6G Dyes by Optical Pumping Process with Designing a Special Electronic Circuit (TTL)

Designing a special electronic circuit (TTL) that controls the parameters of the dye-pumping laser or LED has the ability to:

- Changing the frequency at which the LED operates from (10000 Hz - 150000 Hz)

- Changing the Duty cycle from (10% - 90%), but first will set a Duty cycle (pumping time) at 50% for measuring the fluorescence spectra of the dyes

The independent to change the parameters (frequency , Duty cycle) allows to obtain direct and decisive results for each change in them on the performance of the dye in terms of an increase or decrease in the absorption or emission beams and thus for the efficiency of filling and unloading the energy levels included the laser action in the dye

The organic dyes chosen for the study are R6G and MO dye with different concentration but will chosen optimum concentration for each dye for this study .

The measurement of fluorescence spectra for MO and R6G Dyes by using Spectra Academy device but this time with use the electronic circuit Designed (TTL) that controls the parameters of the dye, pumping by (laser or LED) and this circuit it has the ability to control the laser or LED frequency and the pulse duration .

By using Blue LED for MO dye and Green LED for R6G as pump source with frequencies from (10000-150000) Hz, and install the duty

cycle at 50 % with electronic circuit to control this parameters , and apply the measured data in origin program to find Area under the curve and the full width at half maximum (FWHM) at constant pumping time with different frequencies .

Through this study we will try to find out the extent of changes in dye and reach to the perfect harmony for both frequency and pumping time by reaching the energy levels to saturation limit (filling energy levels) and possibility to estimating fluorescence lifetime . So that can used this property in many application like used it as optical limiter.

The important factor here in the performance of dye is decay time of excitation levels for dye and will calculated from analyze the emission spectrum of dye by using Spectra Academy device ,where it can be observed the energy levels through the fluorescence Spectrum of dye.

So that any change in dye pumping time and frequency parameters will be evident in change of fluorescence spectrum that will lead to change in intensity and output wavelengths .

The measurement of Fluorescence spectra for MO Dye by using Spectra Academy device but this time with use the electronic circuit Designed (TTL) and change in pumping method ,as show in table (4-14) the values of Fluorescence Spectra at different frequency from (10000-150000) Hz and constant pumping time at (50 %) and it can be noticed from Table (4-14), (4-16). the original Fluorescence peak occurs, at wavelengths around 513 nm for MO dye and for R6G dye the original Fluorescence peak occurs, at wavelengths around 561 nm .

But can notice there is many wavelengths (peaks) appeared addition to the original peak start from (220 nm) to (882nm) and these wavelengths (peaks) result from transitions that occurred in the energy level .

The reason for appear these transitions because it was fed with appropriate energy different between levels of the material by changing the frequency and pumping time through our saving mechanism (method) and it is building electronic circuit were able to control the frequency and pumping time, (that meaning there is energy levels outcome from this change and by controlling the pump time and frequency will can see this transitions) .

Therefore, the appearance of these transitions and wavelengths is the result of choosing a frequency range and a time range that revealed what was hidden from peaks and transitions.

From this mechanism it is possible to make a match between frequency and pumping time and get the appropriate amount of energy for the level ,therefore the match that will get is the same amount of increase in efficiency. It is noticeable that a peaks at a wavelength (800.304, 882.403) nm for MO dye with (799.973, 882.11) nm for R6G dye and this wavelengths are not present in previous studies ,but it is present according to the pumping method used in this research .

Through this mechanism it will be able to show the wavelengths and peaks that were actually exist (present in the original) but were not highlighted or previous shown by traditional methods ,but through this method it able to show the peaks in fluorescence spectra of the dyes in figure (4-22).

It is obtained wavelengths that can shown in the figures (4-22),that exist as a result of transitions between energy levels and were not present in previous studies.

After measuring the fluorescence spectra of dyes (R6G, MO), before and after adding Ag nanoparticles , the spectrum was analyzed in a origin

program to find the full width at half maximum (FWHM) and Area under the curve with the wavelengths peaks and intensity for fluorescence spectra.

The effect of increasing the frequency from (10000-150000) Hz on the parameters of fluorescence spectra of the dye which is the fluorescence intensity of MO dye at wavelength (220) nm was almost the same for all frequencies and the highest recorded after the frequency increase was at (40000) Hz while at wavelength (294) nm the highest recorded after the frequency increase was at (20000) Hz also the wavelength at (404) nm the highest recorded after the frequency increase was at (10000) Hz.

However , it is observed that the intensity starting to increase gradually with the increase in frequency at wavelength (486.7, 565.3) nm ,while in other regions there is no such increase and this possible due to the fact that the absorption spectrum of MO dye is located in this region. Therefore ,its emission spectrum has increased in intensity in this region compared to other regions.

After adding Ag nano particles to (MO) dye at concentration (1×10^{-5} M), as show in table (4-15) ,it is clear the effect of Ag nano particles on spectral parameters of dye ,it can notice the decrease in intensity and area under the curve after adding Ag nano particles but there is increase in FWHM because of the scattering of light ,also this increase in FWHM occurred in some peaks like (220.6, 294.8 ,404.4, 565.3, 760.2,and 800.304) nm, because this increase is due to an increase in spectral regions and thus an increase in the spectral line width because have occur a new transitions in energy levels at this wavelengths, lead to increase the

FWHM of the fluorescence spectrum after adding Ag nano particles is shown in table (4-15) and figure (4-22,(b)) ,so the presence of a new ranges and wavelengths will open up horizons for many applications in the future .

Table (4-14) Fluorescence Spectra of the MO Dye (without nanomaterials) at different Frequency from (10000-150000) Hz with constant Pumping time (Duty Cycle = 50%)

Dyes	Frequency (Hz)	Pumping Time T_{ON} (ms)	Area under the curve	FWHM	λ(nm)	Intensity
MO ($1x10^{-5}$M)	10000	0.05	709833.9	34.85465	515.186	15677.56
			1781.068	6.17696	220.61	57.137
			1376.629	5.81597	294.869	69.128
			1113.973	5.08598	404.047	54.846
			5339.469	482.9004	486.79	536.982
			632153.4	34.85465	515.186	15677.56
			67923.45	12.85465	565.351	3236.364
			4104.914	25.2739	643.336	112.6
			1820.562	4.02393	760.602	101.846
			1137.357	1.30792	800.304	77.046
			2464.875	3.27409	882.403	379.282
MO ($1x10^{-5}$M)	20000	0.025	720600.7	35.47566	514.344	15676.96
			1867.616	6.17796	220.61	61.2
			1525.826	6.13625	294.869	72.31
			1110.71	5.07898	404.047	51.264
			5763.245	482.8417	486.79	534.31
			639630.1	35.47566	514.344	15676.96
			69585.77	12.87224	565.351	3288.528
			4441.563	25.60183	643.336	123.573
			1803.415	3.92095	760.254	96.01
			1342.783	1.34407	800.304	78.4
			2917.755	3.2938	882.403	385.246
MO ($1x10^{-5}$M)	30000	0.01666	723548.6	35.77156	513.923	15666.97
			1808.14	5.8482	220.61	59.155
			1407.689	5.75049	294.869	67.337
			1150.902	5.20026	404.047	57.146

			5600.774	482.8123	486.79	542.8
			642426	35.77156	513.923	15666.97
			69649.33	12.9677	565.351	3302.9
			4284.501	22.99824	643.336	121.128
			1773.603	3.9624	760.254	87.791
			1272.312	1.33833	800.304	78.3
			2271.394	3.30054	882.403	281.628
MO ($1x10^{-5}$M)	40000	0.0125	725899.3	36.02885	513.923	15664.35
			1888.06	6.27968	220.61	62.681
			1533.692	5.88361	294.869	66.863
			1169.874	5.05258	404.047	55.5
			5634.28	482.9476	486.79	551.4
			645794	36.02885	513.923	15664.35
			70008.87	12.95475	565.351	3321.609
			4149.12	25.25638	643.336	125.2
			1661.056	3.9488	760.254	90.4
			1025.09	1.29585	800.304	73.163
			2052.228	3.30321	882.403	256.145
MO ($1x10^{-5}$M)	50000	0.01	728942.6	36.25776	513.502	15662.31
			1752.339	5.95988	220.61	57.818
			1385.395	5.69134	294.869	65.854
			911.2726	5.04636	404.047	52.936
			5465.611	482.9045	486.79	550.618
			648242.1	36.25776	513.502	15662.31
			70297.2	12.9399	565.351	3336.636
			4056.052	25.28126	643.336	119.009
			1846.547	4.0164	760.254	103.227
			1108.756	1.50646	800.304	71.745
			1990.656	3.28496	882.11	251.7
MO ($1x10^{-5}$M)	60000	0.00833	731082.4	36.49954	513.502	15659.19
			1566.841	5.80296	220.61	55.846
			1448.7	6.28835	294.869	71.427
			1063.755	5.03711	404.047	55.655
			5355.247	482.9181	486.79	550.091
			651065.1	36.49954	513.502	15659.19
			70500.02	12.95611	565.351	3344.846
			3848.222	25.11122	643.336	118.982
			1424.155	3.93112	760.254	94.773
			1080.26	1.41925	800.304	66.155
			2617.295	3.27667	882.403	372.355

MO ($1x10^{-5}$M)	70000	0.00714	734529.6 1717.747 1285.304 871.1616 5288.684 653946.8 71126.84 3883.969 1572.702 922.5218 1856.838	36.72572 6.05827 6.12632 4.99457 482.9567 36.72572 12.97531 25.1567 3.97 1.44418 3.28204	513.502 220.61 294.869 404.047 486.79 513.502 565.351 643.336 760.254 800.304 882.403	15651.47 56.237 65.073 51.591 562.255 15651.47 3369.609 120.782 93.109 70.628 270.682
MO ($1x10^{-5}$M)	80000	0.00625	737581.8 1775.604 1356.413 955.262 5290.588 656573.7 71589.52 4196.528 1582.517 1215.36 2501.481	36.95509 13.55189 5.78053 4.9976 482.841 36.95509 12.93849 25.0902 3.94816 1.29911 3.28	513.081 183.141 294.869 404.047 486.79 513.081 565.351 643.336 760.254 799.973 882.403	15652.37 57.446 65.137 49.782 562.864 15652.37 3392.364 124.355 85.564 71.491 371.055
MO ($1x10^{-5}$M)	90000	0.00555	738572.4 1635.185 1307.59 938.7326 5417.858 656540.8 71284.31 4022.453 1576.002 1129.721 2297.985	36.98256 13.44752 5.68686 4.99615 482.8885 36.98256 13.07225 22.77557 3.95057 1.54816 3.29894	513.081 185.523 294.869 403.603 486.79 513.081 565.351 643.336 760.254 800.304 882.403	15650.41 55.318 60.609 53.554 567.291 15650.41 3373.454 116.091 86.554 68.927 273.964

MO ($1x10^{-5}$M)	100000	0.005	743644.9	37.40537	512.66	15646.56
			1864.819	6.46144	220.61	59.419
			1364.785	5.83191	294.869	66.991
			1081.117	5.11933	404.047	55.182
			5592.568	482.8709	486.79	571.273
			661554.9	37.40537	512.66	15646.56
			72088.35	13.00289	565.351	3419.237
			4067.874	19.85841	643.336	121.619
			1668.834	3.97583	760.254	87.737
			1161.846	1.49845	800.304	70.064
			2134.724	3.28852	882.403	304.1
MO ($1x10^{-5}$M)	110000	0.00454	745144.9	37.45056	513.081	15641.46
			1656.24	6.07885	220.61	56.255
			1194.69	5.56159	294.869	57.428
			1184.743	5.23036	404.047	57.937
			5878.243	482.8757	486.79	574.109
			661743.6	37.45056	513.081	15641.46
			72281.68	12.92848	565.351	3418.555
			4259.559	19.67014	643.336	127.291
			1781.738	4.04285	760.254	92.928
			982.6099	1.30718	800.304	68.773
			2035.517	3.2798	882.403	275.5
MO ($1x10^{-5}$M)	120000	0.00416	747466.9	37.63667	512.66	15641.64
			1795.378	6.21132	220.61	55.427
			1286.354	6.0145	294.869	62.827
			1106.402	5.10252	404.047	52.527
			5895.29	482.8364	486.79	574
			663743	37.63667	512.66	15641.64
			72612.88	12.95881	565.351	3431.827
			4329.981	24.97302	643.336	124.281
			1845.057	4.03479	760.602	93.291
			1202.187	1.53637	800.304	70.527
			2676.006	3.28955	882.403	364.618
MO ($1x10^{-5}$M)	130000	0.00384	748221.8	37.84392	512.66	15634.47
			1690.449	5.86663	220.61	53.928
			1300.198	5.96688	294.869	62.9
			1085.528	5.04387	404.047	46.982
			5325.342	482.9268	486.79	570.773
			666070.1	37.84392	512.66	15634.47
			72672.51	12.97718	565.351	3452.928

			3914.768	20.29822	643.336	122.655
			1396.056	3.89863	760.602	85.7
			1039.206	1.29632	799.973	68.764
			2251.118	3.29204	882.403	307.5
MO ($1x10^{-5}$M)	140000	0.00357	754223.2	38.2843	512.66	15631.71
			1382.516	5.86068	220.61	52.591
			1135.077	5.81951	294.869	60.718
			783.6622	4.95171	404.047	44.109
			5557.372	482.7904	486.79	581.136
			670874.1	38.2843	512.66	15631.71
			73178.8	12.83219	565.351	3495.282
			4056	19.80194	643.336	120.364
			1748.521	4.01741	760.602	97.691
			891.6527	1.32656	800.304	68.818
			1811.829	3.27965	882.403	261.491
MO ($1x10^{-5}$M)	150000	0.00333	758140.5	38.37512	512.239	15632.46
			1786.458	6.11288	220.61	57.982
			1432.771	6.09417	294.869	64.846
			1007.303	5.09383	404.047	48.982
			5709.949	482.9601	486.79	588.119
			672362.6	38.37512	512.239	15632.46
			73698.03	12.98472	565.351	3493.128
			4510.709	25.19842	643.336	126.891
			1815.124	4.00475	760.254	87.391
			1016.234	1.31295	800.304	68.482
			2206.9	3.28818	882.403	299.346

Table (4-15) Fluorescence Spectra of the MO Dye (with added Ag nano particles) at different frequency from (10000-150000) Hz with Constant Pumping Time (D.C =50 %)

Dyes	*f* (Hz)	Pumping Time T_{ON} (ms)	Area under the curve	FWHM	λ(nm)	Intensity
MO+Ag ($1x10^{-5}$M)	10000	0.05	75330.07	21.71721	454.509	3092.236
			651473.1	33.76124	517.287	15028.23
			1144.957	6.18684	220.61	41.009
			857.121	5.43592	294.869	41.745
			789.673	5.13592	404.047	41.673
			76158.38	21.71721	454.509	3092.236
			576298.4	33.76124	517.287	15028.23
			70449.12	13.15655	565.351	3317.036
			3657.321	24.96762	643.336	111.909
			1196.596	3.99641	760.602	65.591
			639.4987	1.34007	800.304	50.291
			1699.539	3.27206	882.403	237.545
MO+Ag ($1x10^{-5}$M)	20000	0.025	71836.57	21.69776	454.509	2949.991
			616346.3	33.46842	517.287	14288.08
			1042.266	5.59155	220.61	37.745
			828.1677	5.42076	294.869	44.682
			725.9923	5.27757	404.047	45.073
			72588.84	21.69776	454.509	2949.991
			545639.9	33.46842	517.287	14288.08
			66419.23	13.22075	565.351	3124.882
			3268.149	18.96692	643.336	112.655
			1138.338	3.9349	760.254	60.773
			916.9228	1.45357	799.973	51.764
			1447.714	3.27791	882.403	177.227
MO+Ag ($1x10^{-5}$M)	30000	0.01666	73419.86	21.67934	454.509	2975.672
			622555.4	33.52286	517.287	14372.05
			1524.971	7.23202	220.61	50.554
			1373.051	6.19705	294.869	51.809
			1166.727	5.45107	404.047	50.409
			73497.92	21.67934	454.509	2975.672
			549398.5	33.52286	517.287	14372.05
			67624.27	13.33015	565.351	3150.509
			4029.106	25.33237	643.336	116.972

			1217.407	3.96189	760.254	67.227
			656.193	1.26038	799.973	47.827
			1477.057	3.28486	882.403	198.263
MO+Ag ($1x10^{-5}$M)	40000	0.0125	73072.59	21.67429	454.509	2998.345
			628716.2	33.59603	517.287	14493.27
			1624.609	7.14423	220.61	53.173
			1258.57	6.12411	294.869	58.045
			825.8236	5.22831	404.491	47.409
			73849.71	21.67429	454.509	2998.345
			554581.4	33.59603	517.287	14493.27
			68059.22	13.18687	565.351	3188.473
			3710.266	22.18265	643.336	114.364
			1490.12	4.04267	760.254	71.427
			996.8718	1.37113	800.304	52.4
			1559.607	3.29897	882.403	174.609
MO+Ag ($1x10^{-5}$M)	50000	0.01	73028.03	21.68896	454.509	2997.7
			629353.9	33.73592	517.287	14531.76
			1173.138	8.70928	185.523	36.791
			1174.961	6.18733	294.869	52.436
			828.2922	5.2463	404.047	46.027
			73792.99	21.68896	454.509	2997.7
			556463.9	33.73592	517.287	14531.76
			68161.54	13.09313	565.351	3209.027
			3687.618	25.18303	643.336	109.764
			1303.794	3.98123	760.254	68.955
			682.9269	1.27718	800.304	47.536
			1510.05	3.28192	882.403	200.082
MO+Ag ($1x10^{-5}$M)	60000	0.00833	73689.93	21.73086	454.509	3021
			633731.4	33.69783	517.287	14621.93
			1232.761	5.98823	220.61	42.554
			1117.096	5.99717	294.869	50.091
			927.5572	5.25128	404.047	46.954
			74491.79	21.73086	454.509	3021
			560017.3	33.69783	517.287	14621.93
			68860.51	13.15704	565.351	3228.363
			3761.115	24.71451	643.336	116.536
			1151.198	3.97901	760.254	68.1
			725.4224	1.25818	800.304	41.781
			1806.852	3.27496	882.403	263.263
MO+Ag	70000	0.00714	74233.18	21.72329	454.509	3036.8

($1x10^{-5}$M)			637968.3	33.68735	517.287	14709.94
			1287.468	6.2317	220.61	46.837
			1208.114	6.13958	293.945	54.419
			997.3816	5.23936	404.047	46.582
			75018.37	21.72329	454.509	3036.8
			563378.5	33.68735	517.287	14709.94
			69544.59	13.28157	565.351	3245.955
			3970.5	24.32319	643.336	122.628
			1440.511	4.00767	760.254	71.891
			893.8091	1.31886	799.973	54.319
			1328.961	3.36985	882.11	114.791
MO+Ag ($1x10^{-5}$M)	80000	0.00625	74521.74	21.77025	454.509	3047.518
			641816	33.81244	517.287	14788.44
			1361.688	6.33443	220.61	45.954
			1319.525	5.98536	294.869	51.036
			1020.349	5.31047	404.047	48.381
			75319.34	21.77025	454.509	3047.518
			567193.3	33.81244	517.287	14788.44
			69640.59	13.18873	565.351	3270.136
			3885.863	22.58582	643.336	118.99
			1257.297	3.98732	760.254	71.518
			755.2315	1.30559	800.304	55.463
			1624.422	3.29242	882.403	219.19
MO+Ag ($1x10^{-5}$M)	90000	0.00555	75059.55	21.72387	454.509	3054.482
			642030.8	33.81297	517.287	14779.71
			1356.803	6.13954	220.61	46.454
			1062.458	5.68657	294.869	49.573
			948.1797	5.30897	402.272	47.836
			75331.98	21.72387	454.509	3054.482
			566922.8	33.81297	517.287	14779.71
			69713.76	13.15686	565.351	3269.091
			3854.489	22.58512	643.336	118.645
			1269.479	3.94063	760.254	68.018
			870.5973	1.3225	800.304	52.236
			1917.878	3.28116	882.403	262.254
MO+Ag ($1x10^{-5}$M)	100000	0.005	75323.61	21.75319	454.509	3085.8
			650623.4	33.89351	517.287	14953.84
			1483.745	5.99755	220.61	47.01
			1205.719	6.04295	294.869	56.891
			823.6309	5.08397	404.047	43.582

			76188.21	21.75319	454.509	3085.8
			574203.5	33.89351	517.287	14953.84
			71098.35	13.2066	565.351	3324.982
			4208.317	25.01986	643.336	127.51
			1522.569	4.07517	760.254	78.319
			1111.66	1.52582	799.973	54.31
			1799.093	3.28079	882.11	218.21
MO+Ag ($1x10^{-5}$M)	110000	0.00454	75513.49	21.75027	454.509	3083.818
			650972.5	33.99038	517.287	14912.11
			1502.88	6.8667	220.61	53.963
			1276.294	6.0825	294.869	57.809
			1043.235	5.39317	404.047	53.572
			76145.12	21.75027	454.509	3083.818
			573680.6	33.99038	517.287	14912.11
			70715.31	13.1012	565.351	3321.581
			4072.638	19.52664	643.336	124.027
			1592.752	4.00448	760.602	70.59
			934.793	1.30533	799.973	58.009
			1806.864	3.30804	882.403	219.39
MO+Ag ($1x10^{-5}$M)	120000	0.00416	76149.18	21.66805	454.509	3100.827
			654040.7	34.05557	517.287	15002.85
			1136.306	5.84828	220.61	44.273
			1193.018	5.76051	294.869	51.718
			1088.502	5.19926	404.047	46.8
			76343.79	21.66805	454.509	3100.827
			577198.2	34.05557	517.287	15002.85
			71290.59	13.09624	565.351	3345.491
			3939.84	20.18198	643.336	118.645
			1503.285	4.05929	760.602	78.9
			968.7333	1.31587	800.304	54.636
			1865.498	3.27888	882.403	289.336
MO+Ag ($1x10^{-5}$M)	130000	0.00384	76019.34	21.8052	454.509	3108.337
			660210.4	34.05584	517.287	15104.96
			1536.601	6.24561	220.61	50.546
			1198.243	5.79527	294.869	51.764
			972.4708	5.20832	404.047	48.1
			76856.92	21.8052	454.509	3108.337
			581277.4	34.05584	517.287	15104.96
			71977.79	13.08236	565.351	3381.682
			4269.764	22.46982	643.336	123.946

			1688.105	4.08878	760.254	79.409
			922.3757	1.36236	800.304	59.764
			1697.403	3.34087	882.11	162.191
MO+Ag ($1x10^{-5}$M)	140000	0.00357	742883	34.98983	518.127	15489.06
			1466.298	6.21083	220.61	47.191
			1278.663	6.32659	294.869	58.3
			874.568	5.13768	404.047	46.182
			64377.43	21.88438	454.075	2598.027
			594774.8	34.98983	518.127	15489.06
			78463.84	13.02506	565.351	3684.618
			4445.562	20.02161	643.336	136.382
			1477.308	3.99148	760.254	76.655
			1035.247	1.39425	799.973	58.827
			2034.037	3.28396	882.403	287.873
MO+Ag ($1x10^{-5}$M)	150000	0.00333	747931.4	35.26142	518.127	15511.53
			1443.05	6.19437	220.61	50.637
			1380.065	6.23885	294.869	56.091
			1013.054	5.21525	404.047	46.591
			64752.05	21.9695	454.075	2604.91
			598690.3	35.26142	518.127	15511.53
			79186.86	13.20069	565.351	3711.773
			4517.11	25.35217	643.336	145.828
			1514.218	4.02592	760.602	81.6
			867.3874	1.28716	800.304	53.31
			1229.237	3.36623	882.11	96.537

Table (4-16) Fluorescence Spectra of the R6G Dye at different frequency from (10000-150000) Hz with Constant Pumping Time (D.C =50 %)

Dye	Frequency (Hz)	Pumping Time T_{ON} (ms)	Area under the curve	FWHM	λ_f (nm)	Intensity
R6G ($5x10^{-5}$M)	10000	0.05	477623	28.50737	561.262	12060.72
			663.7366	7.81487	220.61	19.982
			703.2746	6.40501	294.869	23.091
			590.7705	5.39359	401.828	16.355
			1241.681	23.62178	478.232	33.009
			186827.5	14.3755	561.262	12060.72
			275899.8	15.40094	565.351	11257.66
			12220.91	18.36926	643.336	473.637
			1385.95	4.37795	760.254	41.319
			384.7304	1.29931	799.973	24.519
			856.2914	3.27403	882.403	108.7
R6G ($5x10^{-5}$M)	20000	0.025	474193.3	28.44755	561.262	12028.24
			570.6114	6.23858	220.61	23.308
			438.3161	5.66241	294.869	19.826
			680.0363	5.37146	404.047	18.844
			1208.557	11.29515	479.089	29.635
			185642.1	14.34057	561.262	12028.24
			275186.5	15.36763	565.351	11236.54
			11677.24	17.41424	643.336	467.608
			929.9774	4.22532	760.254	35.217
			513.2262	1.30567	799.973	26.962
			854.0709	3.32891	882.11	64.772
R6G ($5x10^{-5}$M)	30000	0.01666	477654.5	28.62057	561.262	12079.7
			673.3115	6.11782	220.61	20.672
			871.2467	7.42357	293.945	28.827
			542.9346	5.02801	404.047	16.245
			870.2034	24.75306	477.374	23.309
			186160	14.33021	561.262	12079.7
			277660	15.51805	565.351	11293.09
			11985.31	18.09037	643.336	474.309
			1231.285	4.15539	760.254	41.381
			722.9779	1.30619	799.973	24.445
			954.399	3.38275	882.11	64.591

R6G ($5x10^{-5}M$)	40000	0.0125	481678.2 710.0105 664.6463 663.8679 1294.479 187028.3 280456.1 12142.18 1120.091 710.0013 1176.736	28.67918 7.57123 5.43952 5.09671 13.37626 14.27929 15.60094 18.20313 4.02879 1.45362 3.32023	561.262 185.523 294.869 402.716 479.518 561.262 565.351 643.336 760.254 800.304 882.403	12149.13 26.8 23.782 20.509 34.255 12149.13 11384.15 477.028 43.118 32.673 134.455
R6G ($5x10^{-5}M$)	50000	0.01	275590.2 668.1783 770.8195 510.3435 827.7065 105974.8 160500.3 7258.722 1067.136 528.6896 1051.094	28.32351 5.69858 5.55788 5.01442 5.81435 14.12304 15.32707 19.02494 3.98317 1.35125 3.28685	561.671 220.61 294.869 403.603 447.991 561.671 565.351 643.336 760.602 800.304 882.403	6977.719 26.046 32.619 24.428 30.782 6977.719 6549.355 277.619 46.737 36.537 148.1
R6G ($5x10^{-5}M$)	60000	0.00833	278792.4 719.0865 672.4367 511.1199 1168.582 106816.6 161969.9 7561.035 1197.644 674.3656 1306.297	28.32221 6.64295 5.61565 5.01662 6.28787 14.09899 15.38524 19.03807 4.12221 1.49797 3.27799	561.262 220.61 294.869 403.603 447.556 561.262 565.351 643.336 760.254 800.635 882.403	7025.991 27.536 29.1 27.254 37.991 7025.991 6593.109 281.718 54.909 33.6 167.636

R6G ($5x10^{-5}$M)	70000	0.00714	278182.5	28.32449	561.671	7049.346
			669.4325	5.90383	220.61	28.346
			704.9648	5.70977	294.869	34.391
			666.9167	5.27417	404.047	28.327
			1159.218	5.90662	447.121	37.537
			106854.1	14.0811	561.671	7049.346
			162144.6	15.3755	565.351	6620.309
			7243.018	17.62163	643.336	281.155
			1167.697	4.09844	760.254	56.218
			665.2019	1.30939	800.304	36.527
			1287.672	3.29793	882.403	152.273
R6G ($5x10^{-5}$M)	80000	0.00625	283128.7	28.45475	561.671	7080.536
			795.7662	6.07843	220.61	28.191
			847.8036	6.51698	294.869	37.891
			631.3899	5.36033	404.047	32.909
			1359.451	6.72177	447.991	43.209
			107707	14.0793	561.671	7080.536
			163726.7	15.54041	565.351	6641.518
			7826.301	18.60873	643.336	287.181
			1348.591	4.10593	760.254	58.709
			886.5502	1.60271	800.304	42.627
			1471.272	3.30409	882.11	162.609
R6G ($5x10^{-5}$M)	90000	0.00555	280662.4	28.45637	561.671	7079.755
			902.6611	6.33279	220.61	31.491
			904.4788	6.14594	294.407	35.582
			538.6061	5.05404	404.047	25.046
			1219.254	6.48265	447.991	33.928
			107596.5	14.09396	561.671	7079.755
			163841.2	15.40546	565.351	6667
			7392.251	19.00175	643.336	280.655
			1014.626	3.97002	760.602	52.209
			724.8747	1.32376	800.304	41.346
			1604.052	3.28308	882.403	214.546

R6G ($5x10^{-5}$M)	100000	0.005	289001.5	28.47107	561.671	7175.672
			1000.186	6.23946	220.61	36.291
			865.5737	5.7418	294.869	38.445
			753.3814	5.16758	402.272	33.372
			1287.785	6.41579	447.556	33.882
			109128.5	14.06593	561.671	7175.672
			166137.8	15.4963	565.351	6747.254
			7979.02	19.59852	643.336	287.754
			1645.037	4.19393	760.254	63.782
			1023.13	1.44307	800.304	46.5
			1565.902	3.29565	882.403	207.736
R6G ($5x10^{-5}$M)	110000	0.00454	284112.6	28.4673	561.671	7162.782
			1033.273	6.8929	220.61	42.927
			1137.732	6.57993	294.869	45.736
			719.6487	5.04432	404.047	31.555
			1229.004	5.55046	447.991	40.355
			108761.5	14.05272	561.671	7162.782
			165818.8	15.4777	565.351	6739.927
			7566.971	18.00247	643.336	288.955
			1159.229	3.97791	760.602	57.4
			807.0686	1.31346	800.304	39.509
			1512.458	3.26965	882.403	218
R6G ($5x10^{-5}$M)	120000	0.00416	286785.4	28.48861	561.671	7196.636
			1132.363	7.77789	220.61	37.391
			1077.471	6.63993	294.869	41.791
			673.6568	4.92806	404.047	27.773
			1396.505	6.25972	447.556	46.636
			109403.2	14.05515	561.671	7196.636
			166752.2	15.52918	565.351	6774.364
			7875.789	18.77827	643.336	289.854
			1289.988	4.01447	760.254	63.264
			835.5975	1.32985	800.304	38.582
			1897.776	3.28905	882.403	226.691
R6G ($5x10^{-5}$M)	130000	0.00384	289088.6	28.46668	561.671	7209.545
			887.0998	5.88005	220.61	36.372
			798.7624	5.83723	294.869	38.054
			715.5006	5.26318	403.603	37.109
			1435.478	6.38627	447.121	40.572
			109310.8	14.02821	561.671	7209.545
			166988	15.44791	565.351	6796.791

			7679.708	18.46547	643.336	288.072
			1401.54	4.09237	760.254	59.6
			898.7065	1.29829	799.973	45.654
			1084.801	3.33078	882.11	128.572
R6G ($5x10^{-5}M$)	140000	0.00357	289371.6	28.44969	561.671	7291.191
			795.4489	5.60388	220.61	30.572
			802.8854	6.63989	294.869	41.527
			555.3832	5.10511	404.047	34.482
			1242.255	5.91385	447.556	42.909
			110315.1	14.02188	561.671	7291.191
			168785.3	15.51918	565.351	6865.8
			7474.789	18.91842	643.336	286.582
			1174.488	4.01068	760.254	62.2
			752.7825	1.45186	799.973	45.427
			1082.741	3.29709	882.11	122.309
R6G ($5x10^{-5}M$)	150000	0.00333	291084.1	28.47805	561.671	7320.346
			1073.168	6.24588	220.61	37.418
			1138.536	6.15903	294.869	47.227
			738.4501	5.08011	404.047	31.727
			1083.782	5.66031	447.121	35.237
			110961.2	14.03446	561.671	7320.346
			169656.2	15.54368	565.351	6880.637
			7938.728	18.2113	643.336	296.627
			1352.825	4.05621	760.254	61.637
			744.848	1.27091	800.304	39.318
			1305.467	3.31522	882.11	146.591

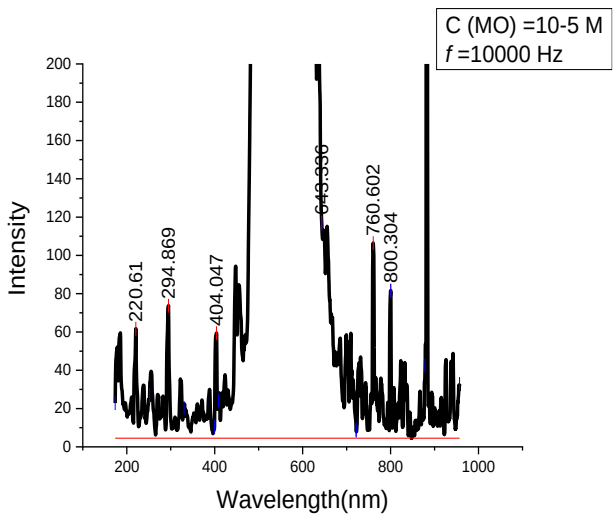

(a) MO dye without AgNPs

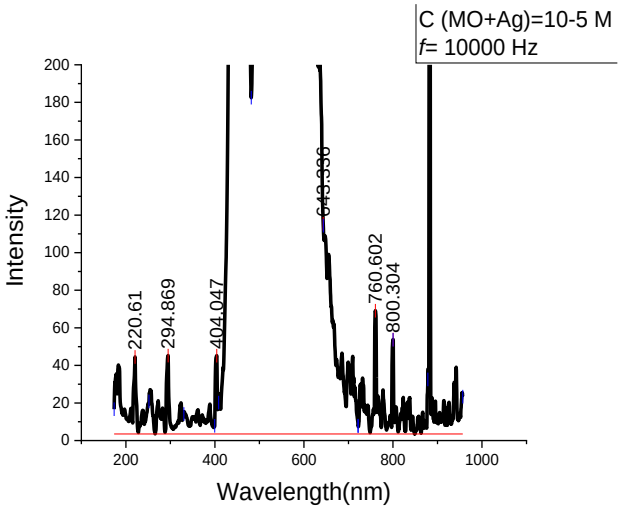

(b) MO dye with AgNPs

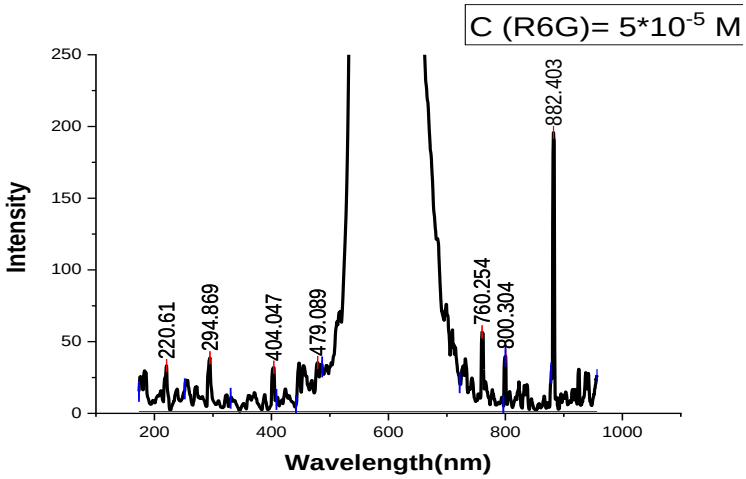

(c) R6G dye

Figure (4-22) Fluorescence Spectra for the MO and R6G Dye at frequency (10000 Hz) with Duty Cycle =50 %, (a)MO dye without AgNPs ,(b) MO dye with AgNPs) ,and(c) R6G dye

4.8 The Estimation of Fluorescence Lifetime

-The dyes extend over a wide range of frequencies as well as over a wide range of energies and to obtain this harmony(consonance) of energies and wavelengths by controlling the frequency ,pulse pumping time and the pumping source that used addition to its concentration and many other factors that effect on the energy magnitude and wavelength of the output laser.

-To obtain the maximum output of the laser ,it is done by controlling the pumping laser pulse with an electronic circuit that acts as a shutter that opens at specific moment and for a calculated period .It controls the time and frequency of the pulse then we can observed the spectrum emitted by the switch which be selected types of dyes. It is done by changing the input parameters of the time and frequency of the laser we get an output that changes with its input .

-An electronic circuit connected with spectra academy device used and designed this circuit is added to control duty cycle and the pulse frequency through this circuit ,we can pumping at different times and we can change the amount of pumping energy given through the following relationship :

$$Dutycycle\,\% = \frac{T_{ON}}{T_{ON} + T_{OF}} \qquad \text{…. (4-1)}$$

$$T_{ON} = DutyCycle \times \frac{1}{f} \qquad \text{…. (4-2)}$$

$$T_{ON} = DutyCycle \times T$$

(T_{ON}) : represent the pumping time (or operation time in sec unite)

(T_{OF}) : is the time when source (Laser ,LED) stops illuminating the material and energy levels stop absorbing

(T) : the time it take to complete a full wave cycle .

The fluorescence lifetime will be estimated by some parameters by using an electronic system that controls frequencies and pumping time to control the operating and off time of the optical pumping source (LED,LASER)

At this stage ,the spectra academy is used ,which is a device that analyzes the spectrum dropped on it and collects it as an intensity over a time relative to the integration time. In this case install the device to measure the intensity of transmittance.

Using a spectrophotometrically studied organic dye (MO,R6G) at an appropriate concentration ,and pump source like green LED for R6G dye and blue LED for MO dye. Then the sample is placed in spectra academy device to analyze the sample according to the change in the parameters of each of the frequencies (f = 10000, 50000, 80000 ,120000 ,150000) Hz and duty cycle (D.C = 10%, 30%, 50% ,70% ,90%)

Practically ,the dyes are pumped with an appropriate pumping source ,then the dyes effectively absorbs the incident wavelength (the electrons will move from lower level to the upper one) and at specific time, it will reaches to saturation state (no absorption occurs) ,it becomes as a optical transmittance medium .It will be closed when it has ability to absorb and nothing passes through it until reaches to saturation state then will be transparent and allows to passes the wavelength through it (becomes open).

Thus the cut-off and permeation continue this means that there are intervals of time in which the filling and discharge of excited and degenerate electrons occur ,which determine the time ,duration and frequency of each pulse. By measuring transmittance intensity which depends on the absorption of the spectral band by energy level of material

so that the intensity is represent as an indicator of the level saturation and the time of emptying the level and this can be seen in the following tables and figures.

There is an important factor in the spectral transitions ,which is the lifetime of the transition , and we practically simulate the transition process that occurs at energy levels through three factors : pumping time ,frequency and integration time in addition to the main factor which is the intensity.

The Data was measured by using spectra academy device and electronic circuit to obtain the Transmittance light intensity of Methyl Orange (MO) Dye at Concentration (1×10^{-5} M) ,Rhodamine 6G Dye at Concentration (5×10^{-5} M) and pumping sources (Blue ,Green) LED with change in pumping time and frequencies at Integration time(t) =30 ms without Ag nanoparticles and with added Ag nanoparticles. It can see from data in table (4.17),(4.18) the intensity magnitude (without adding Ag nano particles) which is as an indicator on absorption and saturation state .

It can see from result in table (4.17) the maximum intensity recorded in transmittance spectra of MO dye is (I=15844.6) at frequency =80000 Hz and pumping time (T_{ON} = 0.01125 ms) (Duty Cycle = 90%) that mean 10% of time the system was OFF and 90% was ON

The result in table (4-18) shows the maximum intensity recorded in transmittance spectra of R6G dye is (I=15943.4) at frequency =80000 Hz and pumping time (T_{ON} = 0.00375 ms) (Duty Cycle = 30%) that mean 70% of time the system was OFF and 30% was ON therefore, at this pumping time and frequency the molecules transitions to upper level and has reach to saturation limit and energy level filled with electrons .At this

time , in this case the processes leading to optical limiting through this technology ,the pumping source of the dye once work as an optical limiter and became a process of filling the upper level ,and it endures along time until it reaches to the saturation state and runs out.

While the lowest intensity of MO dye is (I=13378.7) ,pumping time (T_{ON} = 0.01 ms) and (f=10000 Hz) and lowest intensity of R6G dye is (I=14941.7) ,pumping time (T_{ON} = 0.000625 ms) (Duty Cycle = 50%) and f=80000 Hz at this time there is energy levels that still need to be filled so we can observed the absorption state occur so the photons are still transmittance and an indication of this is the lowest transmittance intensity (it is evidence that energy levels during this time were unstable).

This steps represent a point for calculating the fluorescence lifetime is a measure of the time a fluorophore spends in the excited state before returning to the ground state by emitting a photon.

After measure transmittance spectra of MO and R6G Dye by using Spectra Academy device as can see in figure (4-23) will analyze the data in origin program as shown in figures (4-24), and (4-25) it notice there is many wavelengths (peaks) appear addition to the original peak started from (182 nm) to (882nm) for MO dye and wavelengths peaks of R6G dye started from (220 nm to 882nm) ,this indicates to presence of absorption regions from the beginning and therefore it results in emission regions, and these wavelengths (peaks) result from transitions that occurred in the energy levels ,but the reason for appear these transitions because it was fed with appropriate energy different between levels of the material by changing the frequency and pumping time through the pumping method used which it is building a electronic circuit were able to control the frequency and pumping time.

From this mechanism can make a match between frequency and pumping time and get the appropriate amount of energy for the levels ,therefore the match that we will get is the same amount of increase in efficiency therefore ,obtaining wavelengths resulting from transitions that did not exist previously ,also this number of peaks that we get from this technique refers to the efficiency of the pumping system and this could open up horizon for many applications that are not yet known .

The effect of adding Ag nanoparticles to MO dye on spectrum band and the energy levels were effectively effect by the addition of nano materials to the dye which led to an increase in absorption cross section and that led to scattering light occur ,which can be seen from the increase in intensity, also we can notice after adding Ag nanoparticles to MO dye there is increase in transmittance light intensity and the maximum intensity is (I=15886.7) at pumping time (T_{ON} = 0.00083 ms) (Duty Cycle = 10%) and frequency =120000 Hz, this means electrons transition to upper level and reach to saturation limit in less time (energy levels is full).

Therefore the addition of nanomaterials to dye due to improved the stability of energy level and thus gave an decrease in lifetime that can be observed through the indicator of the intensity of the transmitted light ,and it is clear from the result that after adding nanomaterial to the MO dye the peak wavelength is shifted from (457) nm to (451) nm and this refers that is a blue shift has occurred towards short wavelengths because the absorption occurs in this region of the spectrum as a result of the addition of Ag nano particles as show in table (4-17).

The results of table (4-17),(4-18) is shows in figures (4-26),(4-27) the relationship between the intensity of transmitted light relative to the change in pumping time ,where the top peaks show us that the light transmittance was at high (maximum) intensity at this point when pumped at this time and frequency (it reached to saturation limit).while the bottom in the figures represent the minimum intensity of the transmitted light ,meaning that it is still in absorption state at this pumped time and frequency.

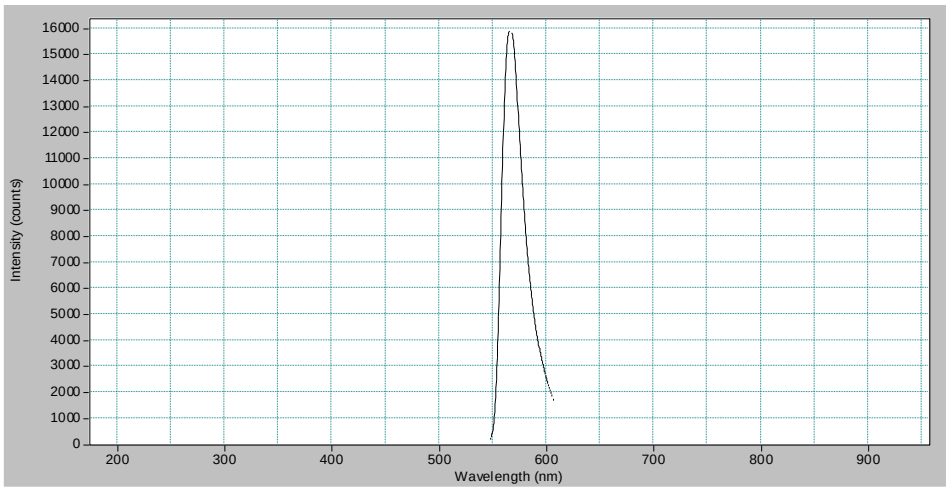

(a) Rhodamine 6G Dye at Concentration (5×10^{-5} M)

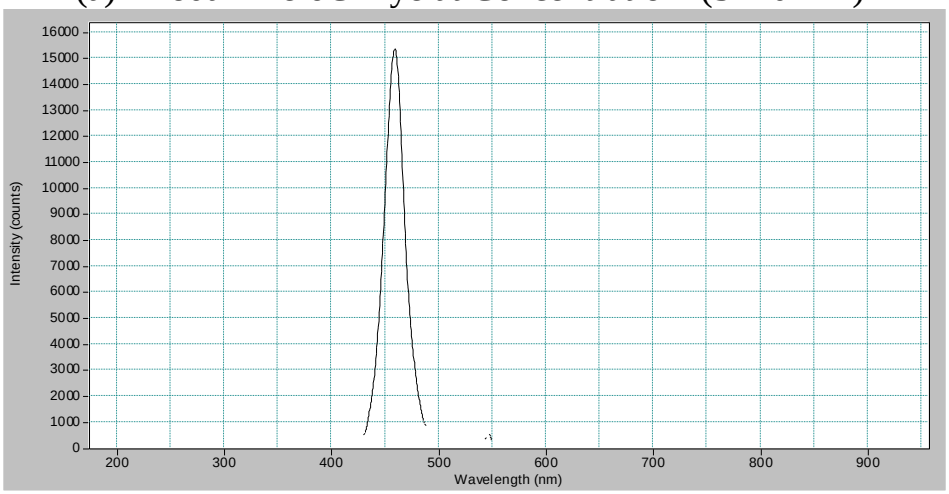

(b) MO Dye at Concentration (1×10^{-5} M)

Fig (4-23) An image showing the Transmittance Spectrum for (a) R6G and(b) MO Dye

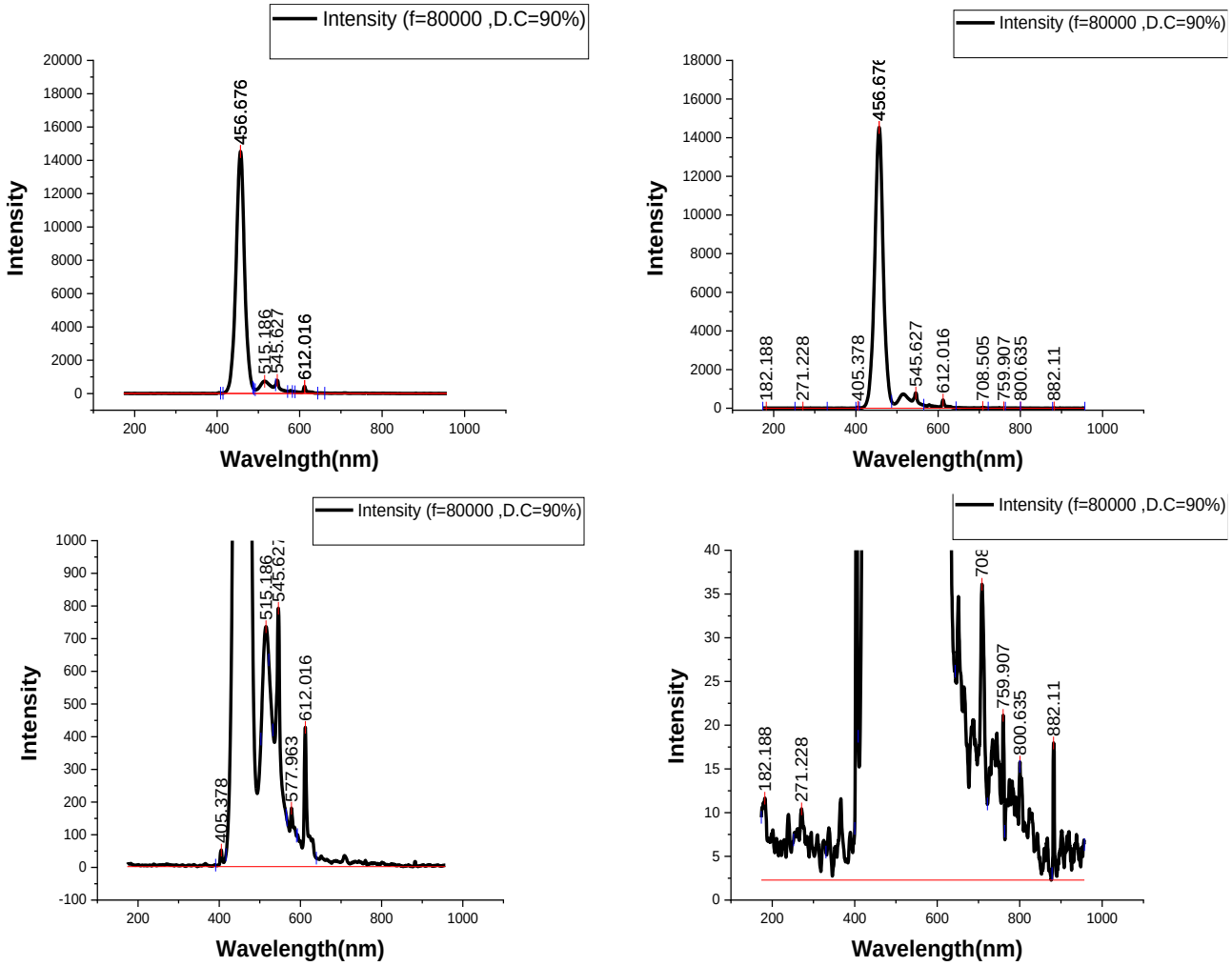

Figure (4-24) The Transmittance spectrum analysis of MO dye in origin program

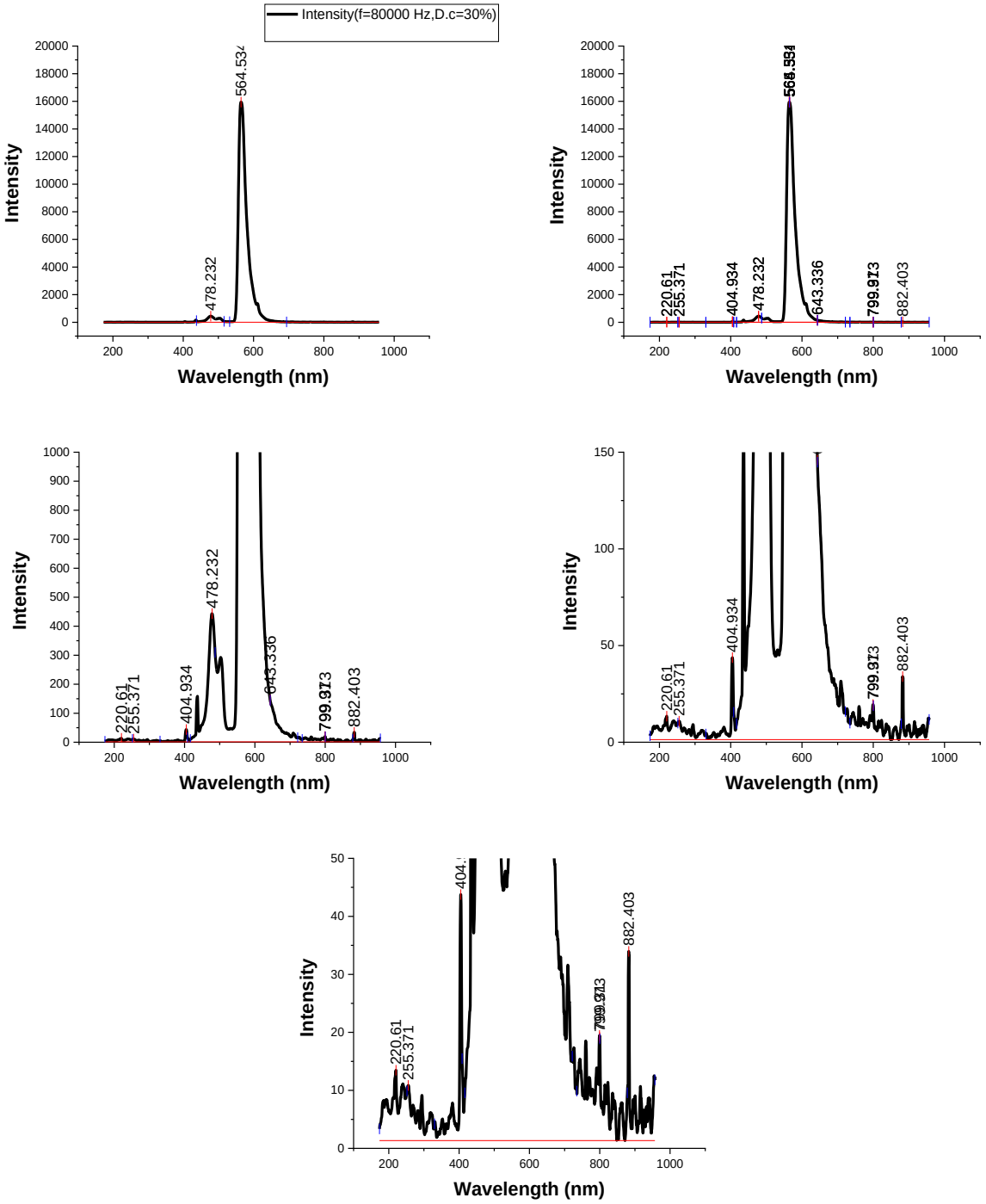

Figure (4-25) The Transmittance spectrum analysis of R6G dye in origin program

Table (4-17) Transmittance light intensity of Methyl Orange (MO) Dye at Concentration (1×10^{-5} M) With change in Pumping Time (ms) and frequencies at Integration time(t) = 30 ms without added Ag nanoparticles and with Added Ag nanoparticles

f (Hz)	Duty Cycle (%)	Pumping Time (T_{ON}) (ms)	Intensity without Ag	Peak Wavelength (nm) without Ag	Intensity with Ag	Wavelength (nm) with Ag
10000	10	0.01	13378.7	457.11	15401.3	451.904
	30	0.03	15211.7	457.11	15673.4	451.904
	50	0.05	14079.2	457.543	15853.8	452.338
	70	0.07	15446.7	457.543	15554.1	452.338
	90	0.09	15838.3	457.11	15858.2	451.904
50000	10	0.002	15842.2	457.11	15762.5	451.904
	30	0.006	15839.7	457.11	15766.8	451.904
	50	0.01	15840.6	457.11	15840.3	451.904
	70	0.014	15841.5	457.543	15801.7	451.904
	90	0.018	15818.6	457.543	15850.9	452.338
80000	10	0.00125	15806.5	457.11	15764.6	451.904
	30	0.00375	15830.1	457.11	15692.4	451.904
	50	0.00625	15797.4	457.543	15847.5	452.338
	70	0.00875	15830.8	457.543	15777	452.338
	90	0.01125	15844.6	457.976	15302.9	452.338
120000	10	0.00083	15844.5	457.11	15886.7	451.904
	30	0.00249	15835.4	457.11	15883.3	451.904
	50	0.00416	15839.1	457.543	15766	451.904
	70	0.00583	15675.7	457.543	15870.3	452.338
	90	0.00749	15770.2	457.976	15862	452.338
150000	10	0.00066	15737.3	457.11	15609.3	452.338
	30	0.002	15788.9	457.11	15874.6	451.904
	50	0.00333	15799.3	457.543	15878	451.904
	70	0.00466	15786.4	457.543	15795.6	452.338
	90	0.006	15799.2	457.976	15860.4	452.338

Duty Cycle (%)	Pumping Time (ms)	*f* (Hz)	Intensity without Ag	Wavelength (nm) without Ag	Intensity with Ag	Wavelength (nm) with Ag
10	0.01	10000	15743	456.676	15758.7	451.904
	0.002	50000	14798.6	456.243	15730.7	451.904
	0.00123	80000	15739.4	456.243	15732.4	451.904
	0.00083	120000	15580.3	456.243	15844.2	451.904
	0.000666	150000	15705.8	456.243	15871.2	451.904
30	0.03	10000	15525.7	456.243	15866.4	451.904
	0.006	50000	15611.6	456.676	15870.9	451.904
	0.00375	80000	15526.5	456.676	15864.8	451.904
	0.00249	120000	15844.5	457.543	15856.3	451.904
	0.002	150000	15652.1	457.543	15863.3	451.904
50	0.05	10000	15832.4	457.543	15459.4	453.641
	0.01	50000	15719	457.543	15846	456.676
	0.00625	80000	15838.3	457.543	15844.9	452.338
	0.00416	120000	15826.9	457.543	15840.8	452.338
	0.00333	150000	15827	457.543	15846.1	451.904
70	0.07	10000	15796	457.543	15660.1	451.904
	0.014	50000	15824	457.543	15840.7	451.904
	0.00875	80000	15809.4	457.543	15846.6	457.543
	0.00583	120000	15820.5	457.543	15782.2	457.543
	0.40066	150000	15821.4	457.543	15633.5	457.11
90	0.09	10000	15737.3	457.976	15838.5	458.409
	0.018	50000	15788.9	457.976	15841.7	460.141
	0.01125	80000	15799.3	457.976	15831.5	452.388
	0.00749	120000	15786.4	457.976	15836.2	451.904
	0.006	150000	15799.2	457.976	15843.8	451.904

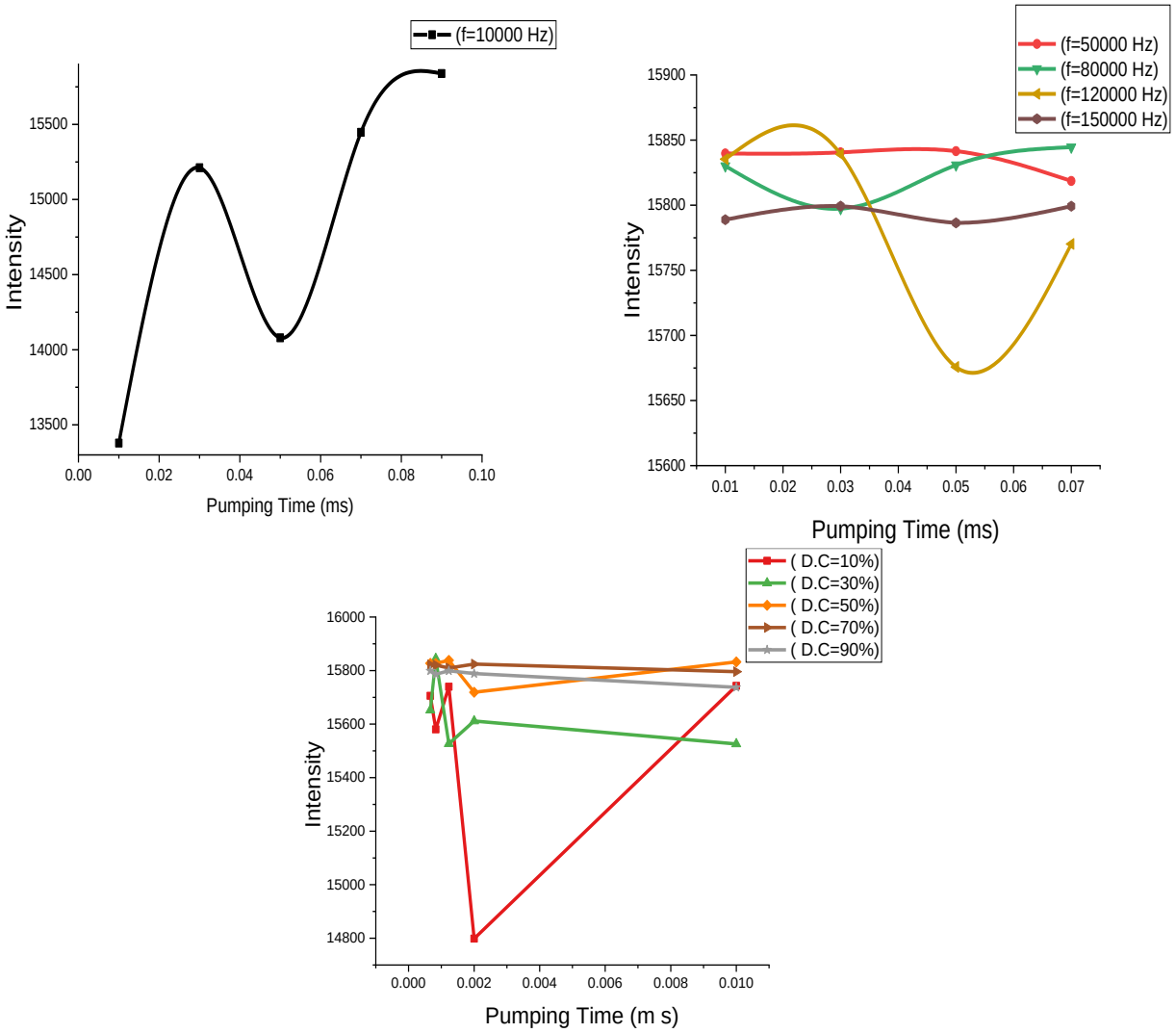

(a) without added Ag nanoparticles

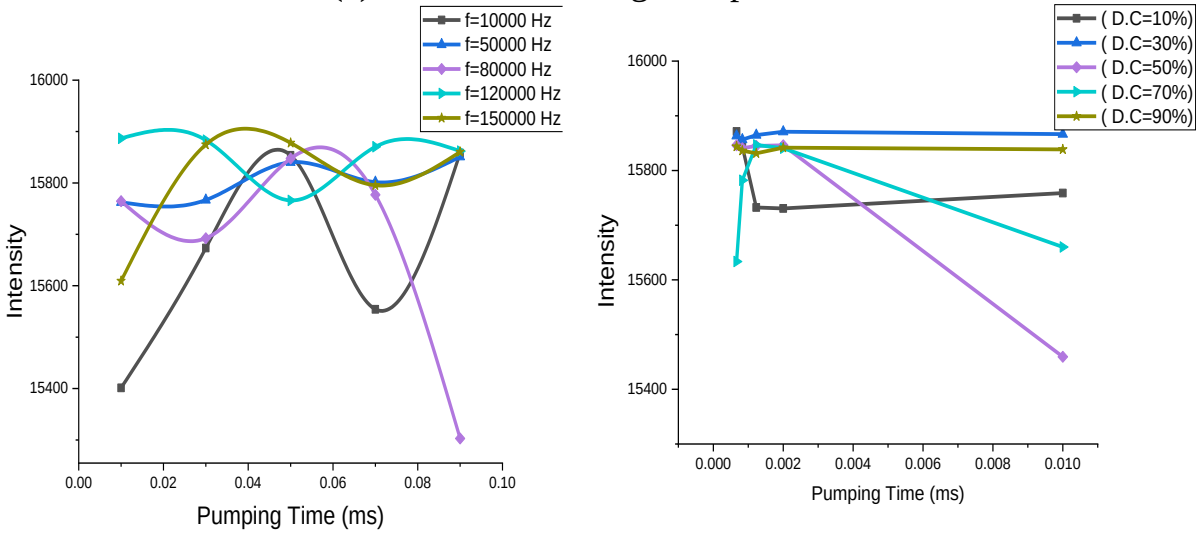

(b) with added Ag nanoparticles

Fig(4-26) The Transmittance light intensity of Methyl Orange (MO) Dye at Concentration (1×10^{-5} M) versus Pumping time (ms) With change in duty cycle and frequencies ,(a) without added AgNPs , (b) with added AgNPs

Table (4-18)Transmittance light intensity of Rhodamine 6G Dye at Concentration (5×10^{-5} M) With change in Pumping Time (ms) and frequencies at Integration time(t) = 30 ms

Frequency (Hz)	Duty Cycle (%)	Pumping time (ms)	Intensity	Wavelength (nm)
10000	10	0.01	15722.6	564.943
	30	0.03	15917.9	564.943
	50	0.05	15924	564.943
	70	0.07	15917.9	564.943
	90	0.09	15922	564.943
50000	10	0.002	15932.6	564.943
	30	0.006	15938.7	564.943
	50	0.01	15881.7	565.351
	70	0.014	15938.2	565.351
	90	0.018	15941.6	565.351
80000	10	0.00125	15794.2	564.126
	30	0.00375	15943.4	564.534
	50	0.00625	14941.7	564.943
	70	0.00875	15932.5	564.943
	90	0.01125	15930.1	564.943
120000	10	0.00083	15843.3	564.534
	30	0.00249	15924.4	565.351
	50	0.00416	15924.2	565.351
	70	0.00583	15921.6	564.943
	90	0.00749	15916.8	565.351
150000	10	0.00066	15893.8	564.126
	30	0.002	15890.6	565.76
	50	0.00333	15802.6	565.351
	70	0.00466	15895	565.351
	90	0.006	15885.8	564.943

Duty Cycle (%)	Pumping time (ms)	Frequency (Hz)	Intensity	Wavelength (nm)
10	0.01	10000	15878.4	564.534
	0.002	50000	15852.4	564.126
	0.00123	80000	15872.8	564.126
	0.00083	120000	15867.5	564.126
	0.000666	150000	14944.1	564.126
30	0.03	10000	15863.7	564.943
	0.006	50000	15828.5	564.943
	0.00375	80000	15852.9	564.943
	0.00249	120000	15851.5	564.943
	0.002	150000	15848	564.943
	0.05	10000	15826.9	564.943
50	0.01	50000	15827.7	565.351
	0.00625	80000	15827.3	565.351
	0.00416	120000	15808.8	564.943
	0.00333	150000	15822.5	564.943
70	0.07	10000	15816.1	564.943
	0.014	50000	15803.4	565.351
	0.00875	80000	15719.8	565.351
	0.00583	120000	15804.6	565.351
	0.40066	150000	15810.6	565.351
90	0.09	10000	15802.4	565.351
	0.018	50000	15793.7	565.351
	0.01125	80000	15801.2	565.351
	0.00749	120000	15794.8	565.351
	0.006	150000	15793.5	565.351

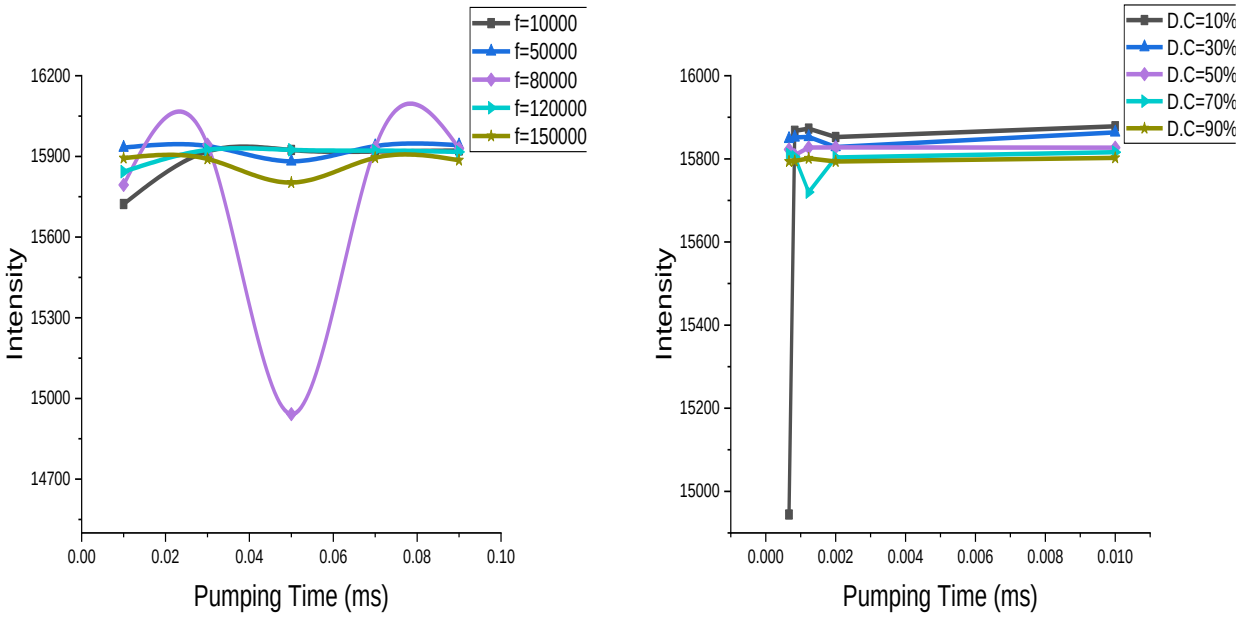

Fig(4-27) Transmittance light intensity of Rhodamine 6G Dye at Concentration (5×10^{-5} M) vs Pumping time (ms) With change in duty cycle and frequencies with Integration Time =30 (ms)

4.8.1 The influence of Different Integration Time (30ms ,60ms and 90 ms) on Transmittance Spectrum Analysis

To improve the accuracy of spectral measurement, extensive efforts are required to minimize external interference and instrument error. Previous studies successfully increased the measurement accuracy by optimizing temperature, humidity , path length , and so on, but few studies have evaluated the influence of integration time, which determines spectrometer sensitivity .

An ideal spectrum should neither be saturated nor be too weak; a saturated spectrum will lose wavelength information and a weak spectrum will lead to a low SNR. Thus, the appropriate integration time is artificially determined to ensure the spectrum is captured in an ideal range .

Although the spectrometer is constantly optimized, due to dynamic changes in sample concentration and limited measurement range of the spectrometer, the integration time for one sample may not be suitable for other samples; which may produce a saturated spectrum that leads to information loss or a weak spectrum that lead to a low SNR. In this case, the integration time must be changed to obtain the ideal spectrum.

The integration time is define as the signal collection time (is the time window during which a given pulse is measured), integration time , it is an important and essential factor in the pumping process, as it represent the amount of time that the detector receives photons also effect on the lifetime of transitions .

The influence of different integration time (30ms ,60ms and 90 ms) on the intensity of transmitted light with different pumping times as shown in table (4-19). It is prove that the integration time is effect on

transmittance intensity by observing the increase in transmittance intensity when increase integration time from 30 ,60 to 90 ms this means any increase in intensity demonstrates full signal collection of spectrum and appropriate integration time ,except there are some result in table (4-19) which are as follows:

- The transmittance intensity was 15841.5 ms at frequency =10000 Hz and pumping time =0.03 ms

- The transmittance intensity was 15380.8 ms at frequency =50000 Hz and pumping time =0.002 ms

- The transmittance intensity was 15716 ms at frequency =80000 Hz and pumping time =0.01125 ms

- The transmittance intensity was 15850.1 ms at frequency =120000 Hz and pumping time =0.00583 ms

- The transmittance intensity was 15789.9 ms at frequency =150000 Hz and pumping time =0.002 ms

- The transmittance intensity was 15764.3 ms at frequency =150000 Hz and pumping time =0.006 ms

All values above are measured at integration time (90ms)

It can see increase in transmittance intensity at integration time 30ms and 60 ms, but some values above the transmittance intensity decrease at integration time 90 ms ,it means this values above there was not matching between frequency and data integration time

Also from the result in table (4-19) from value below ,the transmittance intensity decrease at integration time 60 ms and then it increased again at integration time 90 ms

-The transmittance intensity was 15710.7 ms at frequency =50000 Hz and pumping time =0.01 ms with integration time 60 ms

-The transmittance intensity was 15797.2 ms at frequency =50000 Hz and pumping time =0.014 ms with integration time 60 ms

It conclude from these result ,that the increase in transmittance intensity indicate to the amount of matching between frequency and the data integration time while any decrease in transmittance intensity indicates that the frequency does not match with integration time , which in turn affect on the fluorescence lifetime .

Figure (4-28) shows there is a clear point ,which is practically there is low transmittance and then high transmittance or vice versa as show in results and figures and then the intensity of the transmittance increases for a certain period of time and then it decreases .therefore at this time and frequency the intensity will be high there will be a matching between the transmission time and the data collection time .

Table (4-19) Transmittance light intensity of Methyl Orange (MO) Dye at Concentration (1×10^{-5} M) at different Pumping Times (ms) and frequencies at Integration time(t) = (30, 60 and 90 ms)

f (Hz)	D.C %	T_{ON} (ms)	Intensity with t=30ms	λ (nm) with t=30ms	Intensity with t=60ms	λ (nm) with t=60ms	Intensity with t=90ms	λ (nm) with t=90ms
10000	10	0.01	13378.7	457.11	15822.4	457.543	15901.6	458.409
	30	0.03	15211.7	457.11	15843.5	457.543	15841.5	457.976
	50	0.05	14079.2	457.543	15839.4	457.543	15889.4	457.976
	70	0.07	15446.7	457.543	15847.8	457.543	15893.5	458.842
	90	0.09	15838.3	457.11	15843.1	457.543	15884.8	458. 409
50000	10	0.002	15842.2	457.11	15848.6	457.543	15380.8	457.11
	30	0.006	15839.7	457.11	15852.6	457.11	15878.1	457.11
	50	0.01	15840.6	457.11	15710.7	457.11	15859.8	457.976
	70	0.014	15841.5	457.543	15797.2	457.11	15859.1	457.976
	90	0.018	15818.6	457.543	15853.9	457.11	15870.5	457.976
80000	10	0.00125	15806.5	457.11	15814.6	457.11	15865.6	457.976
	30	0.00375	15830.1	457.11	15852.1	457.11	15858.2	457.543
	50	0.00625	15797.4	457.543	15847.6	457.11	15893.8	458.842
	70	0.00875	15830.8	457.543	15852.7	457.543	15890.5	458.409
	90	0.01125	15844.6	457.976	15845.6	457.543	15716	458.409
120000	10	0.00083	15844.5	457.11	15858.1	457.543	15915.3	457.976
	30	0.00249	15835.4	457.11	15858.5	457.543	15897	457.976
	50	0.00416	15839.1	457.543	15853.9	457.543	15901.6	457.976
	70	0.00583	15675.7	457.543	15855.8	457.543	15850.1	457.976
	90	0.00749	15770.2	457.976	15850.2	457.543	15928.1	458. 409
150000	10	0.00066	15737.3	457.11	15853.1	457.543	15933.2	457.543
	30	0.002	15788.9	457.11	15852	457.543	15789.9	457.976
	50	0.00333	15799.3	457.543	15824.9	457.543	15934.4	457.976
	70	0.00466	15786.4	457.543	15849.8	457.543	15943.9	457.976
	90	0.006	15799.2	457.976	15846.7	457.543	15764.3	458.409

D.C %	T_{ON} (ms)	*f*(Hz)	Intensity with t=30ms	λ (nm) with t=30ms	Intensity with t=60ms	λ (nm) with t=60ms	Intensity with t=90ms	λ (nm) with t=90ms
10	0.01	10000	15743	456.676	15850.6	457.543	15873.9	457.543
	0.002	50000	14798.6	456.243	15845.7	457.11	15949	457.543
	0.00123	80000	15739.4	456.243	15836.7	456.676	15780.9	457.543
	0.00083	120000	15580.3	456.243	15841.9	457.11	15961.4	457.543
	0.000666	150000	15705.8	456.243	15844.5	457.11	15851.3	457.976
30	0.03	10000	15525.7	456.243	15843.2	457.11	15715	457.976
	0.006	50000	15611.6	456.676	15823.9	457.11	15955.2	457.976
	0.00375	80000	15526.5	456.676	15843.4	457.11	15827.8	457.976
	0.00249	120000	15844.5	457.543	15841	457.11	15816.2	457.976
	0.002	150000	15652.1	457.543	15834.2	457.11	15922.7	457.976
	0.05	10000	15832.4	457.543	15838.6	457.543	15938.3	457.976
50	0.01	50000	15719	457.543	15842.3	457.11	15929.1	457.976
	0.00625	80000	15838.3	457.543	15837.1	457.11	15860.2	457.976
	0.00416	120000	15826.9	457.543	15830.1	457.11	15918.3	457.976
	0.00333	150000	15827	457.543	15832	457.11	15920.9	457.976
70	0.07	10000	15796	457.543	15840.6	457.11	15813.5	458.409
	0.014	50000	15824	457.543	15839.5	457.11	15911.7	458.409
	0.00875	80000	15809.4	457.543	15839.1	457.543	15911.9	458.409
	0.00583	120000	15820.5	457.543	15744.4	457.543	15892	458.409
	0.40066	150000	15821.4	457.543	15835.1	457.543	15841.7	458.409
90	0.09	10000	15737.3	457.976	15832.8	457.543	15829.2	458.409
	0.018	50000	15788.9	457.976	15824.8	457.543	15677.5	458.409
	0.01125	80000	15799.3	457.976	15584.5	457.543	15884	458.409
	0.00749	120000	15786.4	457.976	15834.6	457.543	15883.8	458.409
	0.006	150000	15799.2	457.976	15823.1	457.543	15893.7	458.409

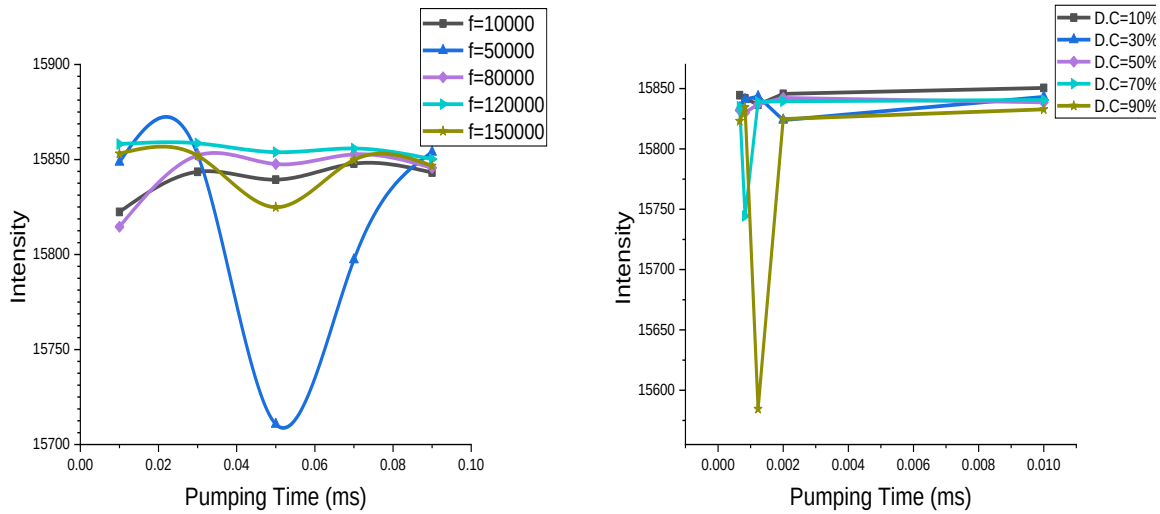

(a) at Integration Time = 60ms

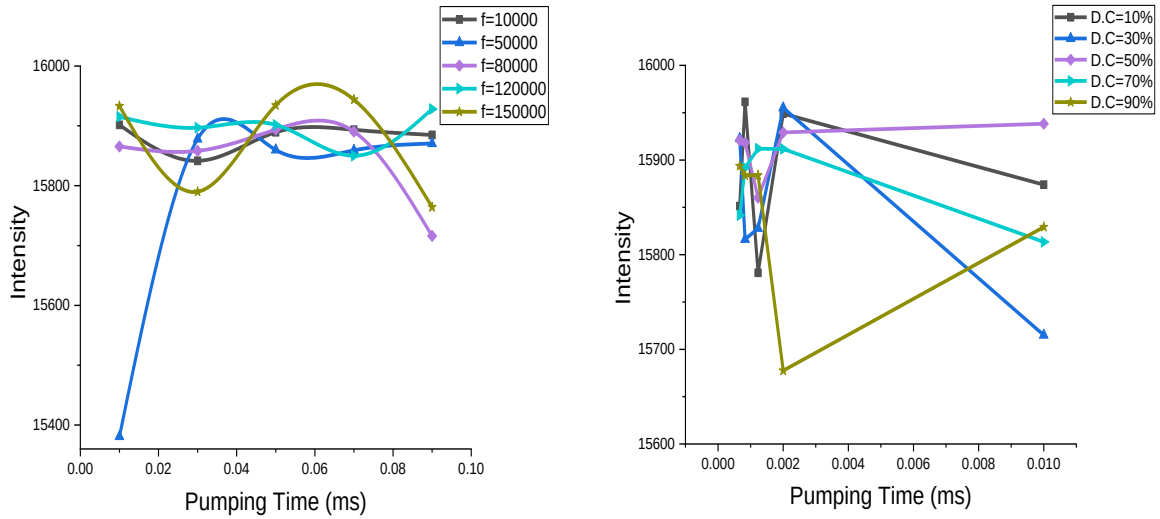

(b) at Integration Time = 90ms

Fig(4-28) Transmittance light intensity of Methyl Orange (MO) Dye at Concentration (1×10^{-5} M) vs Pumping time (ms) With change in duty cycle and frequencies with Integration Time = 60ms and 90ms

5.1 Conclusions

From our study of the organic dyes (R6G ,MO) for different cases, the conclusion of the results are described below.

1. The fluorescence spectra for (R6G ,MO) dyes, drift towards longer wavelengths with increasing concentration of dyes.
2. Added Ag nano particles to MO dye can effect on the absorption and fluorescence spectra
3. The nonlinear optical properties, it was found that the nonlinearity of the dye increases with increasing concentration of the two dyes and depends mainly on the concentration of the dye and the wavelength used.

4. Designing a special electronic circuit (TTL) that can control through it the frequency and pumping time and from the pumping time it will be possible to know how much energy the level needs.

5. Studying the fluorescence spectra of (R6G ,MO) dyes with Spectra Academy device connected with a Special Electronic Circuit and frequencies from (10000-150000) Hz, and install the duty cycle at D.C = 50 %. It is noticeable there is many wavelengths (peaks) appear addition to the original peak start from (220 nm) to (882nm) and these wavelengths (peaks) result from transitions that occurred in the energy level and this due to the mechanism that used

6. It is possible that a peaks can be noticed at a wavelength (800.304 , 882.403) nm for MO dye with (799.973, 882.11) nm for R6G dye and this wavelength is not present in previous studies ,but it is present according to the pumping method used in this research

7. Studying the transmittance spectrum with using Electronic Circuit and analyze the sample at frequencies (f = 10000, 50000, 80000 ,120000

,150000) Hz and duty cycle (D.C = 10%, 30%, 50% ,70% ,90%), for Methyl Orange (MO) and Rhodamine 6G Dye. There was the maximum intensity recorded in transmittance spectra of (R6G, MO) dyes. In this case the processes leads to optical switches through this technology ,this pumping method of the dye can enhance to work as an optical switches and became a process of filling the upper level ,and it endures along time until it reaches to the saturation state and runs out.

8. Any decrease in transmittance intensity indicates that the frequency does not match with integration time despite the increase in the integration time , which in turn affect on the fluorescence lifetime therefore, the amount of matching between frequency and the data integration time is one of the important factors .

9. The possibility of using the organic dyes as an optical switches.

5.2 Future Works

1-Studing the effect of the diameter of the added nanomaterials on the behavior of the dyes used (with the same previous steps ,but using nanomaterials with small or large diameters) and the effect of this on the absorption beams , the absorption cross –section , speed of transitions and filling time.

2- Study the effect of temperature from (20-50) °C on dye behavior and parameters before and after addition of nanomaterials

3-Studing the resulting transitions in some spectral regions and the possibility of using them in suitable applications

References

[1] F.P.Schafer, Dye lasers, Springer-VerIag,Berlin ,(I989).

[2] Krishnamurthy R.R. and Alkondan A., "Nonlinear characterization of mercurochrome dye for potential application in optical limiting", Optica applicata, Vol.XL, No.1, PP.187-196, (2010).

[3] Huang T., Hao Z., Gong H., Liu Z., Xiao S., Li S., Zhai Y., You S., Wang Q. and Qin J., "Third-order nonlinear optical properties of mew copper coordination compound : a promising candidate for all-optical switching", Chemical physics letters, Vol.464, No.4, PP.213-217, (2008).

[4] Nalla V., Rao D.N., Lingamallu G. and Somo V.R., "Femtosecond nonlinear optical properties of alkoxy phthalocyanines at 800 nm studied using z-scan technique", Chemical physics letters, Vol.464, No.4,PP .213-217, (2008).

[5] Boyd R.W., "Nonlinear Optics", Third Edition, Rochester, NewYork, (2007).

[6] Trager F., "Handbook of Lasers and Optics", Springer, (2007).

[7] Sheik-Bahae M., Said A.A., Wei T-H., Hagan D.J. and Van stryland E.W., "Sensitive measurement of optical nonlinearities using a single beam", Ieee journal of quantum electronics, Vol.26, No.4, PP.760-769, (1990).

[8] Chapple P. B., Staromlynska J., Hermann J.A. and Mckay T. J., "Single – beam z-scan: measurement techniques and analysis", Journal of nonlinear optical physics and materials, Vol.6, No.3, PP.251-293, (1997).

[9] Ali Q.M. and Palanisamy P. K., "Investigation of nonlinear optical properties of organic dye by z-scan technique using He-Ne laser", Optik, Vol.116, No.11, PP.515-520, (2005).

[10] Sundari R.M. and Palanisamy P.K., "Optical nonlinearity of atriphenyl methane dye as studied by z-scan and self-diffraction techniques", Modern physics letter B, Vol. 20, No.9, PP.887-897, (2006).

References

[11] Ali Q.M. and Palanisamy P.K., "Z-scan determination of the third order optical nonlinearity of organic dye Nile blue chloride", Modern physics letter B, Vol.20, No.11, PP.623-632, (2006).

[12] Nooraldeen A.Y., Dhinaa A.N. and Palanisamy P.K., "Nonlinear optical properties of acid orange 10 dye by z-scan technique using Ar+ laser ", Journal of nonlinear optical physics and materials, Vol.16, No.3, PP.359-366, (2007).

[13] Qi S., Zhang C., Yang X., Chen K., Zhang L., Yang G., Ling X., Xu T. and Tian J., "effective indexes of refraction and limiting properties of ethyl red", Optik-international journal for light and electron optics,Vol.118, No.9, PP.425-429, (2007).

[14] Qi S., Zhang C., Yang X., Chen K., Zhang L., Yang G., Ling X., Xu T. and Tian J., "Absorption characteristic and limiting effect Congo red doped PVA film", Optical materials, Vol.29, No.11, PP.1348-1351, (2007).

[15] VaLsalamilka B., Sreekumar G.,Muneera C.I., Senahil K. and Vijayan C., "Nonlinear refraction of coomassise brilliant blue dye in PVA matrix", Journal of materials science, Vol. 40, No.3, PP.777-778, (2005).

[16] Nur Farizan Binti Munajat," Study OF Saturable Absorber Materials For Q-Switching Dye Laser" ,Faculty of Science Universiti Teknologi Malaysia , August (2005).

[17] Hassan H. Hammud · Kamal H. Bouhadir ·Mamdouh S. Masoud · Amer M. Ghannoum ·Sulaf A. Assi." Solvent Effect on the Absorption and Fluorescence Emission Spectra of Some Purine Derivatives: Spectrofluorometric Quantitative Studies", Article *in* Journal of Solution Chemistry · Doi: 10.1007/s10953-008-9289-8, July (2008**).**

[18] Sahib Nimma Abdul-Wahid, Methaq Mutter Mehdy Al-Sultany. "study of the optical properties for BDN-I dye solutions which are used to

Q-switch the Nd:YAG laser", Journal of Kerbala University , Vol. Journal 6 No.1 Scientific .March. (2008).

[19] Rekha Rathnagiri Krishnamurthy,Ramalingam Alkondan. "Nonlinear characterization of Mercurochrome dye for potential application in optical limiting".,Optica Applicata, Vol. XL, No. 1, (2010).

[20] Mahmoud E. M. Sakr, Maram T. H. Abou Kana Gamal Abdel Fattah., " Lifetime, Efficiency and Photostability Enhancement of Pyrromethene Laser Dyes by Metallic Ag Nanoparticles", Arab Journal of Nuclear Science and Applications, 47(1), (99-106)(2014).

[21] Hassan A.F., Al-Hamdani A.H. and Abbas F.S., "Study the effect of concentration on spectroscopic properties of fluorescein sodium dye in ethanol", Journal of kufa- Physics,Vol.6, No.1, PP.112-118, (2014).

[22] Florian M. Zehentbauer , Claudia Moretto , Ryan Stephen, Thangavel Thevar , John R. Gilchrist , Dubravka Pokrajac , Katherine L. Richard , Johannes Kiefer ."Fluorescence spectroscopy of Rhodamine 6G: Concentration and solvent effects", Spectrochimica Acta Part A: Molecular and Biomolecular Spectroscopy 121 ,147–151(2014).

[23] Duanduan Wu, Jian Peng, Zhiping Cai,Jian Weng, Zhengqian Luo,Nan Chen, and Huiying Xu " Gold nanoparticles as a saturable absorber for visible 635 nm Q-switched pulse generation" .©2015 Optical Society of America , | Vol. 23, No. 18 |,7 Sep (2015).

[24] Shavakandi S.M., and Sharifi S., "Linear and nonlinear optical properties of fluorescein sodium salt doped droplet", Optical and quantum electronics,Vol.49, No.1,PP.26, (2017).

[25] Husam Sabeeh. "Effects of Adding Nanoparticles to Laser Dyes on Photophysical Processes and Estimating Theoretical Models for Some of These Processes", Mustansiriyah University College of Science, (2019).

References

[26] S Jeyaram, S. Hemalatha, T Geethakrishnan, "Nonlinear refraction, absorption and optical limiting properties of disperse blue 14 dye" Chemical Physics Letters, doi: https://doi.org/10.1016/ j.cplett.2019.137037,(2019).

[27] Hiroki Tanka ,Christian Krankel, and Fumihiko, And Fumihiko Kannari ,"Transition-metal-doped saturable absorbers for passive Q-switching of visible lasers," Optical Materials Express /Vol. 10, No. 8 /1 August (2020) .

[28] Afrah M. Al Hussainey , Ban A. Naser ," Non-Linear Optical Properties of Organic Laser Dye" Annals of R.S.C.B., ISSN:1583-6258, Vol. 25, Issue 6, Pages. 11556 - 11567 (2021).

[29] Duarte F.J.," Tunable laser optics", Elsevier Academic Press, New York, (2003).

[30] Ulrich B., "Laser dyes", Third Edition, Lambda physika AG.D, Germany, (2000).

[31] Sadik Z.S., Al-Amiedy D.H. and Jaffar A.F., "Third order optical nonlinearities of C450 doped polymer thin film investigated by the zscan", Advances in materials physics and chemistry, Vol.2, No.01, PP. 43-49, (2012).

[32] Mahdi Z.F.,"Improement of nonlinear optical properties for mixture laser dyes doped PMMA", Iraqi journal laser, Part A, Vol.9, No.2, PP.9-14, (2012).

[33] Shankarling G.S. and Jarag K.J., " Laser dyes", Resonance, Vol.15, No.9, PP.804-818, (2010).

[34] Henry R. Aldag, David H. Titterton, From Flashlamp-Pumped Liqud Dyes Lasers to Diode- Pumped Solid-State Dye Lasers, SPIE photonics West (2005).

[35] F.P.Schafer,W.Schmidt, J .V01ze, Organic dye solution laser, App.Phys.Le1t. 3306-3309, 9(1966).

References

[36] Watanabe, K., D. Menzel, N. Nilius, H.J. Freund. Chem. Rev., 106, 4301-4320 (2006).

[**37**] Yang, P, W.Zhang, Y.Du and X. Wang. J. Molecular Catalysis A, 4-10,260 (2006) .

[38] T. Pradeep, Nano: The essentials– understanding nanoscience and nanotechnology, Tata Mc Graw Hill Publishing Co. Ltd., Chennai, (2008).

[39] S. K. Kulkarni, Nanotechnology : principles and practices, Third edit, Springer US, (2015).

[40] M. Rai, A. P. Ingle, S. Birla, A. Yadav, C. A. Sanos, J. Crit. Rev. Microbiol. 696, 42(2016).

[41] J. Jiang, Y. Li, J. Liu, X. Huang, C. Yuan, X. Lou, Adv. Mater. 24 ,5166(2012).

[42] C. Clavero, J. Natur. Photon. 8 ,95(2014).

[43] R. Taylor, S. Coulombe, T. Otanicar, P. Phelan, A. Gunawan, W. Lv, G. Rosengarten, R. Prasher, and H. Tyagi, "Small particles, big impacts: A review of the diverse applications of nanofluids," Journal of Applied Physics, vol. 113, no. 1. (2013).

[44] Y. L. Hewakuruppu, L.A. Dombrovsky , C. Chen, V. Timchenko, X. Jiang, S. Baek, and R.A. Taylor, "Plasmonic 'pump-probe' method to study semi-transparent nanofluids.," Appl. Opt., vol. 52, no. 24, pp. 6041–50, (2013).

References

[45] Ramya.M and sylvia Subapriya.M, "Green Synthesis of Silver Nanoparticles". Int. J. Pharm: PP 54-61(2012).

[46] W. M. Haynes, "CRC handbook of chemistry and physics : a ready-reference book of chemical and physical data", 95th ed., CRC Press, (2014).

[47] Sileikaite A., Prosycevas I., Pulso J., Juraitis, A., Guobiene, A., "Analysis of Silver Nanoparticles Produced by Chemical Reduction of Silver Salt Solution", Materials Science 12: pp 287-291,(2006).

[48] Li,W.R.; Xie, X.B.; Shi, Q.S.; Zeng, H.Y.; Ou-Yang, Y.S.; Chen, Y.B. "Antibacterial activity and mechanism of silver nanoparticles on Escherichia coli",Appl. Microbial Biotechnol,85:pp1115-1122,(2010).

[49] Mukherjee, P.; Ahmad, A.; Mandal, D.; Senapati, S.; Sainkar, S.R.; Khan, M.I.; Renu, P.; Ajaykumar, P.V.; Alam, M.; Kumar, R.; et al. "Fungus-mediated synthesis of silver nanoparticles and their immobilization in the mycelial matrix: A novel biological approach to nanoparticle synthesis, Nano Letters, *1* (10),: pp 515–519 (2001).

[50] L. Ge, Q. Li, M. Wang, J. Ouyang, X. Li, and M. M. Q. Xing, "Nanosilver particles in medical applications: Synthesis, performance, and toxicity," International Journal of Nanomedicine, vol. 9, no. 1. pp. 2399–2407,(2014).

[51] Carlson, C.; Hussain, S.M.; Schrand, A.M.; Braydich-Stolle, L.K.; Hess, K.L.; Jones, R.L.; Schlager, J.J. "Unique cellular interaction of silver Nanoparticles:Size-dependent generation of reactive oxygen species" J. Phys. Chem. B , 112:pp 13608–13619,(2008),.

[52] Zhang, Q.; Li, N.; Goebl, J.; Lu, Z.D.; Yin, Y.D. "A systematic study of the synthesis of silver nanoplates: Is citrate a "Magic" Reagent**?**", J. Am. Chem. Soc., 133:pp 18931–18939,(2011).

[53] Gliga, A.R., Skoglund, S., Wallinder, I.O., Fadeel, B., Karlsson, H.L.,"Size dependent cytotoxicity of silver Nanoparticles in human lung cell: The role of cellular take, agglomeration and Ag release",licensee, BioMed Central Ltd (2014).

[54] Sriram, M.I.; Kalishwaralal, K.; Barathmanikanth, S.; Gurunathani, S. "Size-based cytotoxicity of silver nanoparticles in bovine retinal endothelial cells". Nanosci. Methods, 1: pp56–77(2012).

[55] Sharma.V.K, Yngard.R.A, Lin.Y., "Silver Nanoparticles:Green synthesise and their antibacterial antimicrobial activities activities" ,Advance in colloid and interface science 145:pp83-96. (2009).

[56] Eustis, Susie. Gold and silver nanoparticles: characterization of their interesting optical properties and the mechanism of their photochemical formation. Diss. Georgia Institute of technology,(2006).

[57] Singh, Priyanka, Yu-Jin Kim, Dabing Zhang, and Deok-Chun Yang. "Biological synthesis of nanoparticles from plants and microorganisms." Trends in biotechnology 34, no. 7: 588-599, (2016).

[58] Wooten, Frederick. "Optical properties of solids". Academic press, (2013).

[59] Chen, Yan, Peter Renner, and Hong Liang. "Dispersion of nanoparticles in lubricating oil". A critical review." Lubricants 7.1 :7, (2019).

[60] Wu, Changle, Xueliang Qiao, Jianguo Chen, Hongshui Wang, Fatang Tan, and Shitao Li. "A novel chemical route to prepare ZnO nanoparticles." Materials Letters 60, no. 15: 1828-1832., (2006).

[61] Lim, P. Y., R. S. Liu, P. L. She, C. F. Hung, and H. C. Shih. "Synthesis of Ag nanospheres particles in ethylene glycol by electrochemical-assisted polyol process." Chemical physics letters 420, no. 4-6: 304-308, (2006).

[62] Fu, Xinxin, Jingxuan Cai, Xiang Zhang, Wen-Di Li, Haixiong Ge, and Yong Hu. "Top-down fabrication of shape-controlled, monodisperse nanoparticles for biomedical applications.", Advanced drug delivery reviews 132: 169-187, (2018).

[63] Jia, Huiying, Jiangbo Zeng, Wei Song, Jing An, and Bing Zhao. "Preparation of silver nanoparticles by photo-reduction for surface-enhanced Raman scattering". Thin Solid Films 496, no. 2: 281-287, (2006).

[64] Mcgilvray, Katherine L., Matthew R. Decan, Dashan Wang, and Juan C. Scaiano. "Facile photochemical synthesis of unprotected aqueous gold nanoparticles." Journal of the American Chemical Society 128, no. 50: 15980-15981., (2006).

[65] Courrol, Lilia Coronato, Flávia Rodrigues de Oliveira Silva, and Laércio Gomes. "A simple method to synthesize silver nanoparticles by photo-reduction." Colloids and Surfaces A: Physicochemical and Engineering Aspects 305.1-3 : 54-57, (2007).

[66] F.J.Duarte, L.W.Hil1man, "Dye laser Principles", Academic press, New York(1999)

[67] Parker C.A. (1968), "Photoluminescence of solution", Elsevier Publishing Company, Amsterdam

[68] Birks J. (1970), 'Photophyscics of Aromatic molecules', J. Willey and Sons, New York.

[69] Mataga N. and Kubota T. ,"Molecular interactions and electronic spectra", Marcel Dekker Inc., New York(1970).

[70] Becker R.S. "Theory and Interpretation of Fluorescence and Phosporescemce", Wiley Interscience, New York (1969).
[71] Schafer F.P. "Dye Lasers", Applied Physics Series, Springer- Verlag, Berlin(1975).

[72] J .R Lakowicz, "Principles of Fluorescence Spectroscopy", Plenum press, New Y0rk, (Chapter 9) (l983).
[73] A.J.Pesce, C.G.Rosen, T.L. Pasby, "Fluorescence spectroscopy", Marcel Dekker Inc, New York (1971).

[74] Mahmoud E. M. Sakr, Maram T. H. Abou Kana Gamal Abdel Fattah., " Lifetime, Efficiency and Photostability Enhancement of Pyrromethene Laser Dyes by Metallic Ag Nanoparticles", Arab Journal of Nuclear Science and Applications, 47(1), (99-106) (2014).

[75] J.R.Lak0wicz, Radiative Decay engineering: Biophysical and Biomedical applications, Analytical biochemistry 298 ,1-24(2001).

[76] Hassan A.F., Al-Hamdani A.H. and Abbas F.S., "Study the effect of concentration on spectroscopic properties of fluorescein sodium dye in ethanol", Journal of kufa- Physics,Vol.6, No.1, PP.112-118, (2014).

[77] Florian M. Zehentbauer , Claudia Moretto , Ryan Stephen, Thangavel Thevar , John R. Gilchrist , Dubravka Pokrajac , Katherine L. Richard , Johannes Kiefer ."Fluorescence spectroscopy of Rhodamine 6G: Concentration and solvent effects", Spectrochimica Acta Part A: Molecular and Biomolecular Spectroscopy .121 ,147–151(2014).

[78] Hassan H. Hammud · Kamal H. Bouhadir ·Mamdouh S. Masoud · Amer M. Ghannoum ·Sulaf A. Assi." Solvent Effect on the Absorption and Fluorescence Emission Spectra of Some Purine Derivatives:

Spectrofluorometric Quantitative Studies", Article in Journal of Solution Chemistry · July 2008 DOI: 10.1007/s10953-008-9289-8

[79] M. N. B.-S. Bernard Valeur, "Molecular Fluorescence: Principles and Applications", 2nd ed. John Wiley & Sons, (2013).

[80] J. R. Lakowicz, "Principles of Fluorescence Spectroscopy", Springer Science & Business Media, (2006).

[81] Hemerik, Marcel. Design of a mid-infrared cavity ring down spectrometer. Technische Universiteit Eindhoven, (2001).

[82] Turner, Daniel B., Krystyna E. Wilk, Paul MG Curmi, and Gregory D. Scholes. "Comparison of electronic and vibrational coherence measured by two-dimensional electronic spectroscopy." The Journal of Physical Chemistry Letters 2, no. 15: 1904-1911, (2011).

[83] Jannson, Tomasz P. "Tribute to Emil Wolf: science and engineering legacy of physical optics." Vol. 139. SPIE Press, (2005).

[84] Saleh, Bahaa EA, and Malvin Carl Teich. Fundamentals of photonics. john Wiley & sons,(2019).

[85] Kabashin, Andrei V., and M. Meunier. "Synthesis of colloidal nanoparticles during femtosecond laser ablation of gold in water." Journal of Applied Physics 9 4.12 : 7941-7943, (2003).

[86] Arbeloa, F. López, A. Costela, and I. López Arbeloa. "Molecular structure effects on the lasing properties of rhodamines." Journal of Photochemistry and Photobiology A: Chemistry 55.1 :97-103, (1990).

[87] McWeeny, Roy. "Atoms, molecules, matter–the stuff of chemistry." (2007).

[88] R.L.Sutherland, Hand book of nonlinear optics, Marcel Dekker (1996)

[89] Y.R.Shen,The Principles of nonlinear optics, John Wiley and sons, New York(1991).

References

[90] E.G.Sauter, Nonlinear optics, John Wiley and sons Inc. New York (1996)

[91] T.Kobayashi, Nonlinear optics of organics and semiconductors, T.Kobayashi, Nonlinear optics, l ,Springer ~Verlag,Berlin (1991)

[92] R.A.Gannev, nonlinear refraction and nonlinear absorption of various media, J.Opt.A: pure and App.Opt , 7 ,7l7-733(2005).

[93] J.S.Shirk, R.G.S.P0ng ,F.J.Bartoli , A.W.Snow, "Optical limiter using a lead phthalocyanine" ,Appl.Phys.Lett. 63 ,l880(l993).

[94] H.Ditlbacher ,J.R.Krenn, B.Lamprecht, A.Leitner ,F.R.Aussenegg, Spectrally coded optical data storage by metal nanoparticles,Opt.Lett, 25 ,563(2000).

[95] Krishnamurthy, Rekha Rathnagiri, and Ramalingam Alkondan. "Nonlinear characterization of Mercurochrome dye for potential application in optical limiting." Optica Applicata 40.1: 187-196 (2010).

[96] Venkatram, N., D. Narayana Rao, L. Giribabu, and S. Venugopal Rao. "Femtosecond nonlinear optical properties of alkoxy phthalocyanines at 800 nm studied using Z-Scan technique." Chemical Physics Letters 464.4-6: 211-215 (2008).

[97] Boyd, Robert W. Nonlinear optics. Academic press, (2020).

[98] Träger, Frank, ed. Springer handbook of lasers and optics. Springer Science & Business Media, (2012).

[99] Vinitha, G., and A. Ramalingam. "Spectral characteristics and nonlinear studies of methyl violet 2B dye in liquid and solid media." Laser physics 18.1: 37-42 (2008).

[100] De Araújo, Cid B., Anderson SL Gomes, and Georges Boudebs. "Techniques for nonlinear optical characterization of materials: a review." Reports on Progress in Physics 79.3: 036401 (2016).

References

[101] Van Stryland, Eric W., and Mansoor Sheik-Bahae. "Z-scan measurements of optical nonlinearities." Characterization techniques and tabulations for organic nonlinear materials 18.3: 655-692 (1998).

[102] Dhinaa, A. N., and P. K. Palanisamy. "Z-Scan technique: To measure the total protein and albumin in blood." J. Biomed. Sci. Eng 3.03: 285-290 (2010).

[103] Sheik-Bahae, Mansoor, Ali A. Said, and Eric W. Van Stryland. "High-sensitivity, single-beam n 2 measurements." Optics letters 14.17: 955-957 (1989).

[104] Patil, P. S., Shivaraj R. Maidur, S. Venugopal Rao, and S. M. Dharmaprakash. "Crystalline perfection, third-order nonlinear optical properties and optical limiting studies of 3, 4-Dimethoxy-4′-methoxychalcone single crystal." Optics & Laser Technology 81: 70-76 (2016).

[105] Irimpan, Litty, A. Deepthy, Bindu Krishnan, V. P. N. Nampoori, and P. Radhakrishnan. "Nonlinear optical characteristics of self-assembled films of ZnO." Applied Physics B 90.3: 547-556 (2008).

[106] Sutherland, Richard L. "Handbook of nonlinear optics". CRC press, (2003).

[107] Plick, William Nicholas. "Quantum light for quantum technologies." (2010).

[108] Chapple P. B., Staromlynska J., Hermann J.A. and Mckay T. J., "Single – beam z-scan: measurement techniques and analysis", Journal of nonlinear optical physics and materials, Vol.6, No.3, PP.251-293, (1997).

[109] Neethling P., "Determining non-linear optical properties using the z-scan technique", M.Sc. Thesis, Stellenbosch University, in April,(2005).

[110] J. Guo**,** T.Y. Chang, I. McMichael, J. Ma, and J.H. Hong, Opt. Lett. 24, 981 (1999).

[111] R. Frey and C. Flytzanis, Opt. Lett. 25, 838 (2000).

[112] Hagan, D. J., E. W. Van Stryland, Y. Y. Wu, T. H. Wei, M. Sheik-Bahae, A. Said, K. Mansour, J. Young, and M. J. Soileau. "Materials for optical switches, isolators, and limiters." In Proceedings of SPIE, vol. 1105, p. 103, (1989).

[113] Lim, G. -K.; Chen, Z. -L.; Clark, J.; Goh, R. G. S.; Ng, W. -H.;C Tan, H. -W.; Friend, R. H.; Ho, P. K. H. and Chua, L. -L. "Giant broadband nonlinear optical absorption resp onse in dispersed graphene single sheets", Nature Photonics 5(554-560) (2011).

[114] Sahib Nimma Abdul-Wahid, Methaq Mutter Mehdy Al-Sultany. "study of the optical properties for BDN-I dye solutions which are used to Q-switch the Nd:YAG laser", Journal of Kerbala University , Vol. Journal 6 No.1 Scientific .March. (2008).

[115] Mansour, K.; Soileau, M. J. and Van Stryland, E.W. "Nonlinear optical properties of carbon-black suspensions (ink)", J. Opt. Soc. Am. B 9 ,1100-1109(1992).

[116] Riggs, 1. E.; Walker, D. B.; Carroll, D. L. and Sun, Y. P. "Optical limiting properties of suspended and solubilized carbon nanotubes", 1. Phys. Chern. B 104 ,7071-7076 (2000).

[117] Tutt, L. W. and Kost, A. "Optical limiting performance of C60 and C70 solutions", Nature 356 ,225.

[118] Perry, J. W.; Mansoor, K.; Lee, I. Y. S.; Wu, X. L.; Bedworth, P. V.; Chen, C. T.; Ng, D.; Mander, S. R.; Miles, P.; Wada, T.; Tian, M. and Sasabe, H. "Organic optical limiter with a strong nonlinear absorptive response". Science (273) 1533(1996).

[119] Senge. M, O.; Fazekas. M. Notaras, E. G A; Blau, W. J.; Zawadzka, M.; Locos, O. B. and Mlhuircheartaigh. E. M. N. "Nonlinear Optical

Properties of Porphyrins". Adv. Mtater. 19 ,2737-2774 , Doi:10.1364/OE.23.024071 | Optics Express 24071 (2007).

[120] Mathews, S. J.; Kumar, S. C.; Giribabu, L. and Rao, S. V. "Large third-order optical nonlinearity and optical limiting in symmetric and unsymmetrical phthalocyanines studied using Z-scan", Opt. Commun. 280 ,206-212,(2007).

[121] Westlund, R.; Malmstro"m, E.; Lopes, c.; Ohgren, 1.; Rodgers, T.; Saito, Y; Kawata, S.; Glimsdal, E. and Lindgren, M. "Efficient Nonlinear Absorbing Platinum(II) Acetylide Chromophores in Solid PMMA Matrices", Adv. Funct. Mater. 18 ,1939-1948(2008).

[122] P. Prem Kiran,"Optical Limiting and Nonlinear Optical Properties of Photo Responsive Materials: Tetratolylporphyrins, Pure and iron doped $Bi_{12}SiO_{20}$ crystals and Codoped Ag-Cu Metal Nanoclusters", School of Physics University of Hyderabad ,(2004).

[123] Alqaragully, Mohammed Bassim. "Removal of textile dyes (maxilon blue, and methyl orange) by date stones activated carbon." Int J Adv Res Chem Sci 1.1: 48-59 (2014).